(NASA-CR-146074) A FINITE ELEMENT ANALYSIS OF THE EXACT NONLINEAR FORMULATION OF A LIFTING SURFACE IN STEADY INCOMPRESSIBLE FLOW, WITH THE EVALUATION OF THE CORRECT WAKE GEOMETRY M.S. Thesis (Boston Univ.) N76-15079 Unclas G3/02 08523

BOSTON UNIVERSITY

DEPARTMENT OF AEROSPACE AND MECHANICAL ENGINEERING

COLLEGE OF ENGINEERING

BOSTON, MASSACHUSETTS

Boston University

College of Engineering

110 Cummington Street

Boston, Mass. 02215

A FINITE ELEMENT ANALYSIS OF THE EXACT NONLINEAR FORMULATION OF A LIFTING SURFACE IN STEADY INCOMPRESSIBLE FLOW, WITH THE EVALUATION OF THE CORRECT WAKE GEOMETRY

by

Emil O. Suciu

Submitted in partial fulfillment of the requirements for the degree of Master of Science in Aerospace Engineering

1975

APPROVED BY

Chairman Luigi Morino
Associate Professor of Aerospace Engineering

First Reader Daniel J. Udelson
Professor of Aerospace Engineering

Second Reader Isaac Fried
Assistant Professor of Mathematics

ABSTRACT

The problem of steady incompressible flow for lifting surfaces is considered. This problem requires the solution of an integral equation relating the values of the potential discontinuity on the lifting surface and its wake to the values of the normal derivative of the potential which are known from the boundary conditions. The lifting surface and the wake are divided into small quadrilateral (hyperboloidal) surface elements, Σ_i, which are described in terms of the Cartesian components of the four corner points. The values of the potential discontinuity and the normal derivative of the potential are assumed to be constant within each lifting surface element and equal to their values at the centroids of the lifting surface elements. This yields a set of linear algebraic equations.

An iteration procedure is used to obtain the wake geometry: the velocities at the corner points of the wake elements are calculated and the (originally straight) wake streamlines are aligned to be parallel to the velocity vector. The procedure is repeated until convergence is attained.

Numerical results are in reasonable agreement with existing ones.

FOREWORD

I would like to thank Dr. Luigi Morino for his help on many levels. Without his continuous support and encouragement, this work would have never been performed by me. I am also indebted to Profs. Daniel G. Udelson and Isaac Fried for acting as readers of this thesis.

This work was supported by NASA Langley Research Center under NASA Grant NGR 22-004-030. Dr. E. Carson Yates, Jr. is the monitor of the Grant.

TABLE OF CONTENTS

LIST OF SYMBOLS

$\vec{a}_i$	base vectors, defined by Eq. 2.9
A_{hk}	See Eqs. 2.2 and 2.3
AR	Aspect Ratio
B_h	Eq. 2.4
C_L	Lift coefficient
$C_{L\alpha}$	Lift coeefficient per unit angle of attack
c_p	Pressure coefficient
D_k	Defined by Eq. 2.1
$\vec{i}$	Unit vector along x-direction
$\vec{n}_h$	Normal to the surface at P_h
NX, NY	Number of elements along x and y directions, respectively

$\vec{P}\ (x, y, z)$	Control point
$\vec{P}_{++}, \vec{P}_{+-}, \vec{P}_{-+}, \vec{P}_{--}$	See Eq. 2.14
$\vec{P}_k, \vec{P}_1, \vec{P}_2, \vec{P}_3$	See Eq. 2.14
p	Pressure
$\vec{Q}_1, \vec{Q}_2, \vec{Q}_3, \vec{Q}_4$	See Eqs. 2.16 and 2.17
$\vec{V}$	Velocity vector
$\vec{V}_h$	Velocity at point $\overline{P}_h$
$\vec{V}_{hk}$	See Eq. 2.6
x, y, z	Cartesian coordinates
$\overline{x}, \overline{y}, \overline{z}$	See Eq. 2.20
U_∞	Velocity of the undisturbed flow
α	Angle of Attack
β, γ	See Eq. 2.20

ξ^1, ξ^2	See Eq. 2.8
ξ, η	See Eq. 2.13
Σ_o	Surface surrounding body and wake
Σ	Lifting surface and wake surface
σ_k	See Eq. 2.1
Φ	Velocity potential function
ϕ	Perturbation aerodynamic potential
ϕ_k	Value of ϕ at $\overline{P}_k$
ψ, θ	See Eq. 2.23

SPECIAL SYMBOLS

$\vec{\nabla}$	Gradient operator in x, y, z coordinates
L.E.	Leading edge
T.E.	Trailing edge

SPECIAL SYMBOLS (Continued)

Δx_w	Length of wake element along x-direction
u, ℓ	Upper, lower
∞	At infinity

LIST OF FIGURES

LIST OF FIGURES (Continued)

LIST OF FIGURES (Continued)

LIST OF FIGURES (Continued)

SECTION I

INTRODUCTION

1.1 Definition of the Problem

This work deals with a nonlinear finite-element analysis of zero thickness wings (lifting surfaces) in steady, incompressible, inviscid, irrotational flow, including the effect of the rolled-up wake. The problem is formulated in terms of the velocity potential. This problem was considered in Ref. 1 where a zeroth order finite-element (i.e. the potential ϕ prescribed at the centroids of the surface elements) analysis was used, with a straight-vortex-line wake. The present work is an extension of Ref. 1 and includes the analysis of the wake roll-up as well as the nonlinearities in the evaluation of the pressure (Bernoulli's Theorem). Throughout this work, the potential is assumed to have a constant value over the surface element, equal for example with its (unknown) value at the centroid of the element (zeroth order formulation). The first item considered here is the wake roll-up. The rolled-up geometry for the wake is obtained by a process of iteration. The convergence of the iteration scheme is investigated. A second item included here is the effect of the rolled-up wake on the pressure distribution over the lifting-surface, using the nonlinearized Bernoulli equation. The results are compared with the linearized ones.

1.2 Lifting-Surface Theory

The theoretical investigation of pressure and lift distributions over lifting surfaces of various shapes is embodied in many works.[1] An excellent review of the literature in the field is given in Refs. 2 and 3, together with results for lifting surfaces in steady and oscillatory, subsonic and supersonic flows. It may be worth noting that the integral equation used here is analogous to the one used by Jones (Ref. 4) for unsteady incompressible flow. The classical approach for the numerical solutions of lifting-surface theories is by expressing the unknown in terms of a series with N unknown coefficients and by imposing that the equation be satisfied at N control points. Recently, however, a new approach (often referred to as the finite-element method) has been introduced, especially in connection with complex-configurations aerodynamics. A finite-element analysis of lifting surfaces is considered for instance in Ref. 5, which presents results for the loading of a rectangular planar zero-thickness wing using a downwash-velocity potential formulation. Ref. 1 presents a general finite-element solution of a velocity potential formulation for lifting surfaces of arbitrary shapes in steady subsonic flows. This work differs from the one of Ref. 5 in that it uses hyperboloidal (i.e. warped) quadrilateral elements and is therefore applicable to any arbitrary nonplanar shape. Expressions for the velocity at any point are also obtained in Ref. 1. These are suitable for investigating the dynamics of the wake.

1.3 Wake Roll-Up

The interest in the phenomenon of wake roll-up has been spurred by the introduction, a few years ago, of the wide-body aircraft. Many papers have since been written about wing-tip vortices: about their formation, their effect on a trailing aircraft, their detection and their disappearance. Excellent descriptions of the phenomenon can be found in Refs. 6 and 7. A short illustration of it is also presented here. In a few words, behind every aircraft in flight, a pair of counterrotating wing-tip vortices is formed. See Fig. 1. The diameter of the vortex core has been found by measurements to be approximately 3% of the wingspan. The strength of the vortex seems to increase as the weight of the aircraft increases. If a four-engine jet airplane flies sufficiently high for the contrails to appear, it is observed that the exhausts from the two engines on each wing are gradually pushed towards the wing tips, thus making the wing-tip vortices visible. These vortices are quite stable; vortex life spans of more than 15 minutes have been observed, which, compared with the speed of a modern aircraft, means that the wing-tip vortices might persist for 150 miles behind the generating aircraft. The circumferential velocity of the vortex is large, of the order of 30% of the generating aircraft speed. If a small aircraft passes through the wake of a large one, structural damage may occur on the small plane; if the flight path is not sufficiently high, the disturbances induced by the wake of the large aircraft on the velocity field of the small one may lead to loss of lift for the small plane and possibly to its crash. Ref. 7 contains more descriptive and pictorial information about these undesirable occurrences.

Numerous wind tunnel and real life measurements of the wake vortices have been performed. See, for example, Refs. 8 and 9.

Theories dealing with the matter are mainly two-dimensional and generally they do not account for the viscosity effects (Ref. 10). Ref. 11 presents a three-dimensional potential method for the estimation of the wake roll-up geometry for wings with control surfaces. In addition, an "artificial" viscosity coefficient is introduced in the equations describing the velocity field of the vortex sheet to "smoothen" out the singularities inherent in the method.

Reference 12 presents another three-dimensional potential model to obtain a rolled-up wake geometry, as well as the wing-jet interaction.

Reference 13 integrates in time a set of ordinary differential equations describing the position of the wake vortices. The finite vortex sheet of which the wake consists is approximated by a finite number of vortices. An unsatisfactory wake pattern was obtained and the paper contends that the mathematical model used fails at the wing tip.

Reference 14 presents a method for the prediction of the aerodynamic loads on thin lifting surfaces. Nonlinearities (wake deformation) are considered. The method of Reference 14 is conceptually the closest to the one presented in this work.

1.4 Formulation of the Problem

This subsection presents the basic flow equations which will be used throughout the paper. The fluid considered here is incompressible, inviscid and irrotational. For an incompressible fluid, the continuity equation is

$$\vec{\nabla} \cdot \vec{V} = 0 \qquad (1.1)$$

where $\vec{V}$ is the velocity vector. Because of the fact that the fluid is irrotational, or

$$\vec{\nabla} \times \vec{V} = 0 \tag{1.2}$$

a velocity potential Φ exists, such that

$$\vec{V} = \vec{\nabla}\Phi \tag{1.3}$$

It is convenient to introduce the perturbation velocity potential, ϕ, and define $\vec{V}$ as

$$\vec{V} = U_\infty \ (\vec{i} + \vec{\nabla}\phi) \tag{1.5}$$

where $\vec{i}$ is the unit vector along the x-direction. Combining now Eqs. (1.1) and (1.5) the Laplace equation for ϕ is obtained:

$$\nabla^2\phi = 0 \tag{1.6}$$

The boundary condition to be satistfied is that the flow is tangent to the surface, or

$$\vec{V} \cdot \vec{n} = 0 \tag{1.7}$$

From Eqs. (1.5) and (1.7), the boundary condition for the perturbation potential results:

$$\frac{\partial \phi}{\partial n} = -\vec{i} \cdot \vec{n} = -n_x \tag{1.8}$$

As it is well known, on the surfaces of the wing and of the wake the solution is discontinuous (see for instance Ref. 1 and 5). Also, there exists a pressure discontinuity on the surface of the wing, while the surface of the wake is determined by the fact that no pressure discontinuity exists on the wake. Therefore, in order to complete the problem, the condition for the geometry of the wake as well as the expressions for the pressure discontinuity on the wing are obtained here. This can be easily accomplished, starting from the Bernoulli theorem (for steady, incompressible, inviscid flows)

$$p - p_\infty + \frac{\rho}{2} (\vec{V} \cdot \vec{V} - U_\infty^2) = 0 \tag{1.9}$$

If there exists a surface of discontinuity, then, indicating for simplicity with "upper" and "lower" the two sides of the surfaces, one obtains, from Eq. (1.9)

$$p_u - p_\ell + \frac{\rho}{2} (\vec{V}_u \cdot \vec{V}_u - \vec{V}_\ell \cdot \vec{V}_\ell) = 0 \tag{1.10}$$

or

$$p_u - p_\ell + \frac{\rho}{2} (\vec{V}_u + \vec{V}_\ell) \cdot (\vec{V}_u - \vec{V}_\ell) = 0 \qquad (1.11)$$

Indicating with $\vec{V}_a$ the velocity of the point on the surface of discontinuity

$$\vec{V}_a = \frac{\vec{V}_u + \vec{V}_\ell}{2} \qquad (1.12)$$

(average between the upper and the lower surface) and with

$$\Delta \vec{V} = \vec{V}_u - \vec{V}_\ell \qquad (1.13)$$

the velocity discontinuity, Eq. (1.11) may be rewritten as

$$\Delta p = p_u - p_\ell = -\rho \vec{V}_a \cdot \Delta \vec{V} \qquad (1.14)$$

This is the desired expression for the pressure discontinuity. Using Eq. (1.5), Eq. (1.14) may be rewritten as

$$\Delta p = -\rho U_\infty^2 \; (\vec{i} + \vec{\nabla}\phi_a) \cdot \vec{\nabla}(\Delta\phi) \qquad (1.15)$$

or

$$\Delta c_p = \frac{\Delta p}{\frac{1}{2}\rho U_\infty^2} = -2(\vec{i} + \vec{\nabla}\phi_a) \cdot \vec{\nabla}(\Delta\phi) \tag{1.16}$$

which gives the exact (nonlinear) expression for the pressure distribution on the wing.

Equation (1.14) may also be used to obtain the condition for the geometry of the wake. For, the condition that no pressure discontinuity exists on the wake yields

$$\vec{V}_a \cdot \Delta\vec{V} = 0 \tag{1.17}$$

It may be noted that if Eq. (1.17) is satisfied, then the no-pressure-discontinuity condition is automatically satisfied. Equation (1.17) may be interpreted as saying that the velocity discontinuity on the wake is normal to the velocity of the wake. Also, Eq. (1.17) may be rewritten as

$$(\vec{V}_a \cdot \vec{\nabla})\ \Delta\phi = 0 \tag{1.18}$$

i.e. that

$$\Delta\phi = \text{constant along a streamline} \tag{1.19}$$

Therefore, the geometry of the wake may be obtained from the streamlines emanating from the trailing edge which have the property of being tangent to $\vec{V}$. Equation (1.17) (and hence the condition of no-pressure-discontinuity) is then satisfied by imposing that $\Delta\phi$ be constant along a streamline (Eq. (1.19)). It may be worth mentioning that Eq. (1.17) is equivalent to saying that the vortex lines coincide with the streamlines since a surface of velocity discontinuity (with continuous normal component) is equivalent to a layer of vortices with vortex lines parallel to the lines of constant $\Delta\phi$ (which, in turn, are normal to the directions of $\Delta\vec{V}$)*.

It is worth noting that the above formulation is exact, in the sense that no small-perturbation hypothesis has been used. In order to assess the relevance of using the exact formulation, the results obtained with such a formulation will be compared with the ones obtained from a small-perturbation formulation. If the small-perturbation hypothesis

$$|\vec{\nabla}\phi| = O(\varepsilon) << 1 \tag{1.20}$$

is invoked, Eq. (1.5) yields

$$V = U_\infty \vec{i} + O(\varepsilon) \tag{1.21}$$

and therefore Eq. (1.16) may be rewritten as

---

*See for instance Ref. 15

$$\Delta c_p \approx -2\vec{i} \cdot \vec{\nabla}(\Delta\phi) + O(\varepsilon) \tag{1.22}$$

while the wake may be assumed to be composed of straight vortex lines emanating from the trailing edge. A more convenient expression for Δc_p is

$$\Delta c_p = -2 \frac{\partial}{\partial s} \Delta\phi + O(\varepsilon) \tag{1.23}$$

where s is the arc length along the lifting surface in the planes y = constant.

1.5 Method of Solution

In Ref. 1, it is shown that the distribution of the perturbation aerodynamic potential around a body of arbitrary shape is given by the following integral expression:

$$4\pi E\phi = - \oiint_{\Sigma_o} \left[\frac{\partial\phi}{\partial n} \frac{1}{r} - \phi \frac{\partial}{\partial n}\left(\frac{1}{r}\right) \right] d\Sigma \tag{1.24}$$

where

$E = 0$ inside Σ_o

$E = 1/2$ on Σ_o

$E = 1$ outside Σ_o

Σ_o is a surface surrounding the body and its wake, and $\vec{n}$ is the normal to the surface.

If the distance between the upper and lower sides of the body surface goes to zero (zero-thickness body), one obtains a lifting surface formulation:

$$\phi = \iint_{\Sigma} D \frac{\partial}{\partial n_u} \left(\frac{1}{r}\right) d\Sigma \tag{1.25}$$

where Σ extends over the lifting surface and its wake,

$$D = \frac{\phi_u - \phi_\ell}{4\pi} \tag{1.26}$$

and the subscripts u and ℓ stand for upper and lower surfaces, respectively. Equation (1.25) shows that the potential can be represented by a doublet distribution on the body and on the wake. The value of D is constant along streamlines of the wake and equal to the value at the trailing edge of the wing (Eq. 1.19).

The boundary condition, Eq. (1.8), must be satisfied. Using Eq. (1.25), the following integral equation results:

$$\frac{\partial \phi}{\partial n_o} = \iint_{\Sigma} \frac{\partial}{\partial n_o} \left[D \frac{\partial}{\partial n} \left(\frac{1}{r}\right)\right] d\Sigma \tag{1.27}$$

where $\partial\phi/\partial n_o$ (the subscript zero denotes the control point) is known and given by E. (1.8).

The surface of the wake is assumed to be known (say from independent calculations).

The numerical solution of Eq. (1.27) will be analyzed in detail in this work.

After Eq. (1.27) has been solved for D, the velocity at any point, P, in the field, may be obtained as:

$$\vec{V}_P = \vec{\nabla} \iint_{\Sigma} D \frac{\partial}{\partial n_u} \left(\frac{1}{r}\right) d\Sigma \qquad (1.28)$$

From $\vec{V}_p$, the pressure, as well as a new geometry for the wake is obtained.

1.6 Outline of the Work

In Ref. 1, the numerical formulation for the integral equation describing the distribution of the perturbation aerodynamic potential over a lifting surface has been obtained. Expressions for the velocity vector, $\vec{V}$, at any point in the field have also been obtained. In Section II of this work, a summary of Ref. 1 is presented. A description of the iteration scheme used for obtaining a rolled-up wake geometry, as well as the calculation of the nonlinear pressure coefficient are added.

Section III presents results obtained with the lifting surface formulation of Ref. 1, shown in comparison with existing theoretical and experimental results.

The convergence of the solution is illustrated in Appendix A. In Appendix B, the convergence of the iteration scheme is presented. A flow chart and list of the computer program implementing the theoretical formulation is contained in Appendix C.

SECTION II

NUMERICAL FORMULATION

2.1 Introduction

This section presents the numerical formulation used here, including the wake roll-up iteration procedure and the calculation of the pressure coefficient, using the linearized Bernoulli Equation, as well as the nonlinearized one. This formulation is an extension of the one of Ref. 1, where wake roll-up is not included. For completeness, the formulation of Ref. 1 is summarized here.

As mentioned in the previous section, the finite-element formulation yields the distribution of the doublet strength at the centroids of the lifting surface elements. Once this is known, the velocity at any point in the field, in particular at the corner points of the wake elements may be obtained. These may be used to obtain the geometry of the wake.

In Subsection 2.2, the gradient of Eq. (1.25) is expressed in terms of the values of D at the centroids of the elements; the boundary condition, Eq. (1.8) is satisfied at the centroids of the elements (control points). In Subsection 2.3, a new type of surface element, the hyperboloidal quadrilateral element, first introduced in Ref. 16, is briefly presented, together with the vector expressions for the velocity induced by an element at a control point. In Subsection 2.4, the iteration scheme used for obtaining the rolled-up wake pattern is presented. The element grid used for performing the numerical calculations is described in Subsection 2.5. In Subsection 2.6, the finite-difference procedure for calculating the pressure coefficient in terms of the planform geometry is indicated.

2.2 Discretization

The lifting surface and its wake are divided into small surface elements. See Fig. 2. Assume that the value of D is constant within each element, say it is equal to D (unknown) at the centroid of the element σ_k. Then Eq., (1.27) reduces to:

$$\frac{\partial \phi}{\partial n_o} = \sum_{k=1}^{N+L} D_k \iint_{\sigma_k} \frac{\partial^2}{\partial n \partial n_o} \left(\frac{1}{r}\right) d\sigma_k \tag{2.1}$$

where N is the number of surface elements on the wing and L is the number of elements on the wake. Note that D is constant along streamlines of the wake and equal to its value at the trailing edge or approximately equal to D at the centroids of the wing elements in contact with the trailing edge. If we impose that the boundary condition, Eq. (1.8) is satisfied at the centroids $P_o = P_h$ of the wing surface elements σ_h, the following system of linear algebraic equations is obtained:

$$[A_{hk}] \; \{D_k\} = \{B_h\} \tag{2.2}$$

where

$$A_{hk} = \left[\iint_{\sigma_k} \frac{\partial^2}{\partial n \partial n_o} \left(\frac{1}{r}\right) d\sigma_k \right]_{P_o = P_h} \tag{2.3}$$

and

$$B_h = \left(\frac{\partial \phi}{\partial n}\right)\Bigg|_{P_o = P_h} \tag{2.4}$$

In addition, according to Eq. (1.28),

$$\vec{V}_h = \Sigma \, D_k \; \vec{V}_{hk} \tag{2.5}$$

where

$$\vec{V}_{hk} = \left[\vec{\nabla} \iint_{\sigma_k} \frac{\partial}{\partial n} \left(\frac{1}{r}\right) d\sigma_k \right]_{P_o = P_h} \tag{2.6}$$

Note that, by definition,

$$A_{hk} \equiv \vec{n}_h \cdot \vec{V}_{hk} \tag{2.7}$$

2.3 Hyperboloidal Quadrilateral Element

In order to evaluate Eqs. (2.3) and (2.6), a typical quadrilateral surface element is approximated by a portion of a hyperboloidal paraboloid passing through the four corner points. This type of surface element is called the hyperboloidal quadrilateral element, introduced in Ref. 16 and briefly described here.

The geometry of a surface element is described in vector form as:

$$\vec{P} = \vec{P}\ (\xi^1,\ \xi^2) \tag{2.8}$$

where ξ^1 and ξ^2 are the generalized curvilinear coordinates on the surface elements with the base vectors

$$\begin{aligned} \vec{a}_1 &= \frac{\partial\ \vec{P}}{\partial \xi^1} \\ \vec{a}_2 &= \frac{\partial\ \vec{P}}{\partial \xi^2} \end{aligned} \tag{2.9}$$

The unit normal to the surface is

$$\vec{n} = \frac{\vec{a}_1 \times \vec{a}_2}{|\vec{a}_1 \times \vec{a}_2|} \tag{2.10}$$

The surface element is (see Fig. 3)

$$d\sigma = |\vec{a}_1 d\xi^1 \times \vec{a}_2 d\xi^2| = |\vec{a}_1 \times \vec{a}_2| d\xi^1 d\xi^2 \tag{2.11}$$

The hyperboloidal element approximating the real surface element is described by the expression (see Fig. 4):

$$\vec{P} = [1,\ \xi,\ \eta,\ \xi\eta] \left\{ \begin{matrix} \vec{P}_k \\ \vec{P}_1 \\ \vec{P}_2 \\ \vec{P}_3 \end{matrix} \right\} \tag{2.12}$$

with

$$\begin{aligned} -1 \le \xi \le 1 \\ -1 \le \eta \le 1 \end{aligned} \tag{2.13}$$

where $\vec{P}_k$ represents the centroid of the element σ_k. The coordinates of the corners of the element are related to $\vec{P}_k$, $\vec{P}_1$, $\vec{P}_2$ and $\vec{P}_3$ as

$$\begin{Bmatrix} \vec{P}_{++} \\ \vec{P}_{+-} \\ \vec{P}_{-+} \\ \vec{P}_{--} \end{Bmatrix} = \begin{bmatrix} 1 & 1 & 1 & 1 \\ 1 & 1 & -1 & -1 \\ 1 & -1 & 1 & -1 \\ 1 & -1 & -1 & 1 \end{bmatrix} \begin{Bmatrix} \vec{P}_{k} \\ \vec{P}_{1} \\ \vec{P}_{2} \\ \vec{P}_{3} \end{Bmatrix} \tag{2.14}$$

The vectors $\vec{P}_k$, $\vec{P}_1$, $\vec{P}_2$, and $\vec{P}_3$ are given by

$$\begin{Bmatrix} \vec{P}_{k} \\ \vec{P}_{1} \\ \vec{P}_{2} \\ \vec{P}_{3} \end{Bmatrix} = \frac{1}{4} \begin{bmatrix} 1 & 1 & 1 & 1 \\ 1 & 1 & -1 & -1 \\ 1 & -1 & 1 & -1 \\ 1 & -1 & -1 & 1 \end{bmatrix} \begin{Bmatrix} \vec{P}_{++} \\ \vec{P}_{+-} \\ \vec{P}_{-+} \\ \vec{P}_{--} \end{Bmatrix} \tag{2.15}$$

Combining Eqs. (2.6) and (2.12), one obtains for $\overline{V}_{hk}$: (See Ref. 1)

$$\vec{V}_{hk} = \left[\vec{\nabla} \iint_{\sigma_k} \frac{\partial}{\partial n} \left(\frac{1}{r}\right) d\sigma_k \right]_{P = P_h} =$$

$$\frac{\vec{Q}_4 \times \vec{Q}_1}{|\vec{Q}_4 \times \vec{Q}_1|^2} \left[\frac{\vec{Q}_4 \cdot \vec{Q}_4 - \vec{Q}_1 \cdot \vec{Q}_4}{|\vec{Q}_4|} + \frac{\vec{Q}_1 \cdot \vec{Q}_1 - \vec{Q}_1 \cdot \vec{Q}_4}{|\vec{Q}_1|} \right] +$$

$$\frac{\vec{Q}_1 \times \vec{Q}_2}{|\vec{Q}_1 \times \vec{Q}_2|^2} \left[\frac{\vec{Q}_1 \cdot \vec{Q}_1 - \vec{Q}_1 \cdot \vec{Q}_2}{|\vec{Q}_1|} + \frac{\vec{Q}_2 \cdot \vec{Q}_2 - \vec{Q}_1 \cdot \vec{Q}_2}{|\vec{Q}_2|} \right] +$$

$$\frac{\vec{Q}_2 \times \vec{Q}_3}{|\vec{Q}_2 \times \vec{Q}_3|^2} \left[\frac{\vec{Q}_2 \cdot \vec{Q}_2 - \vec{Q}_2 \cdot \vec{Q}_3}{|\vec{Q}_2|} + \frac{\vec{Q}_3 \cdot \vec{Q}_3 - \vec{Q}_2 \cdot \vec{Q}_3}{|\vec{Q}_3|} \right] +$$

$$\frac{\vec{Q}_3 \times \vec{Q}_4}{|\vec{Q}_3 \times \vec{Q}_4|^2} \left[\frac{\vec{Q}_3 \cdot \vec{Q}_3 - \vec{Q}_3 \cdot \vec{Q}_4}{|\vec{Q}_3|} + \frac{\vec{Q}_4 \cdot \vec{Q}_4 - \vec{Q}_3 \cdot \vec{Q}_4}{|\vec{Q}_4|} \right]$$

where (see Fig. 5):

$$\begin{aligned} \vec{Q}_1 &= \vec{P}_{++} - \vec{P}_h \\ \vec{Q}_2 &= \vec{P}_{-+} - \vec{P}_h \\ \vec{Q}_3 &= \vec{P}_{--} - \vec{P}_h \\ \vec{Q}_4 &= \vec{P}_{+-} - \vec{P}_h \end{aligned} \tag{2.17}$$

2.4 Iteration Scheme for Wake Roll-up

As mentioned in Section I, the wake is initially assumed to consist of straight vortex lines starting at the trailing edge of the wing. It was also found that these vortex lines should be tangent to the velocity vector $\vec{V}$, and this provides the condition for obtaining the rolled-up wake geometry. The following iteration scheme is used for aligning the initially straight-wake streamlines with the velocity vector: compute the doublet strength distribution at the centroids of the elements, with the wake influencing only the A_{hk} terms of the elements, in contact with the trailing edge. Then compute the velocities in the x, y and z directions on the wake, at the corners of the surface elements. Align segments of the wake streamlines with the velocity vector evaluated at the upstream segment extremity. (See for example Fig. 6, where the position of the point $\vec{P}_{pm}$ is changed according to the velocity at the point $\vec{P}_{mm}$ on a typical wake surface element). The position of the point $\vec{P}_{pm}$ is changed as follows:

$$\vec{P}_{pm} = \vec{P}_{mm} + \Delta\vec{P} \tag{2.18}$$

where

$$\Delta\vec{P} = \vec{V} \; |\Delta\vec{P}| \; / \; |\vec{V}| \tag{2.19}$$

and $|\Delta\vec{P}|$ is the original distance between the points $\vec{P}_{pm}$ and $\vec{P}_{mm}$. The doublet strength distribution is calculated again (notice a very small change, due to the new wake geometry), then the wake velocities and geometry are reevaluated. The process repeats itself until the difference between successive wake geometries becomes sufficiently small, thus indicating the convergence of the scheme (or the fact that the streamlines are indeed tangent to the velocity vector).

The iteration scheme described here is not the best possible one. A number of improvements are suggested in Appendices A and B.

2.5 Element Grid

The pressure coefficient for the wing is computed by using the finite-difference method. In order to properly illustrate the scheme, a description of the element grid is in order.

Let c(y) be the chord and b that span of the wing, $\bar{x}$ and $\bar{y}$ the Cartesian coordinates for the wing at zero degrees angle of attack (see Fig. 2). Let

$$\gamma = \frac{\bar{x} - x_{L.E.}(\bar{y})}{c(\bar{y})}$$

$$\beta = \frac{2\bar{y}}{b} \tag{2.20}$$

Then the parametric form of the wing planform equation is:

$$\bar{x} = c\gamma + x_{L.E.}$$

$$\bar{y} = \frac{b}{2}\,\beta$$

$$\bar{z} = 0 \quad \text{for a flat lifting surface} \tag{2.21}$$

If, in addition, the wing is at an angle of attack, α, different from zero, the geometry may be rewritten as:

$$x = \bar{x}\cos\alpha$$

$$y = \bar{y}$$

$$\dot{z} = -\bar{x} \sin \alpha \tag{2.22}$$

Since the potential (doublet strength) varies faster near the leading edges and tips of the wing, it was found convenient to use smaller boxes in these regions and larger ones elsewhere. See also Ref. 15. This is accomplished by the following transformation:

$$\gamma = \psi^2$$

$$\beta = 1 - (1 - \Theta)^2 \tag{2.23}$$

The boxes have constant sizes in the plane ψ and Θ, given by:

$$\psi = 1/NX$$

$$\Theta = 1/NY \tag{2.24}$$

where NX and NY are the numbers of boxes along the x direction and along the semispan, respectively.

2.6 Pressure Coefficient

As shown in Subsection 1.4, the linearized pressure coefficient Δc_p is given by

$$\Delta c_p = -2\frac{\partial}{\partial s} (\Delta\phi) + O(\varepsilon) \tag{2.25}$$

where s is the arclength on the wing on the planes y = constant. As mentioned before, by solving Eq. (2.2), the potential distribution is obtained at the centroids of the wing elements. By interpolation, a continuous distribution can be obtained.

The wings used here for the numerical examples are all rectangular flat surfaces, for which $s = \bar{x}$. The derivative of the potential in Eq. (2.25) can be written as:

$$\frac{\partial(\Delta\phi)}{\partial\bar{x}} = \frac{\partial(\Delta\phi)}{\partial\psi} \quad \frac{\partial\psi}{\partial\gamma} \quad \frac{\partial\gamma}{\partial\bar{x}} \tag{2.26}$$

At any point $\bar{x}_i$, on an element borderline along the semispan, the derivative of the potential, by finite - differences, is:

$$\frac{\partial\ \Delta\phi}{\partial\ \bar{x}_i} = \frac{1}{c}\,\frac{\Delta\phi_{i+1/2} - \Delta\phi_{i-1/2}}{\psi_{i+1/2} - \psi_{i-1/2}} \cdot \frac{1}{2\sqrt{\psi_i}} \tag{2.27}$$

where $i \pm 1/2$ represents adjacent element centroids on planes y = constant.

The non-linearized pressure coefficient is given by Eq. (1.16), reproduced here:

$$\Delta c_p = -2(\vec{i} + \vec{\nabla}\phi_a) \cdot \vec{\nabla}(\Delta\phi) = 2\vec{V} \cdot \vec{\nabla}(\Delta\phi) \tag{2.28}$$

Denote by $\vec{i}$, $\vec{j}$ and $\vec{k}$ the unit vectors along the x, y, z coordinates and by $\vec{i}_w$, $\vec{j}_w$, $\vec{k}_w$ the unit vectors along the $\bar{x}$, $\bar{y}$, $\bar{z}$ coordinates. One can express the velocity $\vec{V}$ in terms of the wing coordinates and in terms of the x, y, y coordinates as:

$$\vec{V} = V_1 \vec{i}_w + V_2 \vec{j}_w + V_3 \vec{k}_w$$

$$= V_x\vec{i} + V_y\vec{j} + V_z\vec{k} \tag{2.29}$$

and

$$\vec{\nabla}(\Delta\phi) = \frac{\partial(\Delta\phi)}{\partial \bar{x}} \vec{i}_w + \frac{\partial(\Delta\phi)}{\partial \bar{y}} \vec{j}_w \tag{2.30}$$

Therefore, combining Eqs. (2.28), (2.29) and (2.30), the pressure coefficient becomes:

$$\Delta c_p = 2V_1 \frac{\partial(\Delta\phi)}{\partial \bar{x}} + 2V_2 \frac{\partial(\Delta\phi)}{\partial \bar{y}} \tag{2.31}$$

On the plane y = 0, a simpler expression may be obtained, since, for the symmetric cases considered here

$$\frac{\partial(\Delta\phi)}{\partial \bar{y}} = 0 \tag{2.32}$$

Therefore, on y = 0

$$\Delta c_p = 2V_1 \frac{\partial(\Delta\phi)}{\partial \bar{x}} \tag{2.33}$$

where V_1 is given by

$$V_1 = \vec{V} \cdot \vec{i}_w = V_x \cos\alpha - V_z \sin\alpha \tag{2.34}$$

with

$$V_x = 1 + \frac{\partial\phi_a}{\partial x}$$

$$V_z = \frac{\partial\phi_a}{\partial z} \tag{2.35}$$

$\frac{\partial\phi_a}{\partial x}$ and $\frac{\partial\phi_a}{\partial z}$ are obtained from Eq. (2.5).

Finally,

$$\Delta c_p \Big|_{y=0} = 2\left[(1 + \frac{\partial\phi_a}{\partial x})\cos\alpha - \frac{\partial\phi_a}{\partial z} \sin\alpha\right]\frac{\partial(\Delta\phi)}{\partial \bar{x}} \tag{2.36}$$

where $\frac{\partial(\Delta\phi)}{\partial \bar{x}}$ is computed according to Eqs. (2.26) and (2.27).

SECTION III

NUMERICAL RESULTS

3.1 Introduction

As mentioned in the beginning of Sections I and II, this work is an extension of Ref. 1. The zeroth order formulation described in Section II was implemented into a computer code, ILSAWR (acronym from Incompressible Lifting Surface Aerodynamics with Wake Roll-up). ILSAWR performs the iteration routine described in Subsection 2.4. The way the program is set up, the wake geometry is automatically generated, with each row of elements along the x-direction having equal lengths. The Kutta condition is satisfied by imposing that the first row of wake elements is tangent to the wing. The iteration scheme is performed for the rest of the rows only.

All numerical results presented here were obtained for rectangular planar lifting surfaces and all the graphs show results only for the semispan of the wings.

3.2 Parametric Analysis of the Effect of the Angle of Attack

A parametric analysis of the effect of the angle of attack on the wake roll-up is presented here. The case considered is a rectangular wing of aspect ratio AR = 8. This value was chosen because of existing results of Ref. 11 (see Section 3.3). Results are presented for three values of the angle of attack: $\alpha = 5°$, $10°$ and $15°$. The case $\alpha = 5°$ is presented in detail. In Figures 7a, b, c, and d, the converged wake pattern for a rectangular planform of aspect ratio AR = 8 at an angle of attack $\alpha = 5°$, with an element grid having NX = 4, NY = 10, with the length of the wake elements $\Delta x_W = .5c$ is plotted in great detail for 10 chord lengths behind the trailing edge. Figures 7a and 7b show the rolled-up wake plotted at stations 1 through 10 chord lengths behind the trailing edge. Figure 7c is a side view of the rolled-up wake (the vertical scale is enlarged), showing the vertical displacement of the streamlines. The numeration system for the streamlines is also shown, with streamline number 1 being at $y = 0$ and the last streamline starting at the wingtip. Figure 7d shows a top view of the rolled-up wake behind the wing, with the side displacement of the streamlines visible. The streamline numeration system is clearly shown here.

It may be noted that the analysis of convergence (presented in Appendix A) indicates that the solution is close to convergence, although improvements appear to be desirable at the trailing edge, especially near the wingtip.

Results for $\alpha = 5°$, $10°$ and $15°$ are presented in Figures 8 and 9, for a rectangular planform of aspect ratio AR = 8, with an element grid of NX = 4, NY = 10, $\Delta x_W = .5c$. Figure 8 shows the effect of the angle of attack on the wake roll-up, plotted at 5 chord lengths behind the trailing edge. The wake displacement becomes more pronounced as α increases from 5° to 10° and 15°. The effect of the angle of attack is shown also in Figure 9a, b and c, where streamlines 1, 10 and 11 are plotted in a side view.

The analysis of the convergence of the iteration scheme is presented in Appendix B.

3.3 Comparisons with Existing Results

In order to assess the validity of the method, a number of comparisons with existing results are presented here.

3.3.1 Comparison with the Artificial Viscosity Method of Bloom and Jen

Figure 10 presents the wake roll-up for a rectangular planform of aspect ratio AR = 8 at an angle of attack $\alpha = 6.25°$, for an element grid of NX = 4, NY = 10, with the wake elements length of $\Delta x_w = .5c$. Converged wake patterns are shown at stations 1, 5 and 9 chord lengths behind the trailing edge and the results of the present method are compared with the artificial viscosity results of Ref. 11. In Ref. 11, the lift coefficient was $C_L = 1$ and no angle of attack was specified. Therefore, the lift coefficient per unit angle of attack, $C_{L\alpha}$, was evaluated with the present method and the angle of attack was found according to

$$\alpha = \frac{C_L}{C_{L\alpha}} \tag{3.1}$$

The lift coefficient per unit angle of attack was found to be $C_{L\alpha} = 9.174$. For this value of the $C_{L\alpha}$, the value of the angle of attack which gives a lift coefficient of 1 is $\alpha = 6.25°$.

3.3.2 Comparison with the Experimental Results of Chigier and Corsiglia

In Ref. 8, the position of the vortex centerline is experimentally determined as the locations where the tangential velocity is zero. The results of Ref. 8 (Chigier and Corsiglia) have been obtained for a rectangular wing of aspect ratio AR = 6, at an angle of attack of $\alpha = 12°$. For the present method, there is (as yet) no precise way for determining the location of the vortex centerline. The last streamline is taken to represent the vortex centerline for the planform with an element grid of NX = 4, NY = 10 and $\Delta x_W = .5c$. Figure 11 results obtained with the present method, compared with the ones of Chigier and Corsiglia.

3.3.3 Comparison with Results of Shollenberger

As mentioned in Section I, Ref. 12 (Shollenberger) uses a three-dimensional potential method and an iteration procedure to obtain the rolled-up wake. The wing planform used has an aspect ratio AR = 6 and it is at an angle of attack $\alpha = 10°$. The results obtained with the present method, in comparison with the ones of Ref. 12, are shown in Figure 12. The wake geometries are plotted for 1, 2, 3 and 4 chord lengths behind the trailing edge.

3.4 Pressure Coefficient

In Subsection 2.6, the finite-difference procedure used in calculating the pressure coefficient was described in detail. The results obtained by using the linearized and nonlinear Bernoulli Equations with and without wake roll-up are presented here. Table I shows the values of Δc_p at $y = 0$, linear and nonlinear, with straight and rolled-up wakes. The results are obtained for a rectangular wing with aspect ratio AR = 8, at an angle of attack $\alpha = 5°$, with an element grid of NX = 7, NY = 7, with $\Delta x_w = .5c$. Figure 13 shows a plot of the pressure coefficient presented in Table I. Note the negligible effect of the wake roll-up on Δc_p. However, as previously mentioned, the wake roll-up is believed to have an important effect in the case of wing-tail interaction.

Finally, Figure 14 presents the potential distribution at the trailing edge of the wing, $\Delta\phi_{T.E.}$, for the same planform as the one used in Figure 13. It can be seen from Figure 14 that at $y = 0$, $\partial(\Delta\phi)/\partial\overline{y} = 0$. The effect of the wake roll-up is negligible.

x/c	Linearized Δc_p		Nonlinear Δc_p	
	Straight Wake	Rolled-up Wake	Straight Wake	Rolled-up Wake
.055	.8800	.8706	.8699	.8600
.136	.4523	.4530	.4471	.4470
.258	.2799	.2860	.2767	.2827
.421	.1921	.1921	.1899	.1899
.624	.1276	.1274	.1261	.1259
.868	.0732	.0729	.0723	.0720

Table 1. Pressure Coefficient at $y = 0$, for a rectangular wing planform of aspect ratio $AR = 8$, at angle of attack $\alpha = 5°$, with element grid of $NX = 7$, $NY = 7$ and $\Delta x_w = .5c$.

CONCLUDING REMARKS

A method for analyzing the wake roll-up has been described and numerical results have been presented. At this point, it might be interesting to quote Ashley and Rodden (Ref. 17) from their review on wing-body aerodynamic interaction: "It should be evident from the foregoing all too brief account of interaction theory that it is both a complicated subject and one in which computer automation is more nearly in a state of revolution than of evolution. Within a few years, programs should be available that will solve the linear potential equation, with boundary conditions satisfied by placing appropriate discrete singularity elements at a close approximation to all the true wing and body surfaces. The following 'nonlinearities' will be included: pressure velocity relations such as" the nonlinear Bernoulli Theorem; "boundary conditions that partially account for x - velocity perturbations...; wakes trailing streamwise from the actual positions of trailing edges; and/or estimates of self-deformation of wing wakes as they affect aft tail surfaces and the like."

All the nonlinearities mentioned above (with the exception of the wing-tail interaction and the zero-thickness limitations of lifting-surface theory) have been included in the present work. The only approximations introduced are numerical ones, and they are negligible, as the convergence analysis indicates.

Finally, the main innovations and advantages of the mehod are discussed. First, the method is based upon an exact (rather than discrete) formulation. Only numerical approximations are introduced (other methods use approximate physical models such as discrete vortices): this implies that the formulation is apt to refinements (first-order finite-element representation for D is now under investigation). Second, the wake is represented as doublet distribution: this implies that the method may be extended to steady and unsteady, subsonic and supersonic aerodynamics around complex configurations, in a relatively straightforward method, using the formulation of Ref. 18. Third, the convergence of the solution is exceptionally fast (as is the more general method of Ref. 18). Fourth, the method is relatively fast: the results for NX = 4, NY = 7, N_{wake} = 10 require 3 minutes of C.P.U. time per iteration on the I.B.M. 370/145 computer of Boston University. Finally, the convergence of the iteration scheme is already good, although considerable improvements can be obtained by using alternative, more sophisticated iteration schemes which are now under investigation.

Most of the theoretical results on wake roll-up are of a rather recent origin (from 1973 onward) and comparisons with experimental results show that some refinements of the mathematical model are still in order. Viscosity effects, thickness effects, aerodynamic interaction still remain to be accounted for.

REFERENCES

1. Morino, L., and Suciu, E.O., "A Finite-Element Method for Lifting Surfaces in Steady Incompressible Subsonic Flow", Boston University, College of Engineering, Department of Aerospace Engineering, TR-74-05, December, 1974.

2. Ashley, H., Widnall, S., and Landahl, M.T., "New Directions in Lifting Surface Theory", AIAA Journal, Vol. 3, No. 1, January 1965, pp. 3-16.

3. Landahl, M.T., and Stark, V.J.E., "Numerical Lifting-Surface Theory - Problems and Progress", AIAA Journal, Volume 6, No. 11, November 1968, pp. 2049-2060.

4. Jones, W.P., "The Calculation of Aerodynamic Derivative Coefficients for Wings of Any Plan Form in Non-Uniform Motion", R & M 2470, 1952, Aeronautical Research Council, Great Britain.

5. Haviland, J.K., "Downwash - Velocity Potential Method for Lifting Surfaces", AIAA Journal, Vol. 9, No. 11, November 1971, pp. 2268-2269.

6. Chigier, N.A., "Vortexes in Aircraft Wakes", Scientific American, Vol. 230, No. 3, pp. 76-83, March, 1974.

7. Tombach, I. "Observations of Atmospheric Effects on Vortex Wake Behavior", Journal of Aircraft, Vol. 10, No. 11, November 1973, pp. 641-646.

8. Chigier, N.A., and Corsiglia, V.R., "Wind-Tunnel Studies of Wing Wake Turbulence", Journal of Aircraft, Vol. 9, No. 12, December 1972, pp. 820-825.

9. Mason, W.H., and Marchman, J.F. III , "Far Field Structure of Aircraft Wake Turbulence", Journal of Aircraft, Vol. 10, No. 2, February 1973, pp. 86-92.

10. Chorin, A.J. and Bernard, P.S., "Discretization of a Vortex Sheet, with an Example of Roll-Up", Journal of Computational Physics, Vol. 13, 1973, pp. 423-429.

11. Bloom, A.M., and Jen, H., "On the Roll-Up of Aircraft Trailing Vortices Using Artificial Viscosity", Joint Institute for Acoustics and Flight Sciences, NASA Langley Research Center, Hampton, Va., 1973.

12. Shollenberger, C.A., "A Three-Dimensional Wing/Jet Interaction Analysis Including Jet Distortion Influences", McDonnell Douglas Research Laboratories St. Louis, Missouri, 63166, 1974.

13. Moore, D.W., "The Discrete Vortex Approximation of a Finite Vortex Sheet", AFOSR-1804-69, October, 1971.

14. Kandil, O.I., Mook, D.T., and Nayfeh, A.H., "Non-linear Prediction of the Aerodynamic Loads on Thin Lifting Surfaces", Dept. of Engineering Science and Applied Mechanics, Virginia Polytechnic Institute and State University, Blacksburg, Virginia, 1975.

15. Morino, L., "A General Theory of Unsteady Compressible Potential Aerodynamics", NASA CR-2464, December 1974.

16. Morino, L., "A Finite Element Formulation for Subsonic Flows Around Complex Configurations", Boston University, College of Engineering, TR-73-05, December 1973.

17. Ashley, H. and Rodden, W.P., "Wing-Body Aerodynamic Interaction", Annual Review of Fluid Mechanics, Vol. 4, 1972, pp. 431-472.

18. Morino, L., Chen, L.T. and Suciu, E.O., "Steady and Oscillatory Subsonic and Supersonic Aerodynamics around Complex Configurations", AIAA Journal, Vol. 13, No. 3, March 1975, pp. 368-375.

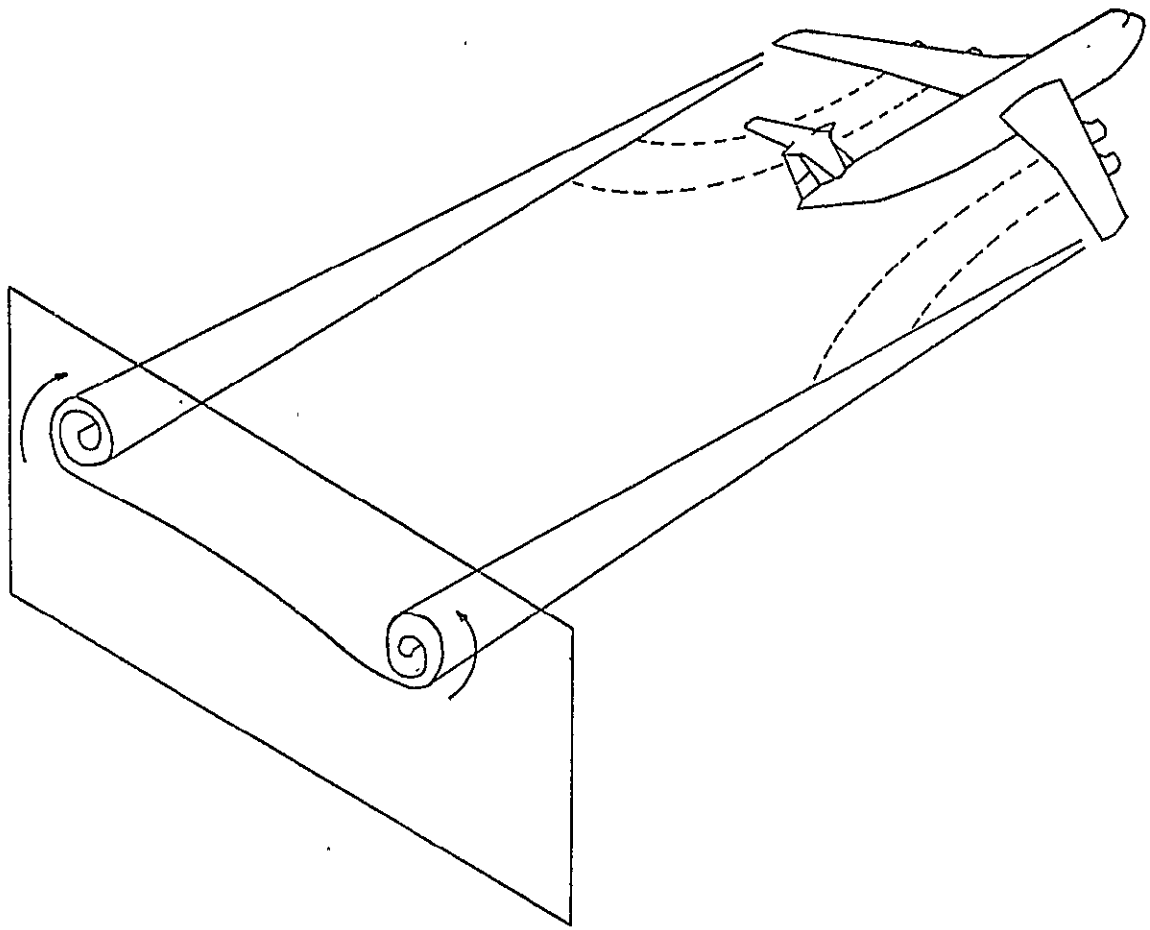

Figure 1. Formation of the Wing - Tip Vortices.

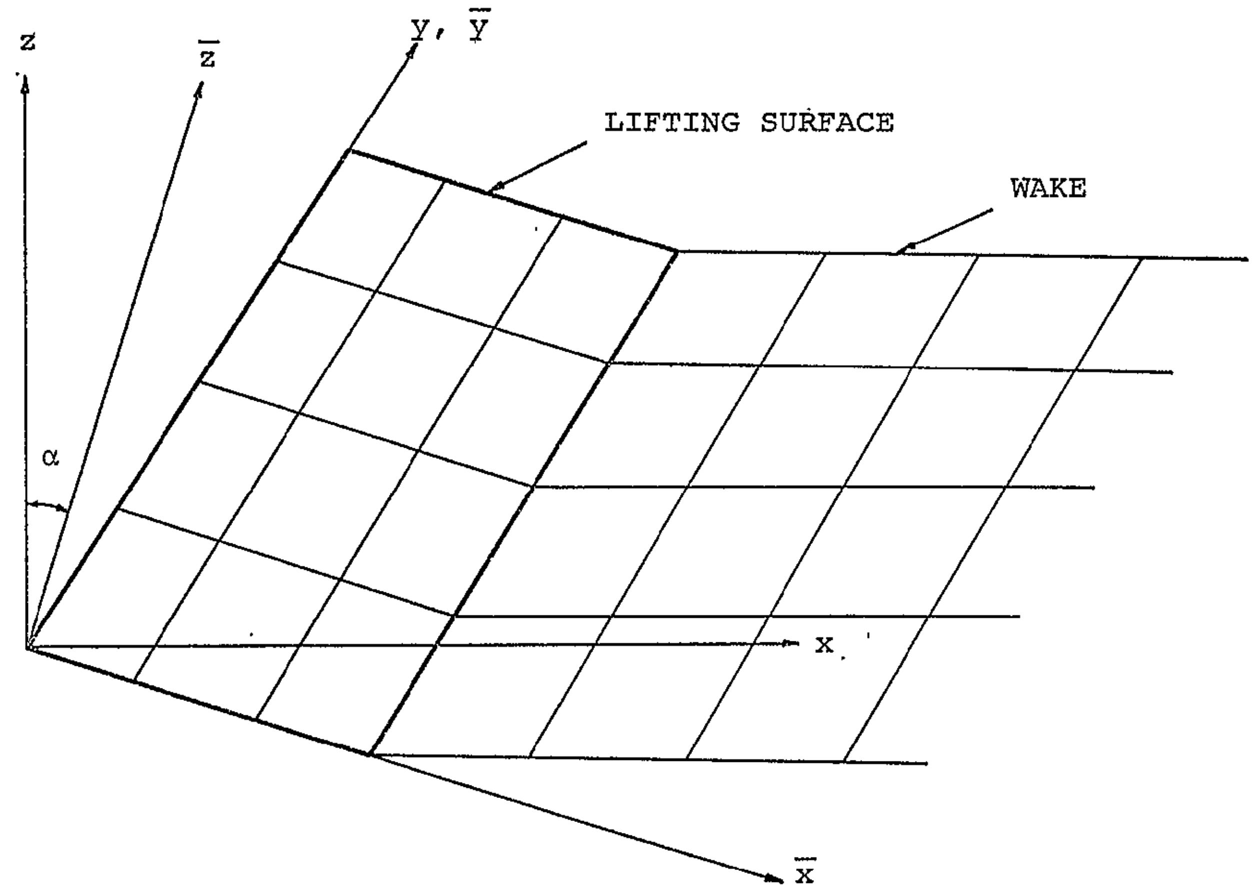

Figure 2. Lifting Surface and Wake Geometries.

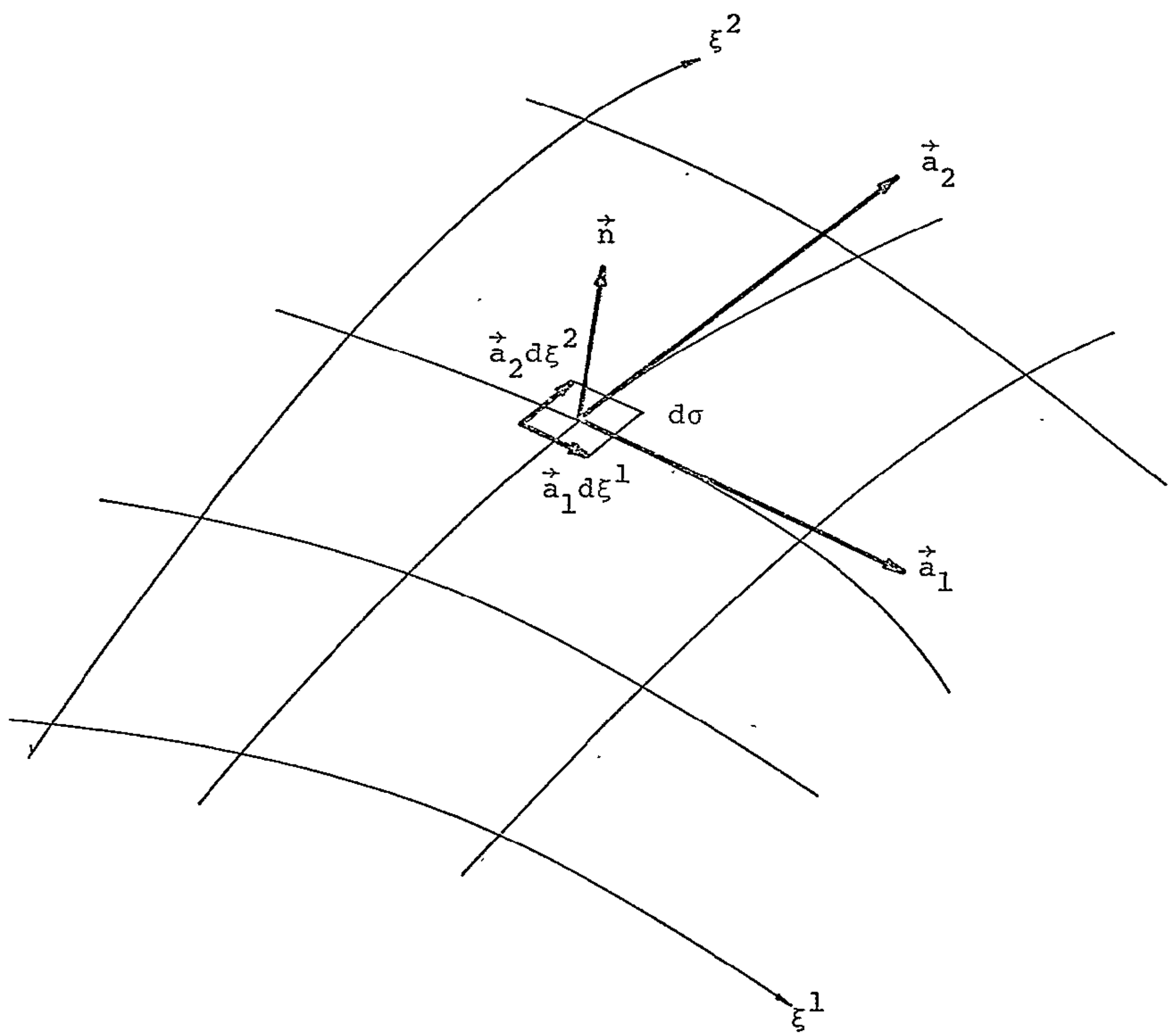

Figure 3. Surface ry.

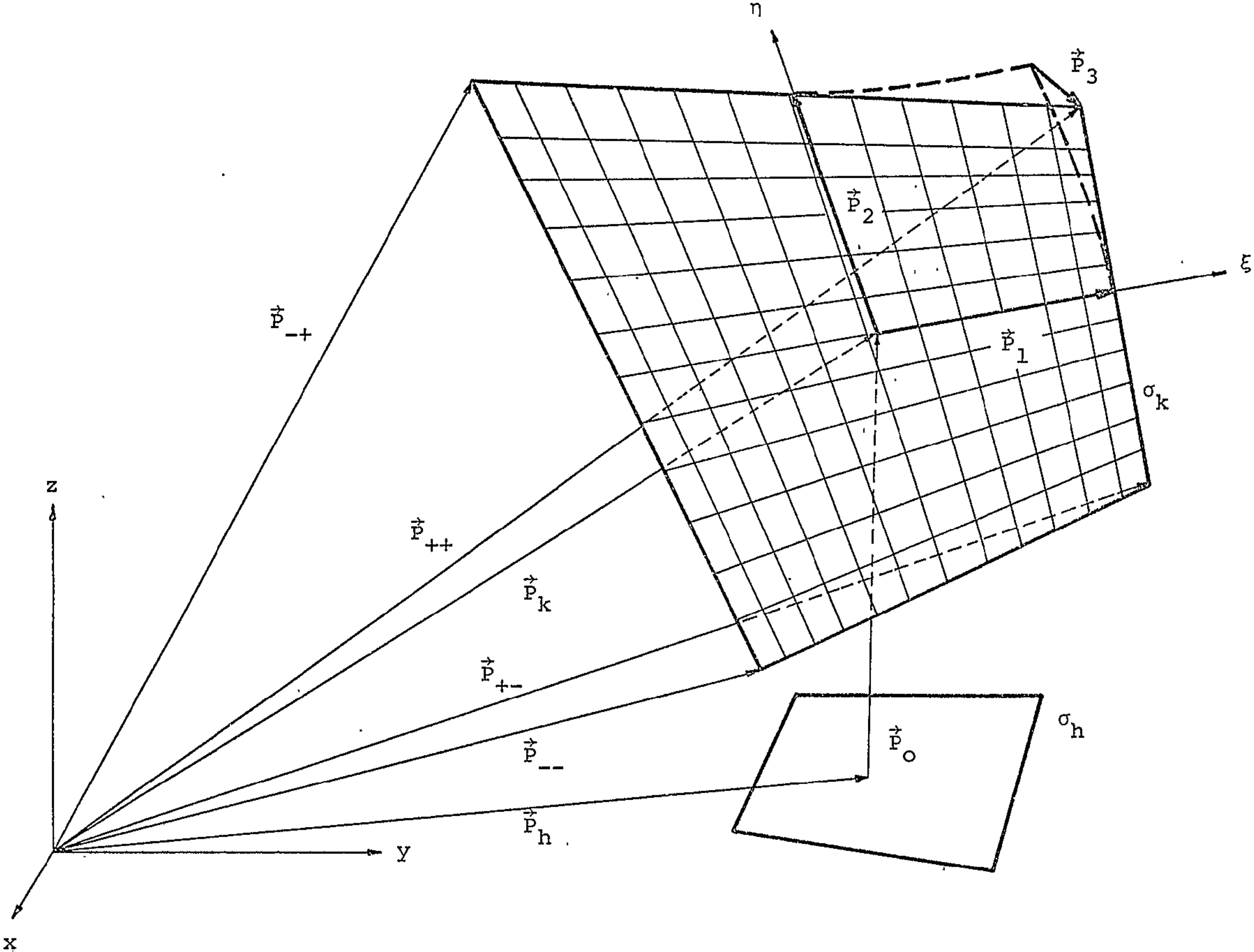

Figure 4. Hyperboloidal Quadrilateral Element.

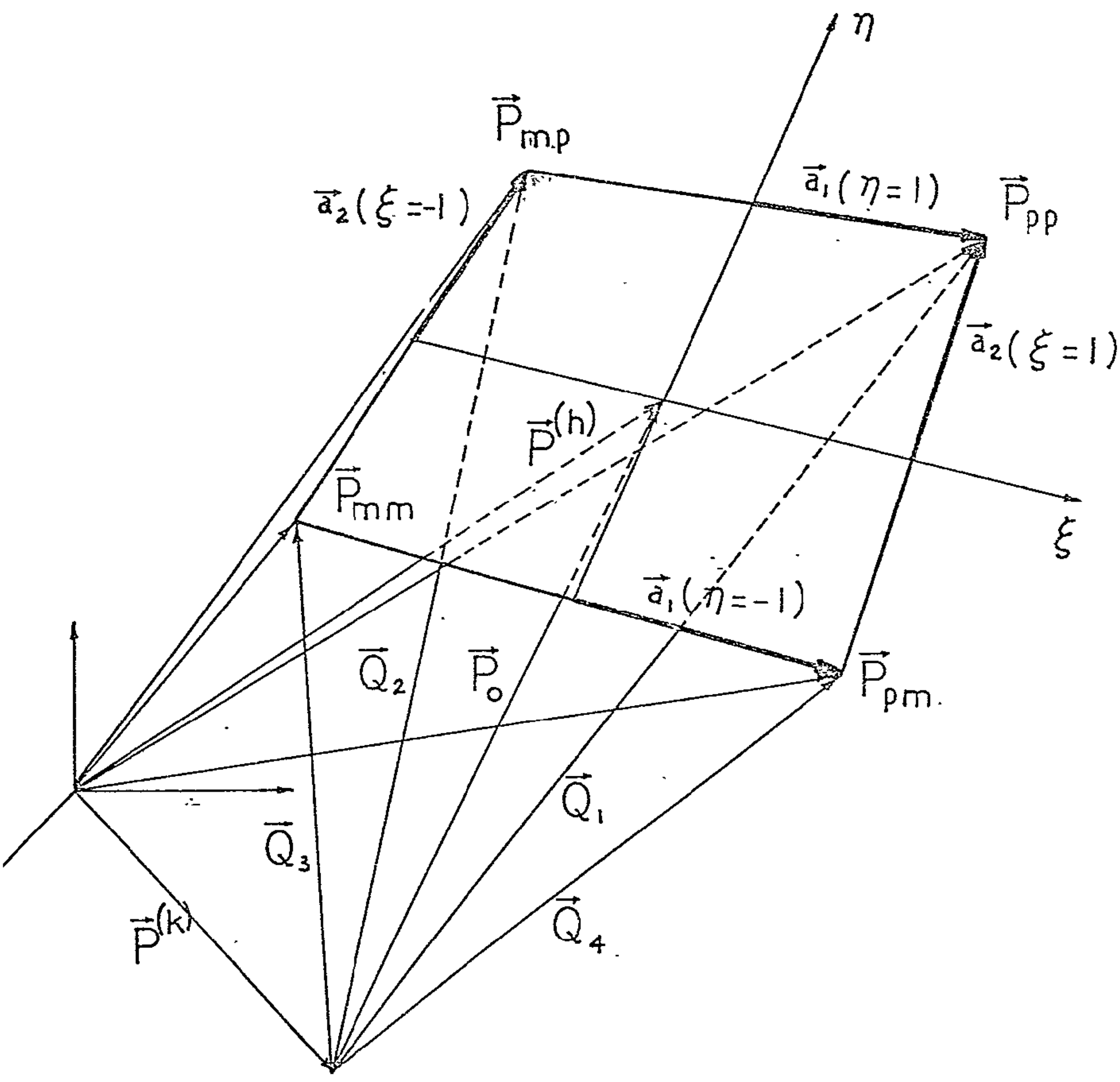

Figure 5. Hyperboloidal Element with Definition of Vectors $\vec{Q}_1$, $\vec{Q}_2$, $\vec{Q}_3$, $\vec{Q}_4$.

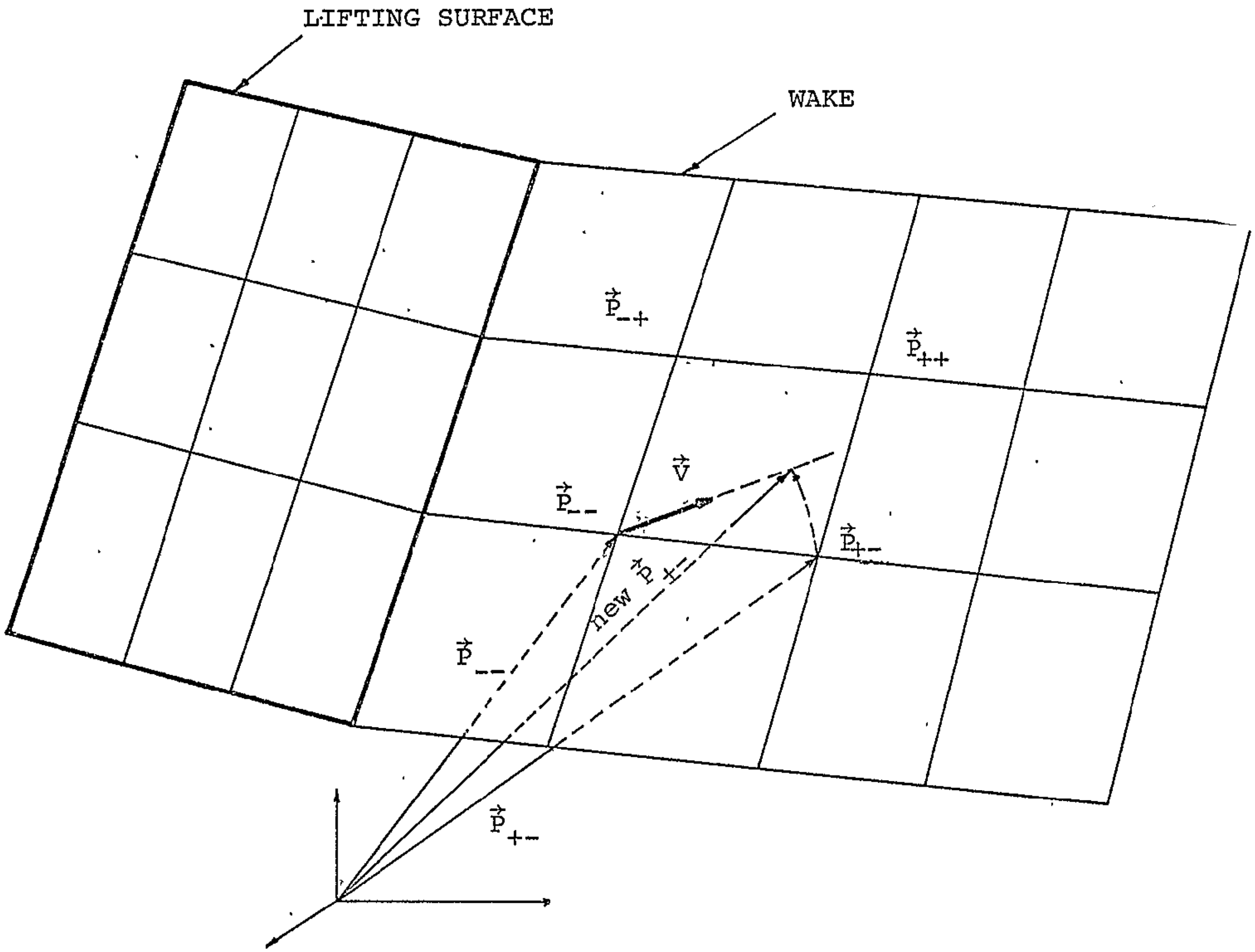

Figure 6. The process of Aligning the Streamlines with the Velocity $\vec{V}$ in a Typical Wake Surface Element.

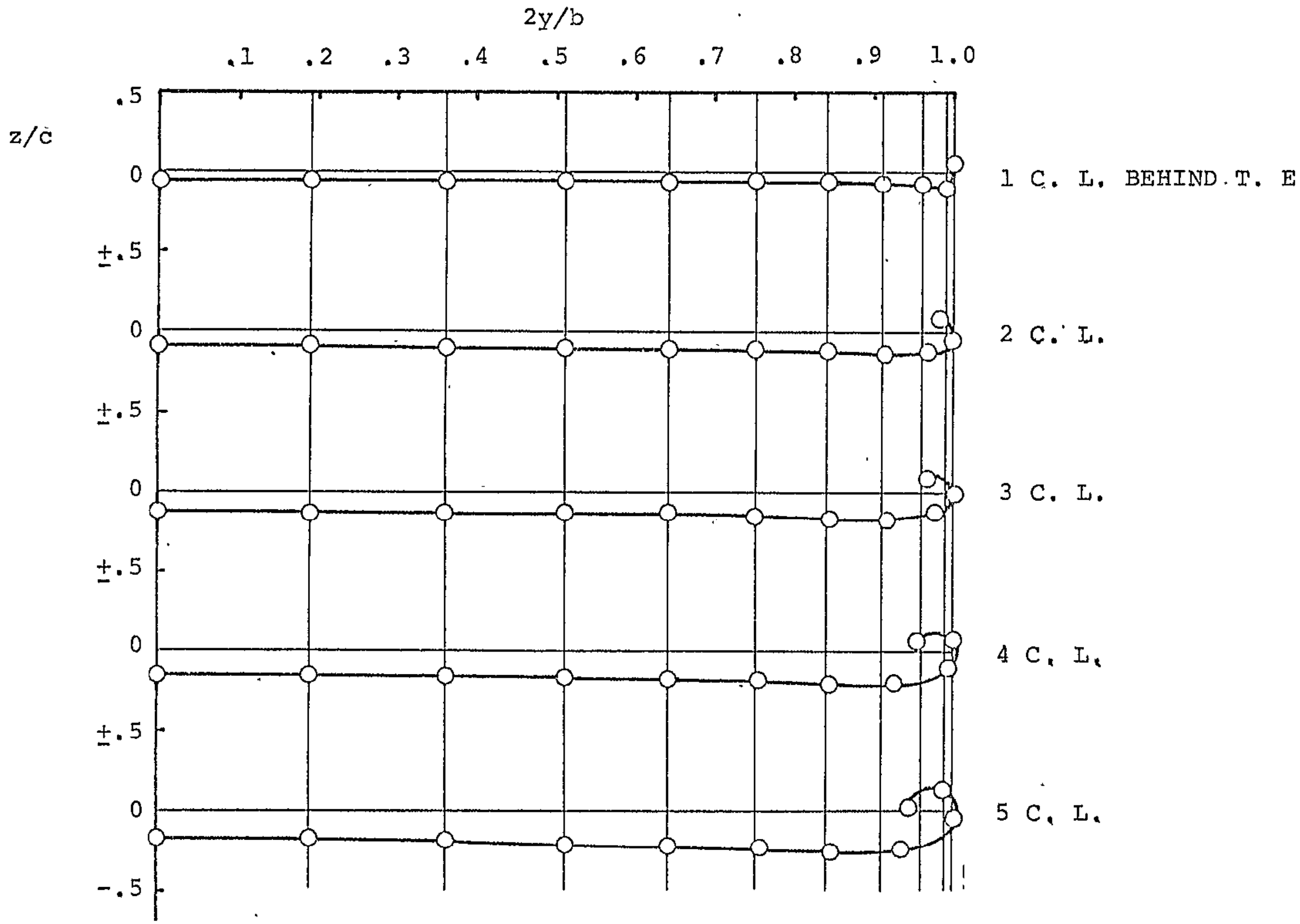

Figure 7a. Converged Wake Pattern for a Rectangular Wing Planform of AR = 8, with $\alpha = 5°$, Element Grid with NX = 4, NY = 10, Length of Wake Elements $\Delta x_w = .5c$, Plotted for 10 Chord Lengths Behind the Trailing Edge. Continued on Next Page.

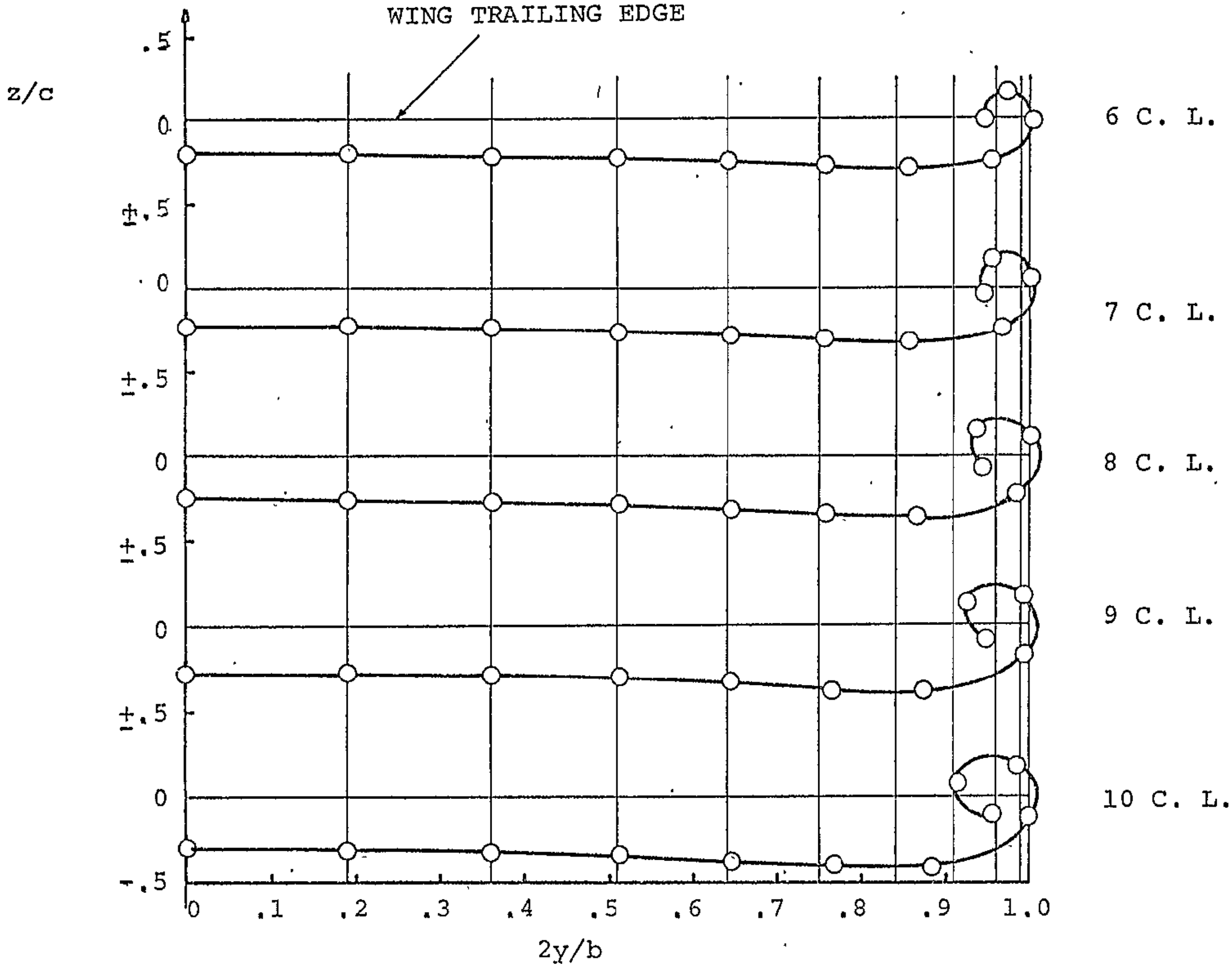

Figure 7b. Continuation of Figure 7a.

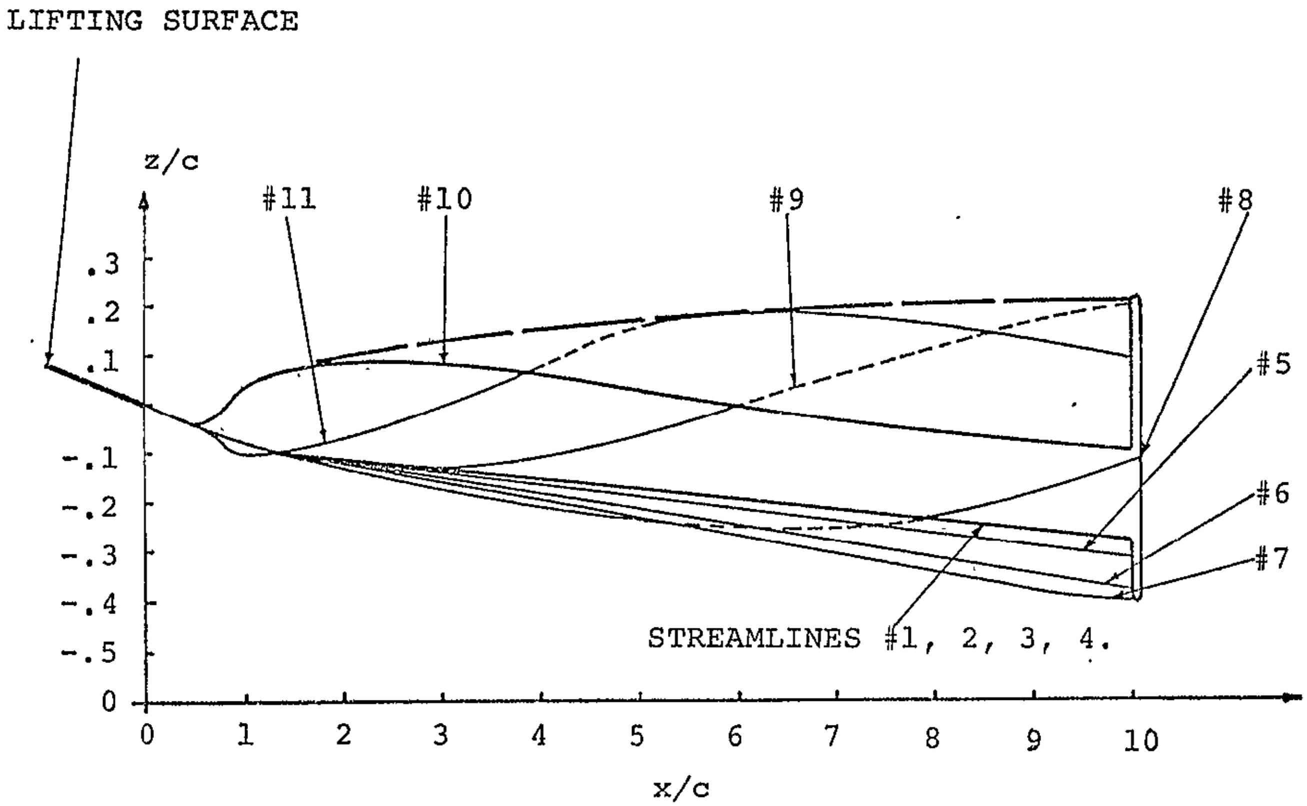

Figure 7c. Side View of the Rolled-up wake for the Wing of Figure 7a.

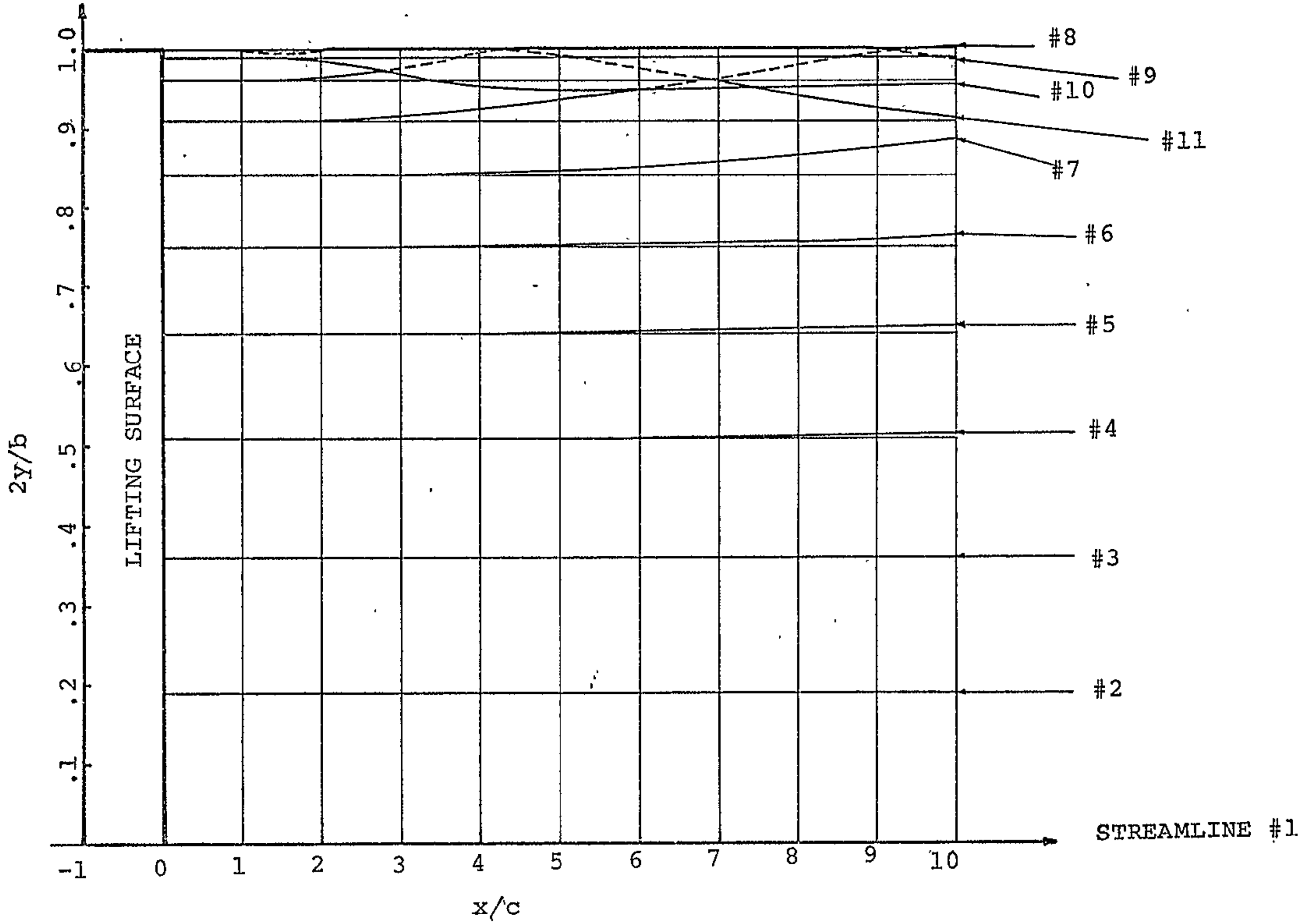

Figure 7d. Top View of the Rolled-up Wake for the Wing of Figure 7a.

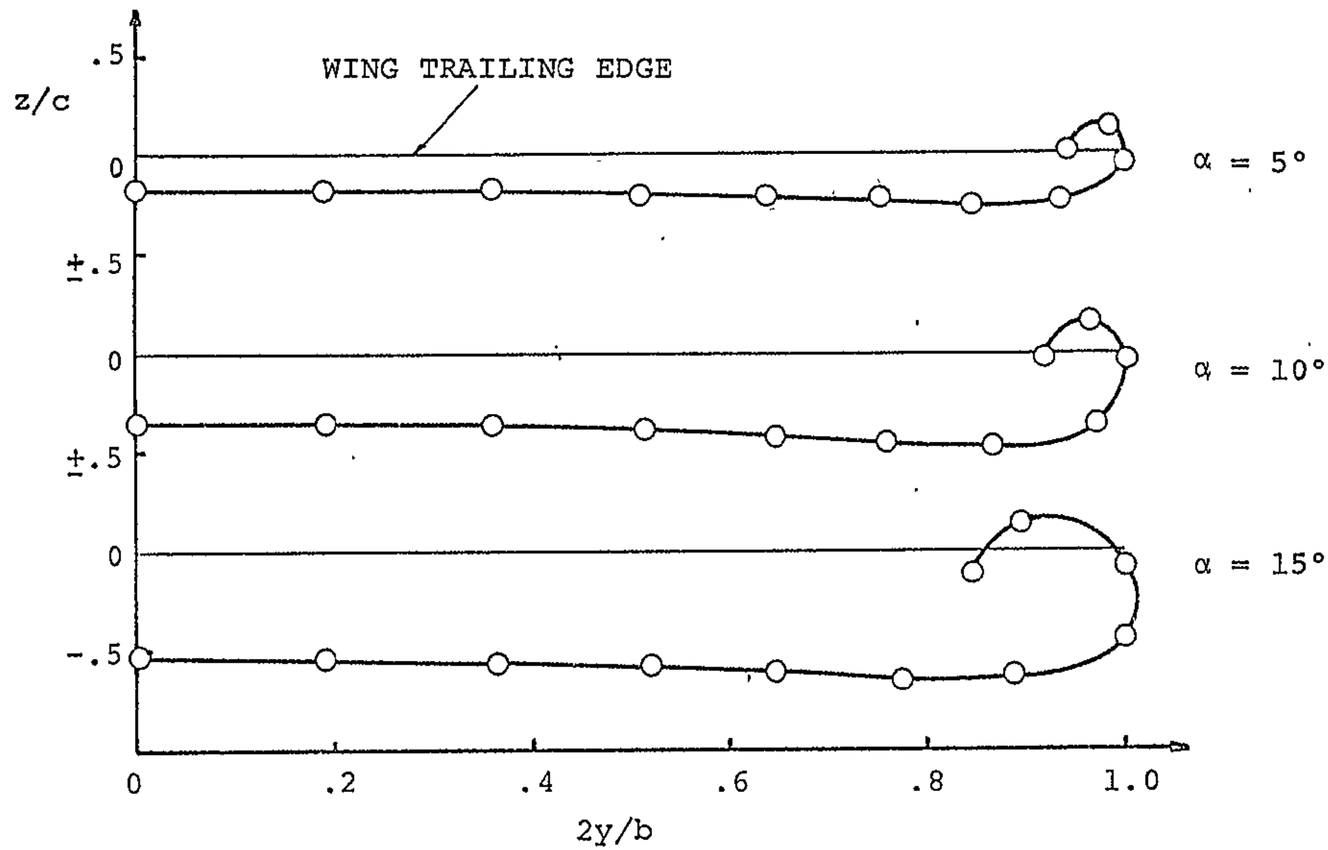

Figure 8. The Effect of the angle of attack, α, on the Wake Roll-up for a Rectangular Lifting Surface of AR = 8, Plotted at 5 Chord Lengths Behind the Trailing Edge. The Element Grid has NX = 4, NY = 10 and $\Delta x_w = .5c$.

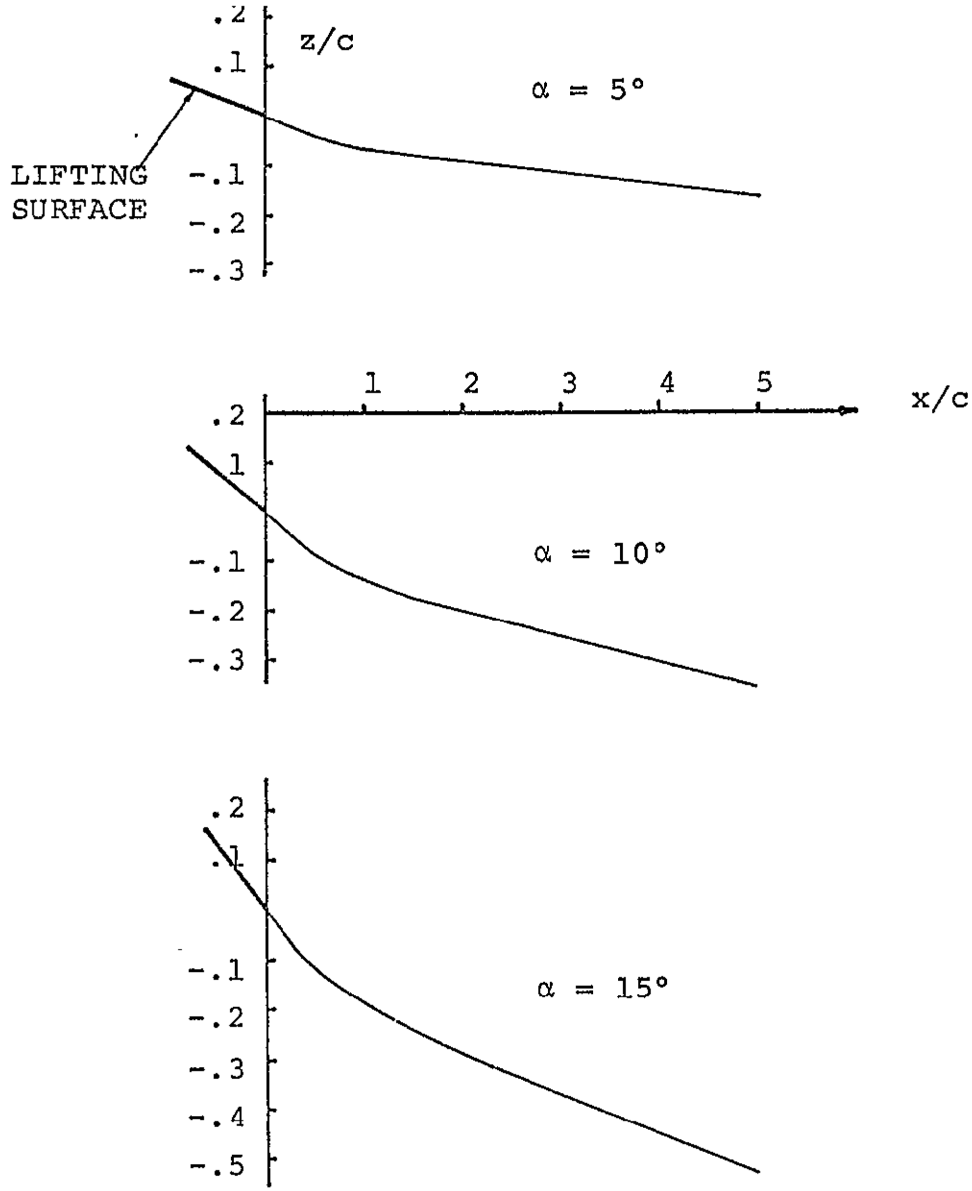

Figure 9a. Streamline #1 of a Rectangular Lifting Surface of AR = 8, with NX = 4, NY = 10, Δx_w = .5c, Plotted for Various Values of the Angle of Attack.

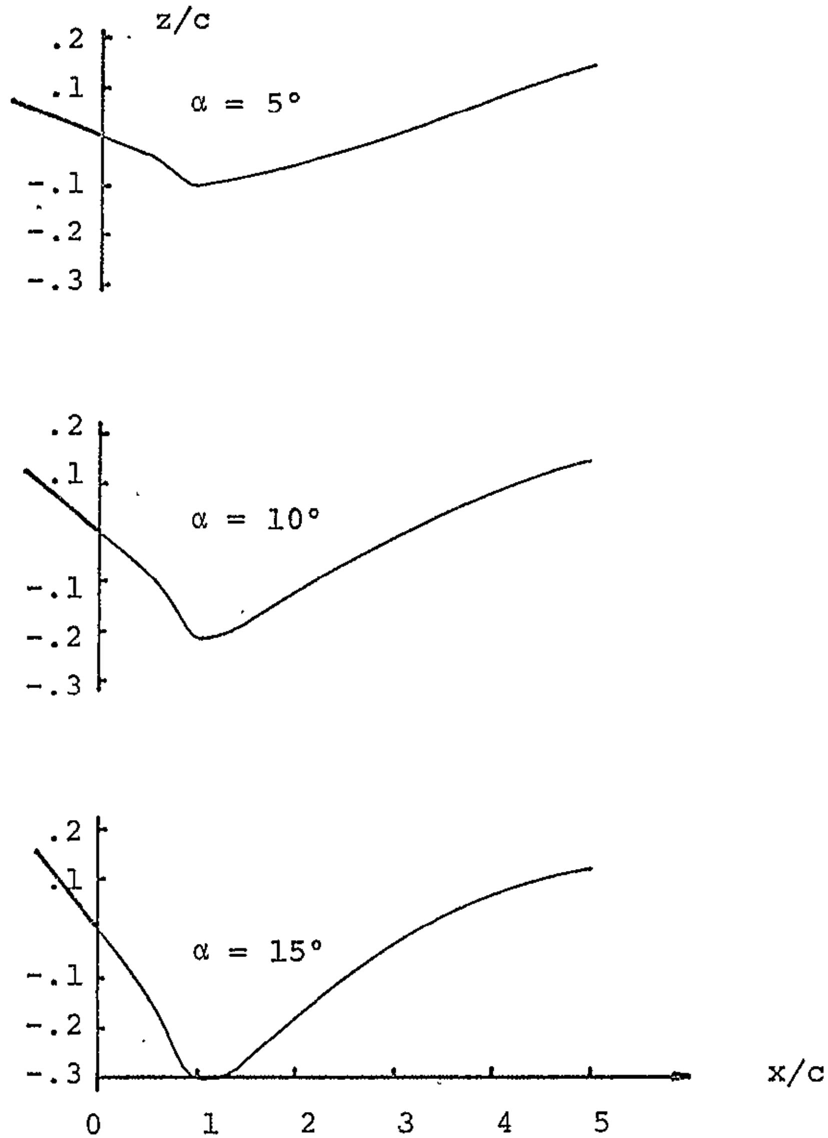

Figure 9b. Streamline #10 for the Planform of Figure 9a, Plotted for various Values of α.

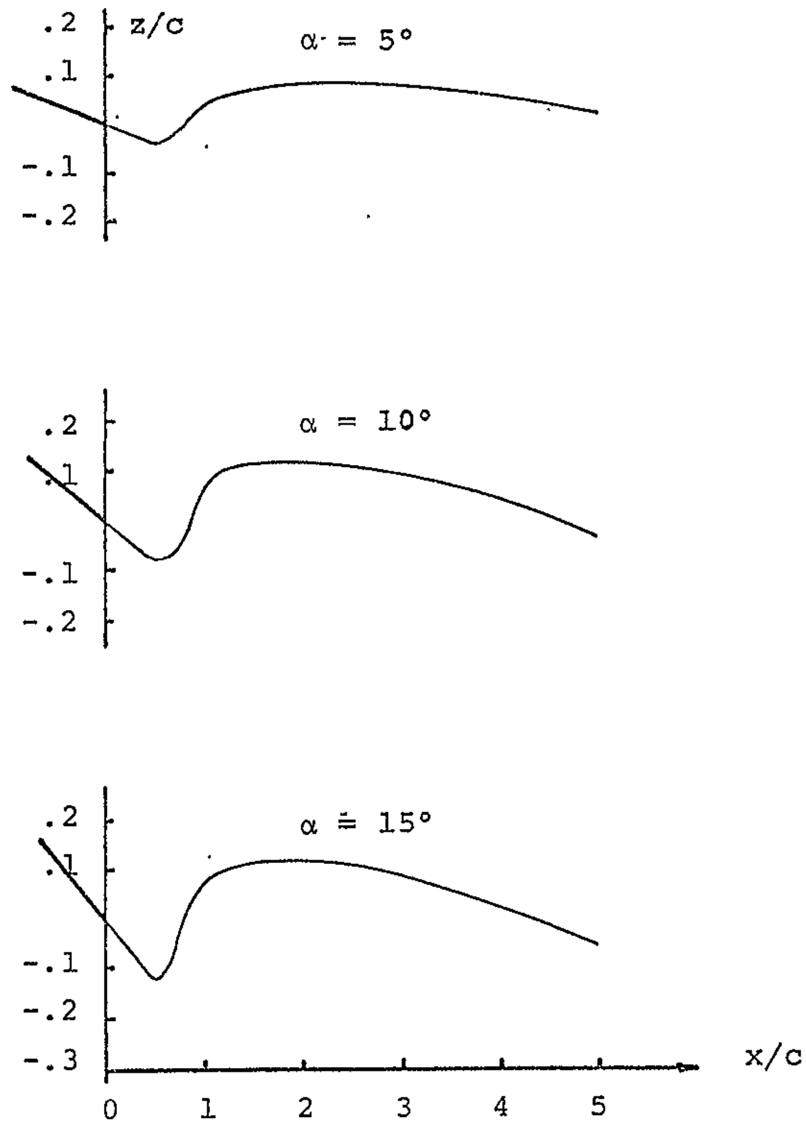

Figure 9c. Streamline #11 for the Planform of Figure 9a, Plotted for various values of α.

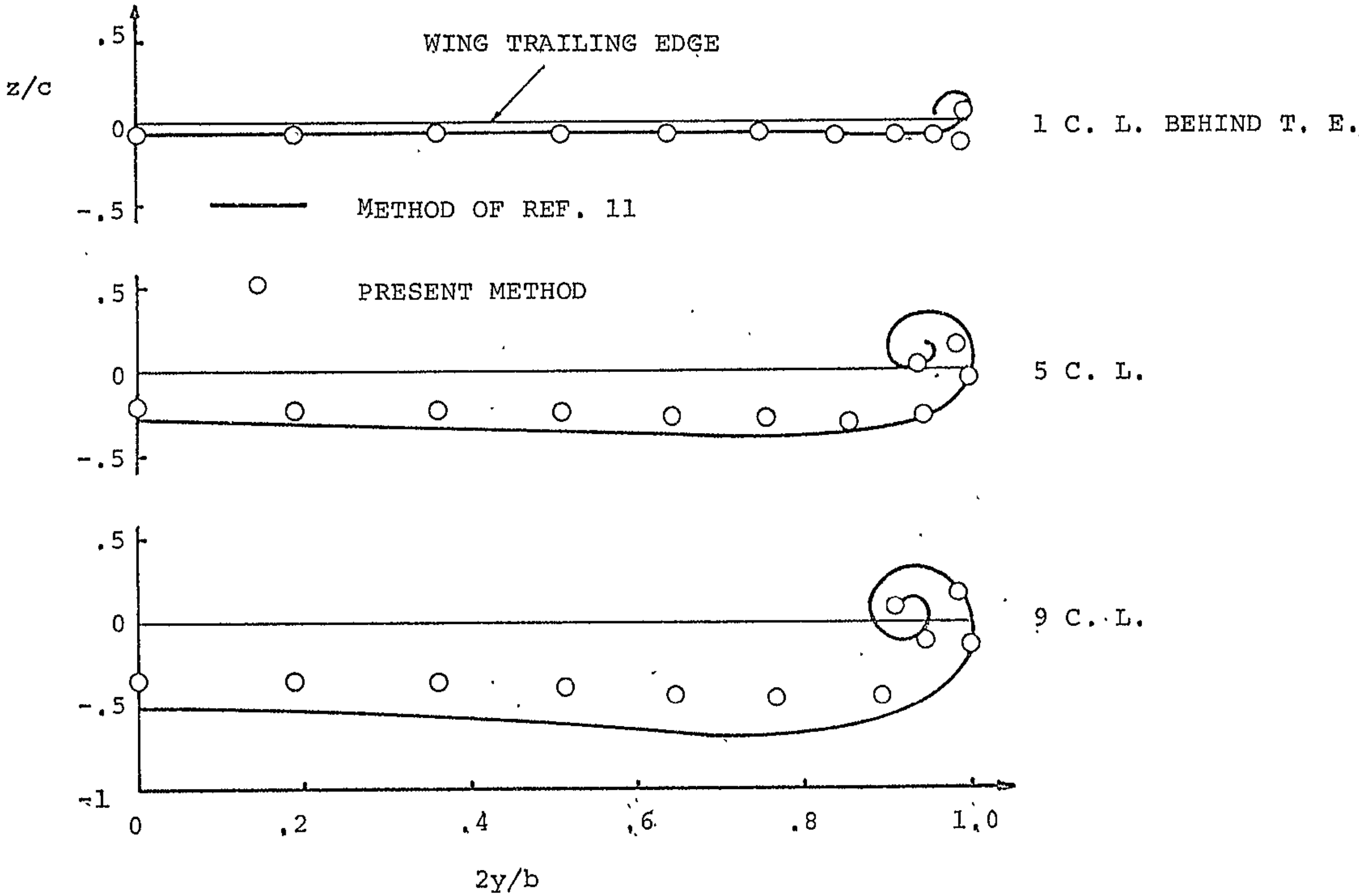

Figure 10. Wake Roll-up for a Rectangular Lifting Surface of AR = 8, Angle of Attack $\alpha = 6.25°$, Element Grid with NX = 4, NY = 10, $\Delta x_w = .5c$ and Comparison with the Results of Ref. 11.

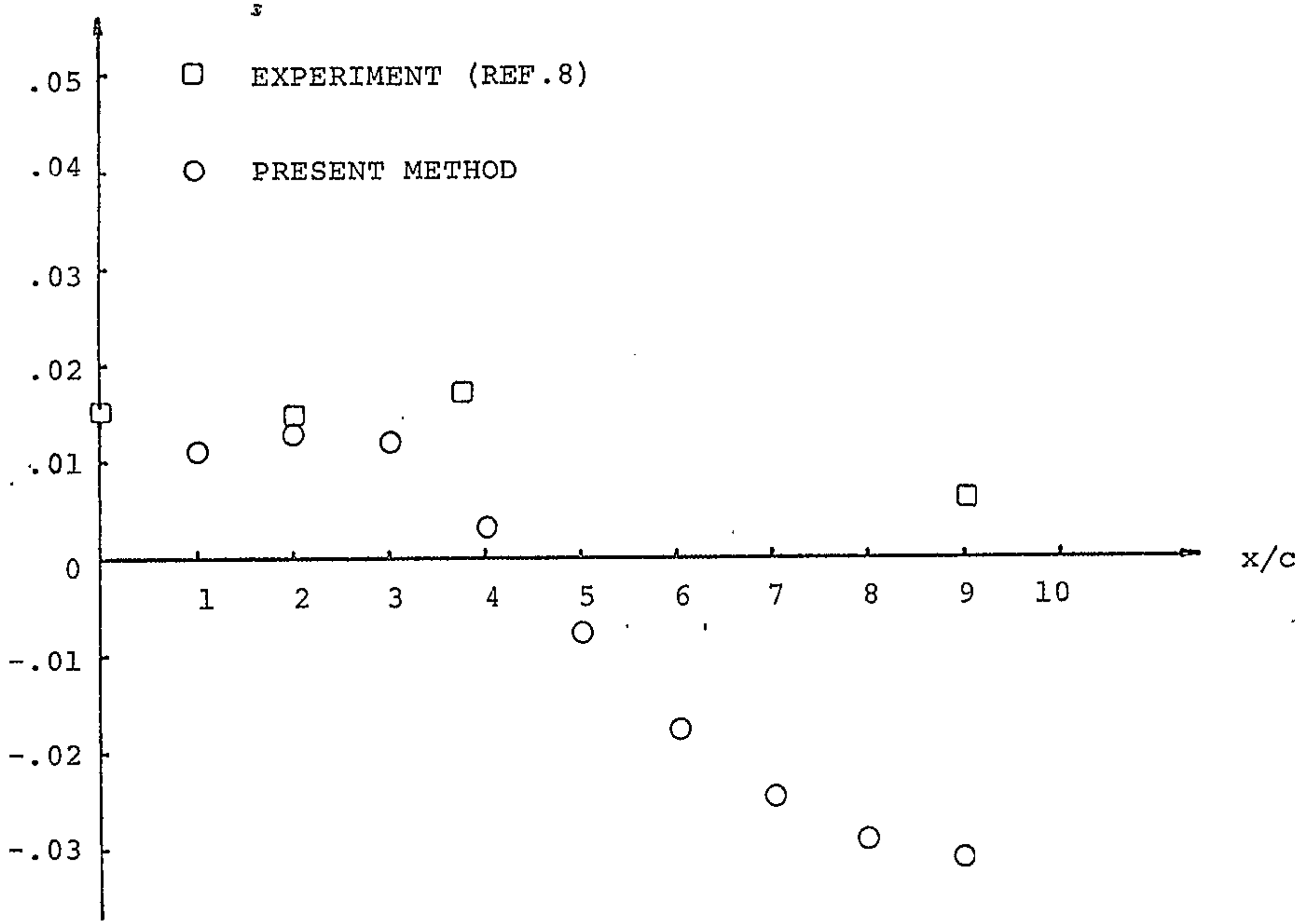

Figure 11. Location of the Vortex Centerline for a Rectangular Lifting Surface of AR = 8, for $\alpha = 12°$, Element Grid with NX = 4, NY = 10, $\Delta x_w = .5c$ and Comparison with the Result of Ref. 8.

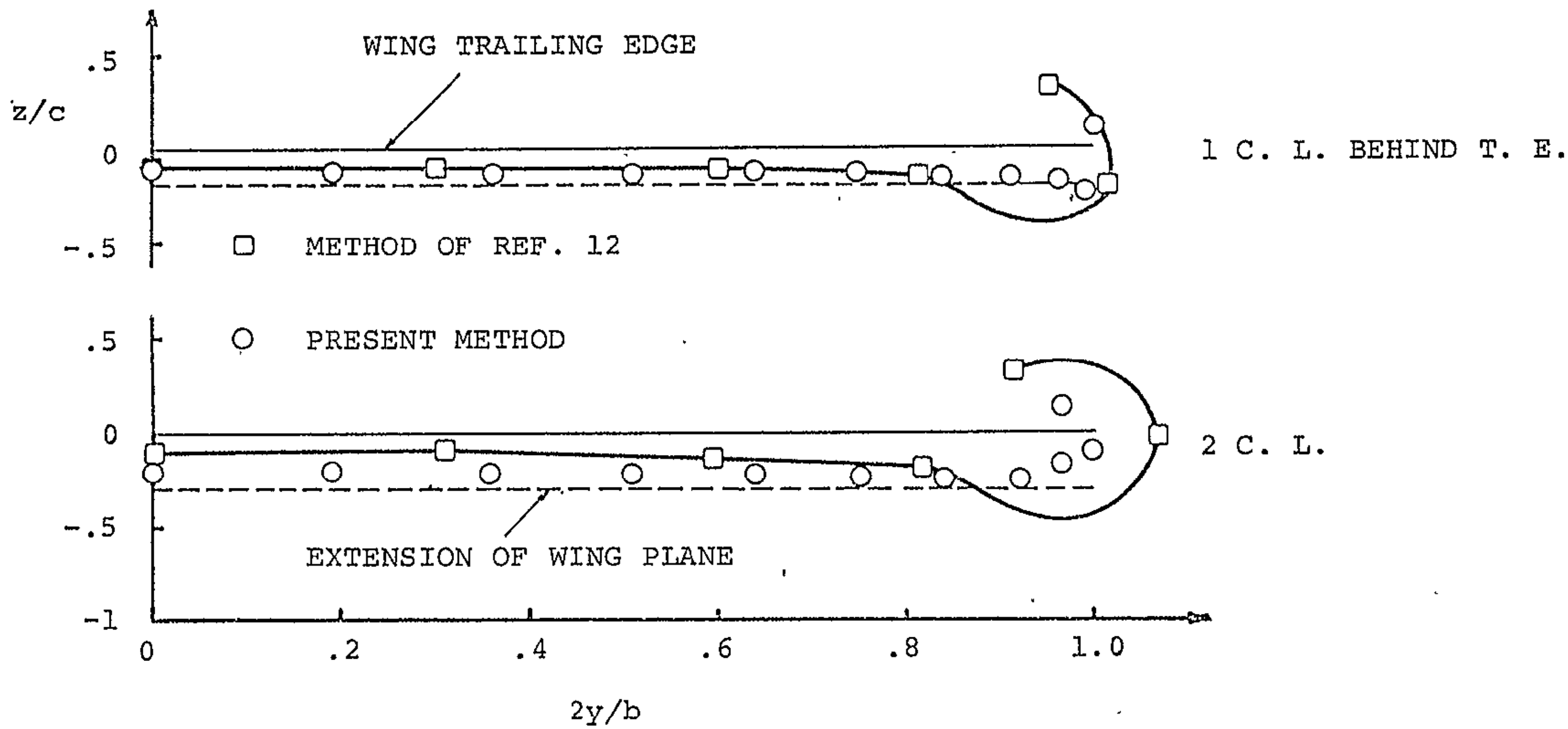

Figure 12. Wake Roll-up for a Rectangular Lifting Surface of AR = 8, at $\alpha = 5°$, with NX = 4, NY = 10, Length of Wake Elements $\Delta x_w = .5c$ and Comparison with Results of Ref. 12. Continued on Next Page.

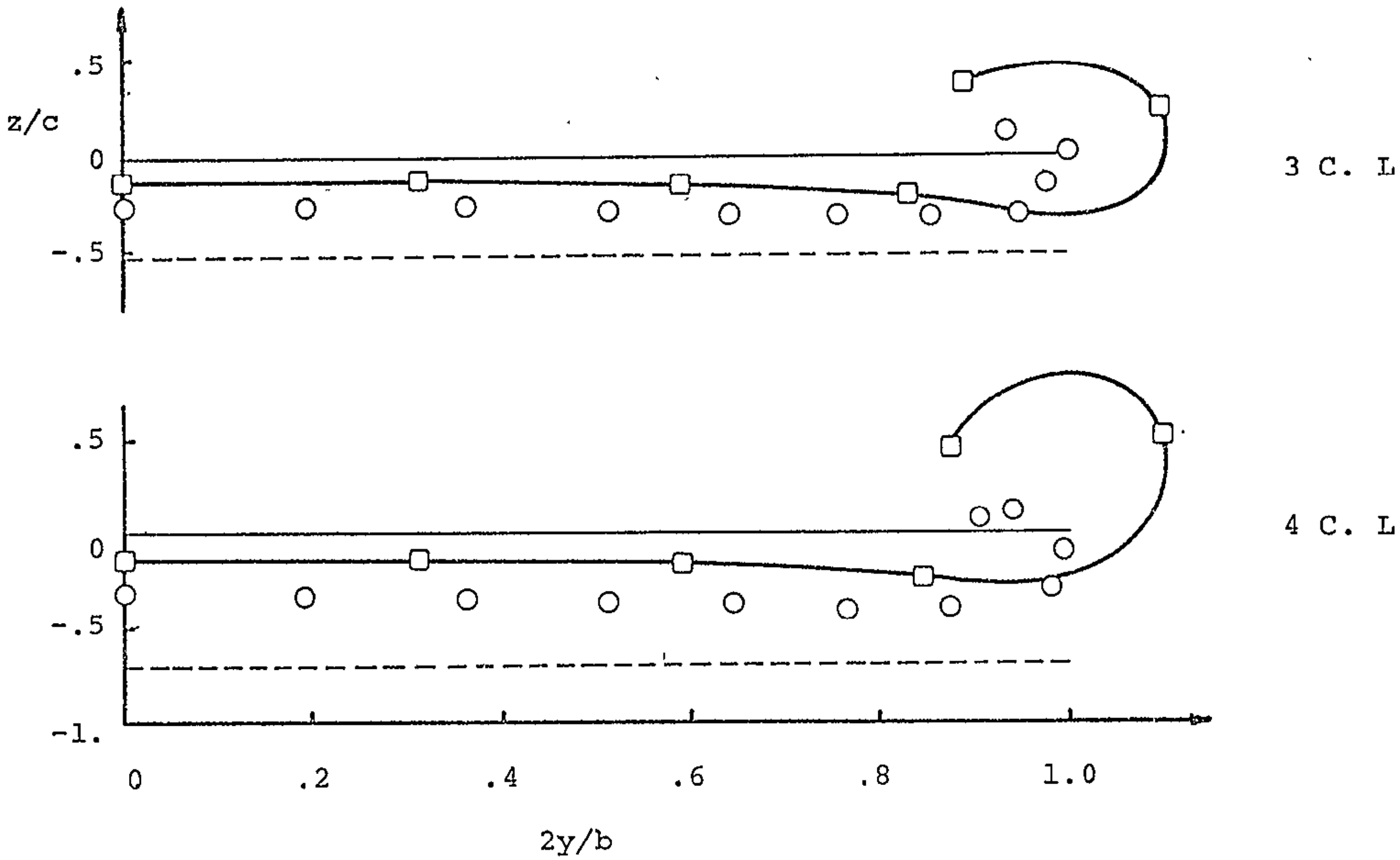

Figure 12, Continued.

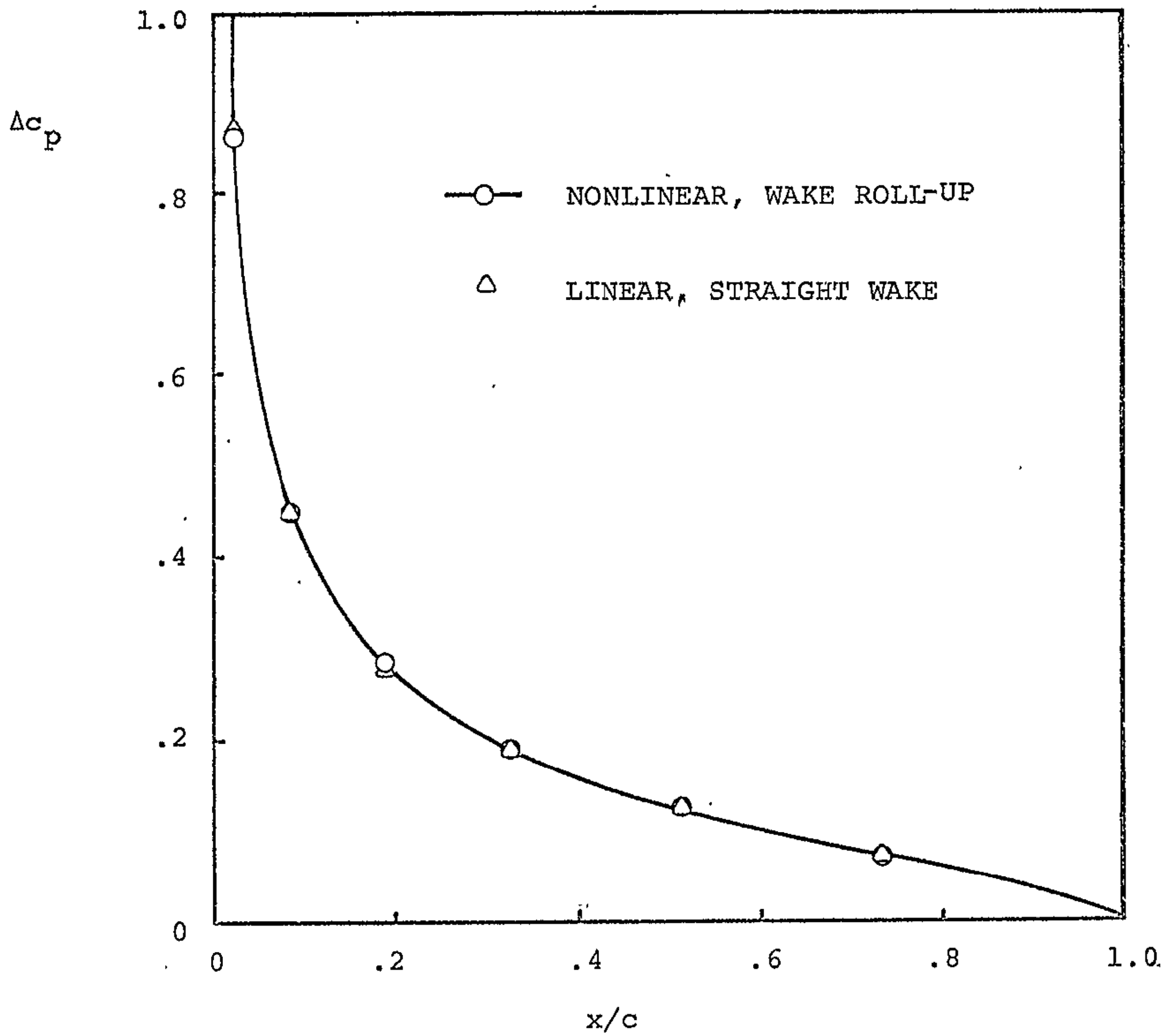

Figure 13. Nonlinear Section Pressure Coefficient at $y = 0$, for a Rectangular Planform of $AR = 8$, at $\alpha = 5°$, with $NX = 7$, $NY = 7$, $\Delta x_w = .5c$.

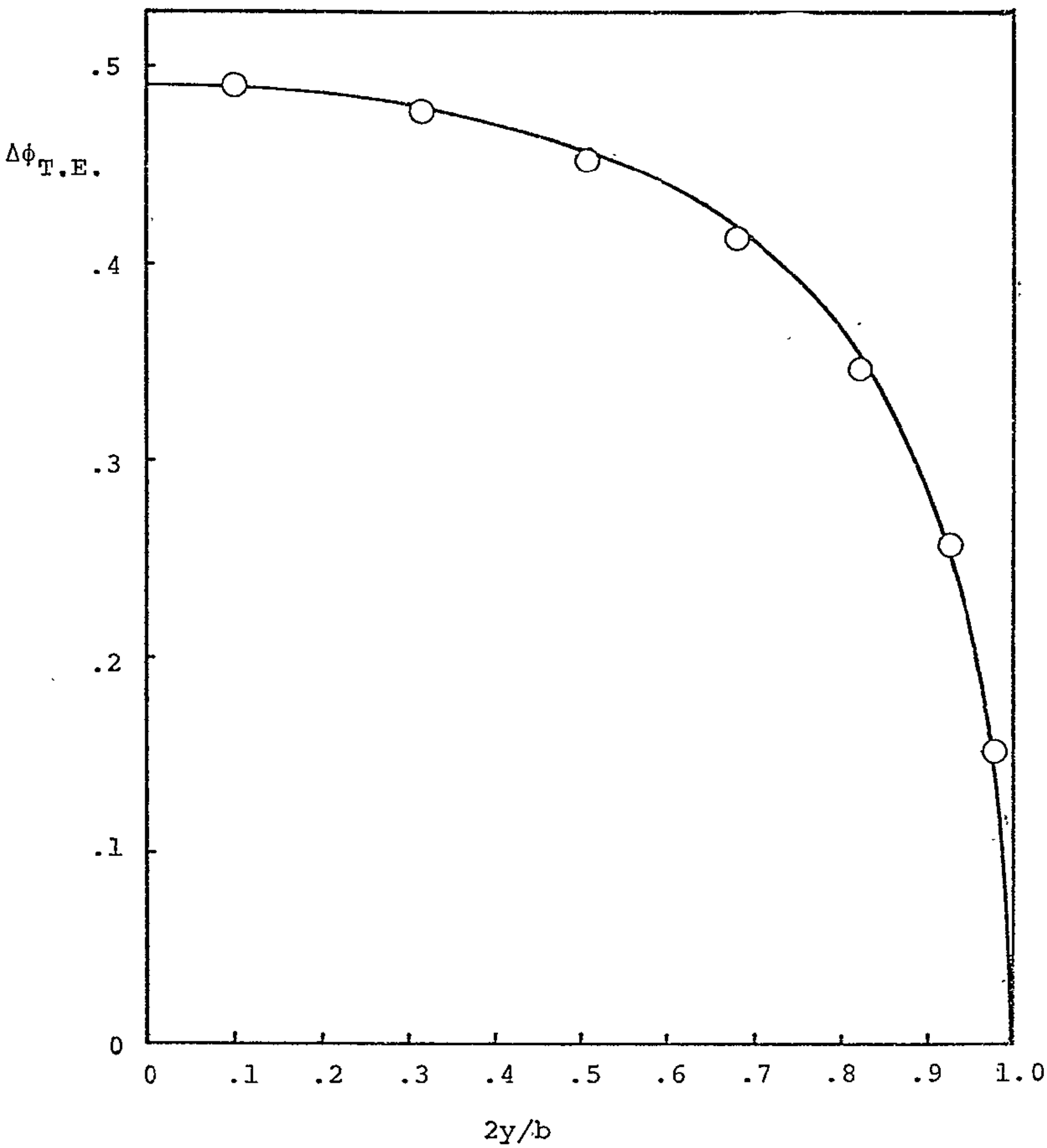

Figure 14. Potential Distribution at the Trailing Edge of a Rectangular Planform of AR = 8, with $\alpha = 5°$, NX = NY = 7 and $\Delta x_w = .5c$.

APPENDIX A

CONVERGENCE OF SOLUTION

In this Appendix, a numerical study is performed on the influence that the parameters NW (the number of wake elements along the x direction), Δx_w and NY have on the convergence of the solution. The only case presented here is relative to a rectangular wing planform of aspect ratio AR = 8 at $\alpha = 5°$.

In Figures A1a, b and c, the effect of the length of the wake elements on the wake roll-up is shown. The element grid for the planform has NX = 4 and NY = 10. The length of the wake elements Δx_w is allowed to vary from .5c to .75c and 1c. Rolled-up wake patterns are plotted for stations located at 3, 6 and 9 chord lengths behind the trailing edge. Note that, as Δx_w increases, the wake pattern becomes "larger", as it is easy to see from Figure A1. Note also that the difference between wake patterns for various values of Δx_w becomes smaller as the distance from the trailing edge increases. In Figure A2 one might find an explanation to this difference, as well as a suggestion for the improvement of the numerical model. In this figure, the same rectangular planform with an element grid of NX = 4, NY = 10 is used. The figure shows streamlines (counted from the line of symmetry of the wing, the mid-line included) numbers 1, 10 and 11, plotted for values of Δx_w of .5c, .75c, and 1c, for 10 chord lengths.

The first streamline shows remarkable closeness (on this enlarged vertical scale) for the various Δx_w. The difference increases as we approach the wing-tip streamlines. Note that the streamlines are approximately parallel; the difference between them is due to the fact that, by imposing the Kutta condition, the first row of wake elements lies in the same plane as the wing, and since Δx_w varies, the streamlines will start at .5c, .75c, and 1c behind the trailing edge. Also, the downwash is larger in the vicinity of the trailing edge and decreases as we move farther behind. Therefore, the wake slopes can be expected to be larger in the vicinity of the trailing edge. Note the sharp jump between the first element and the next in streamline number 11. It may be worth noting that, since the streamline displacement is obviously influenced by the length of the wake elements, we might obtain a smoother profile in the vicinity of the trailing edge by using smaller elements in this region, for one or two chord lengths. This remains to be implemented.

Next, consider the influence of NW. If the number of wake elements is increased, it is observed that the newly added rows of elements have no effect whatever on the wake roll-up of the previous ones.

The effect of the number of wake strips on the wake roll-up is shown in Figure A3, for the rectangular wing having an element grid of NX = 4, with NY varying between 7 and 10,

$\Delta x_w = .5c$ and NW = 11. All cases are converged and lie practically on the same line.

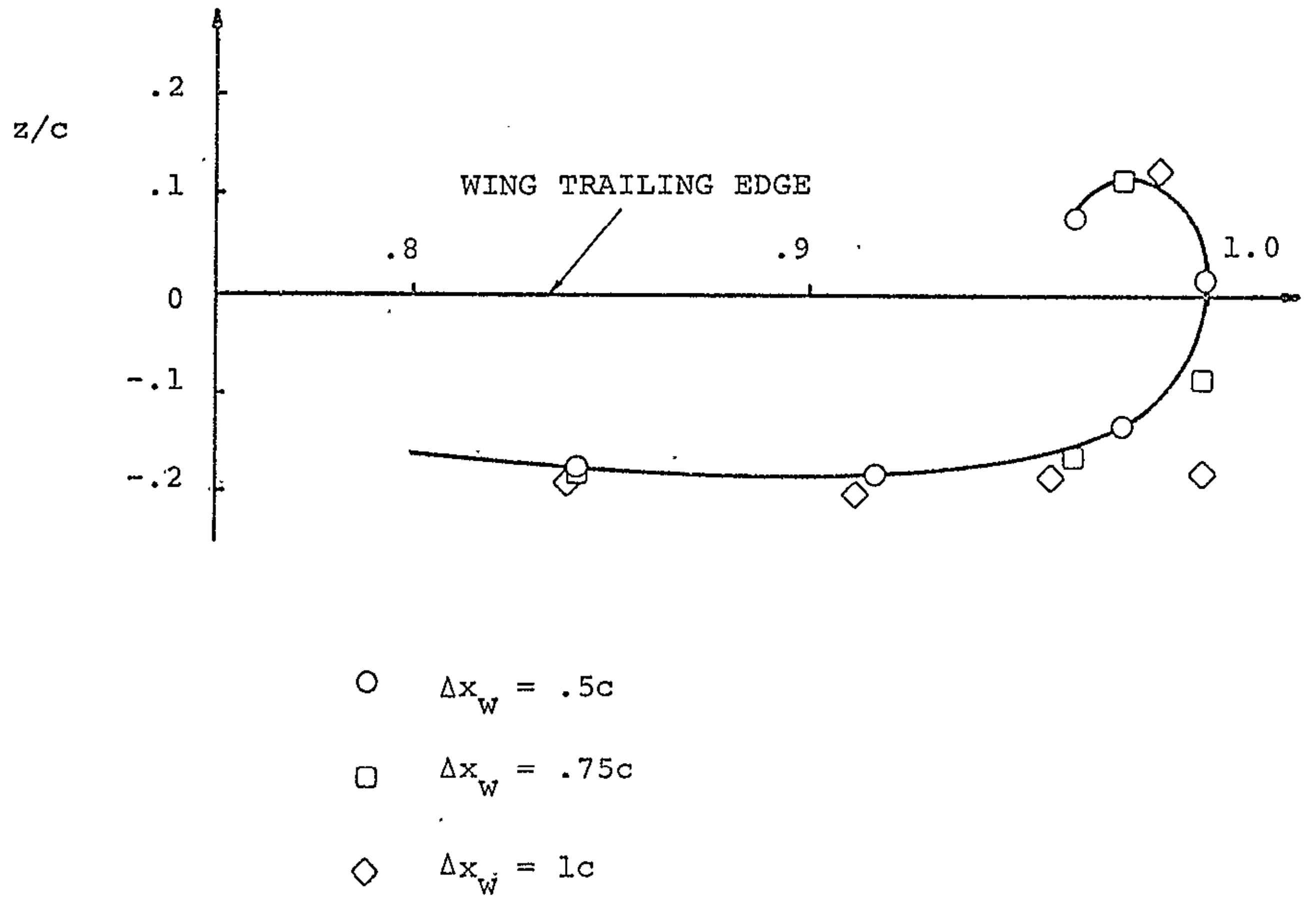

Figure A1a. Influence of the Length of the Wake Elements Δx_w on the Rolled-up Wake for a Rectangular Wing of AR = 8, for $\alpha = 5°$, at a Station Situated 3 Chord Lengths Behind the Trailing Edge. The Element Grid has NX = 4, NY = 10.

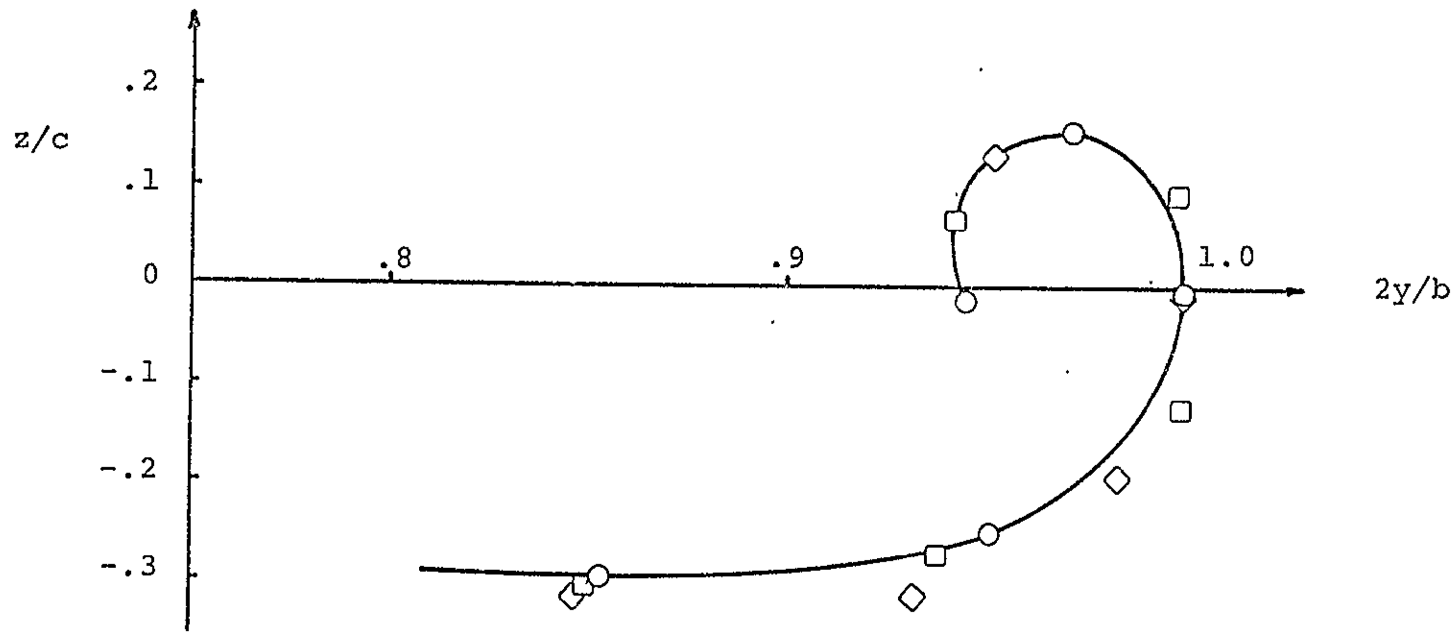

Figure A1b. Influence of the Length of the Wake Elements Δx_w on the Rolled-up Wake for the Wing of Figure A1a, at a Station Situated 6 Chord Lengths Behind the Trailing Edge.

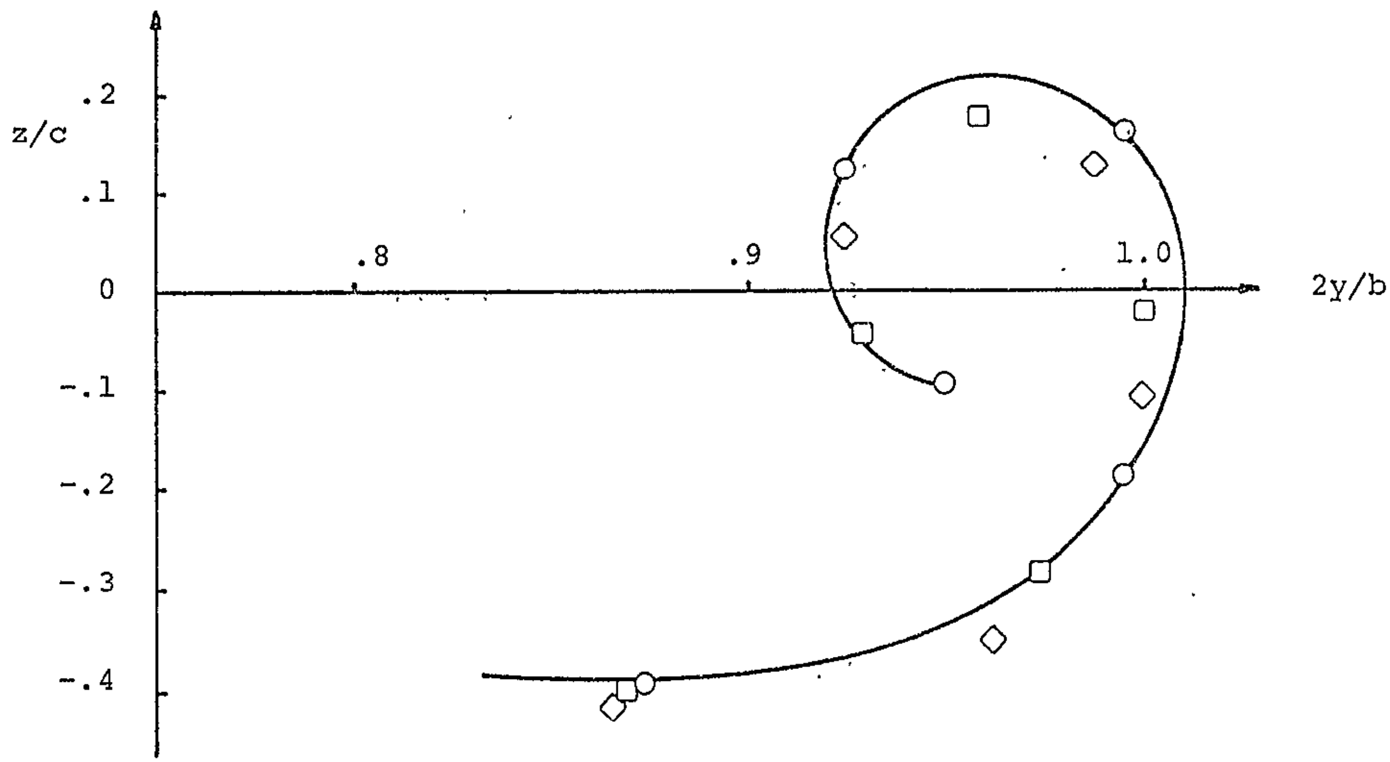

Figure A1c. Influence of the Length of the Wake Elements Δx_w on the Rolled-up Wake for the Wing of Figure A1a, Plotted at a Station Situated 9 Chord Lengths Behind the Trailing Edge.

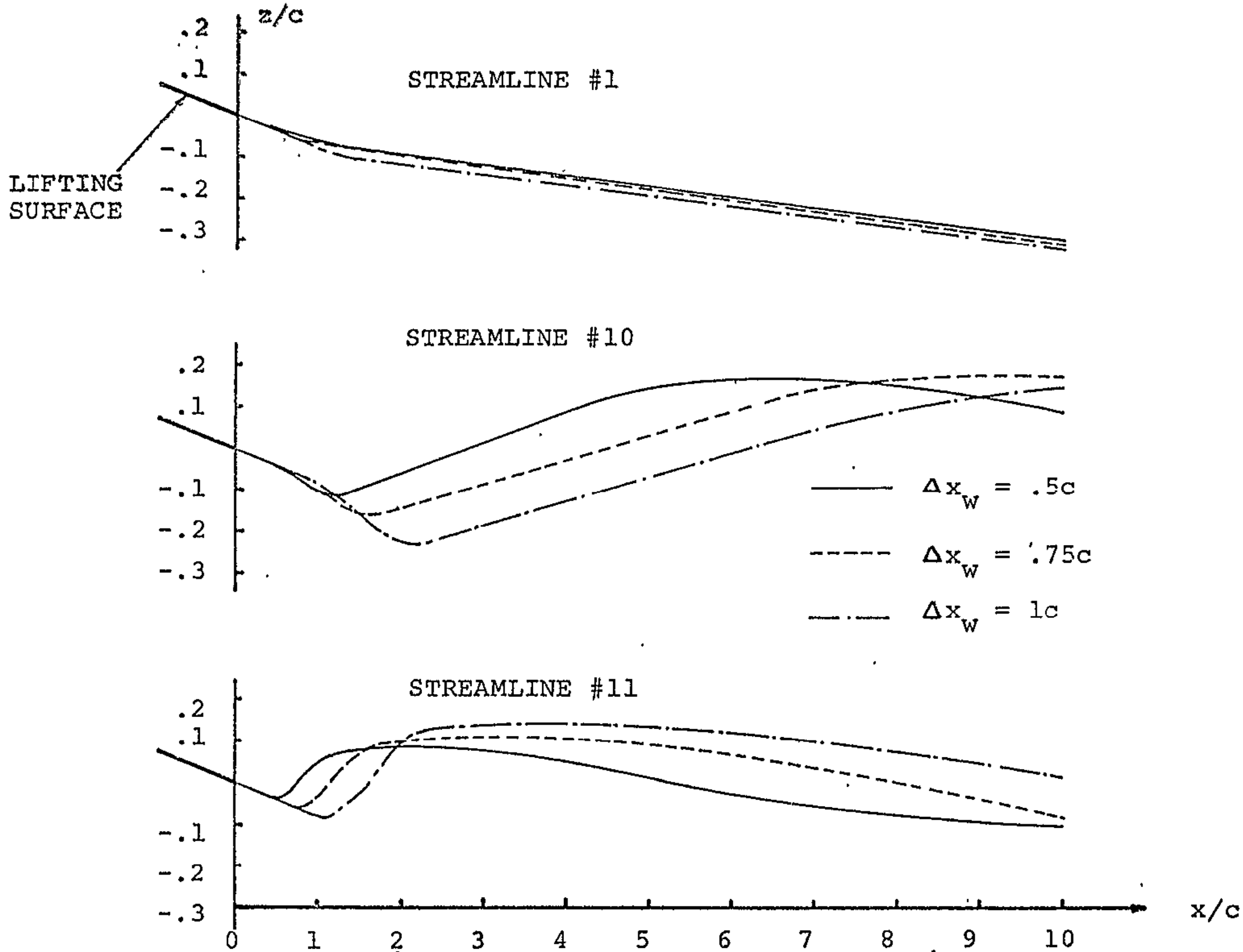

Figure A2, Influence of the Length of the Wake Elements Δx_W on the Wake Roll-up for a Wing of AR = 8, with $\alpha = 5°$, NX = 4, NY = 10. Plotted are the Streamlines #1, 10 and 11.

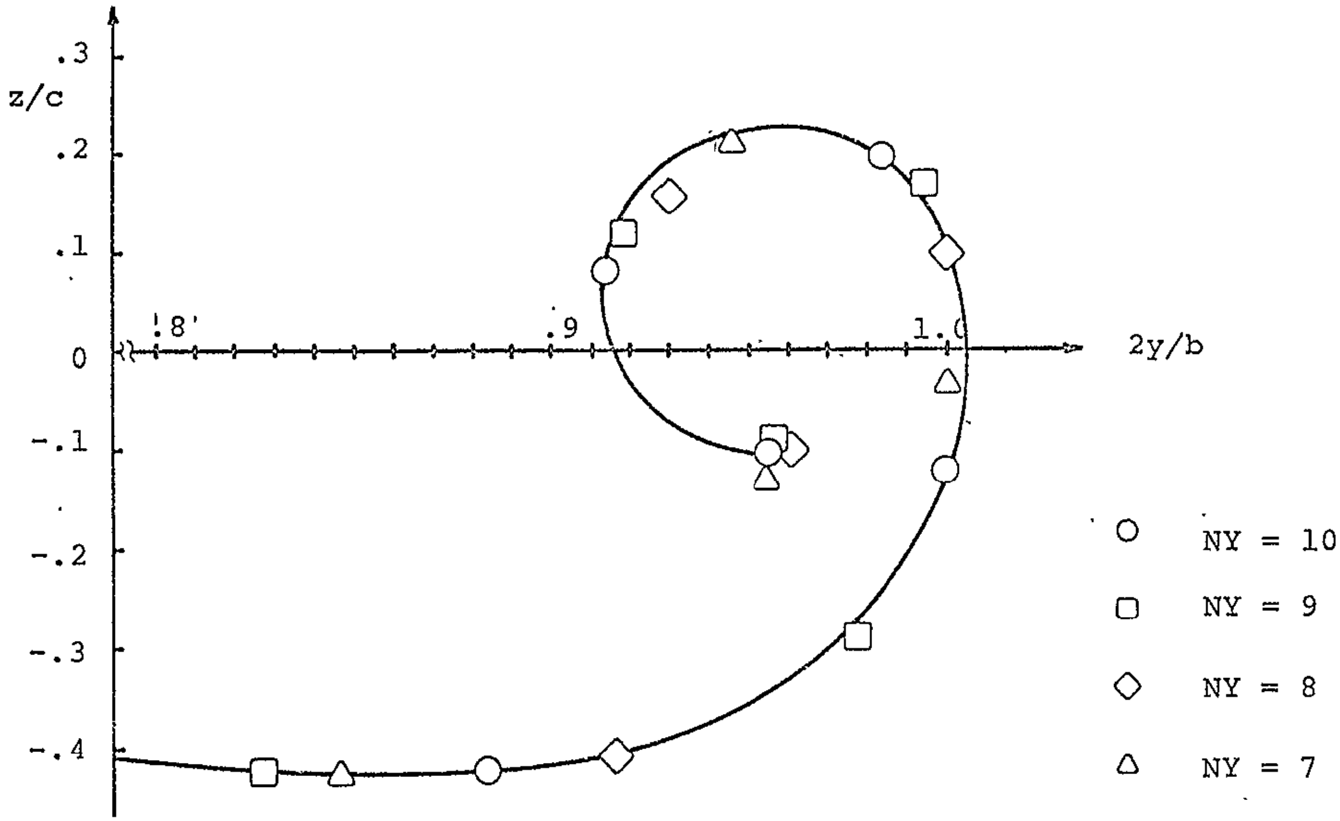

Figure A3. Convergence Problem: Influence of NY on the Wake Roll-up for a Rectangular Wing of $AR = 8$, at $\alpha = 5°$, with $NX = 4$ and $\Delta x_w = .5c$, Plotted at a Station Situated 10 Chord Lengths Behind the Trailing Edge.

APPENDIX B

CONVERGENCE OF ITERATION SCHEME

In this Appendix, an analysis of the convergence of the iteration scheme is presented, for a rectangular wing of AR = 8, at an angle of attack $\alpha = 5°$, with an element grid having NX = 4, NY = 10 and $\Delta x_w = .5c$. Figures B1a, b, c, d show the evolution of the rolled-up wake pattern through successive iterations until convergence is reached. The plots are for stations at 1, 2, 5 and 10 chord lengths behind the trailing edge. Figures B2a, b, c, d show the evolution of the wake streamlines numbers 1, 9, 10 and 11 through successive iterations until convergence, plotted for 10 chord lengths behind the trailing edge.

A common feature of Figs. B1 and B2 is that the plots of the initial iterations show very large displacements of points on the wake. The largest displacement takes place near the wing-tip and far behind the trailing edge. Convergence is attained faster near the trailing edge and the rate of convergence decreases as we move from the wing root toward the wing-tip.

The computation time required to obtain the convergence of the iteration scheme (described in Subsection 2.4) for a wake having 210 elements is of the order of one hour and 20 minutes on Boston University's IBM 370/145 computer. A number of improvements of the present iteration scheme can be tried.

First, since the calculated potential distribution on the wing is essentially the same with a straight wake as well as with a rolled-up one, the potential distribution could be computed for the straight wake and then recomputed for instance every fifth iteration. This should lead to some savings in computational time. Second, a much better iteration scheme can be used (suggested by the plots of Figures B1 and B2). This scheme should converge much faster than the one used in this paper and account for significant time savings. The first iteration should only change the position of the second row of boxes on the wake; (the first one is kept tangent to the wing plane according to the way the Kutta condition is satisfied) the rest of them will have the same y and z coordinates as the second row. Only the velocities at the influencing corners are calculated. The third row of corners should be realigned according to the velocities at the second row; the rest of the boxes will have the same y and z coordinates as the second row. The process should be repeated until convergence is reached everywhere.

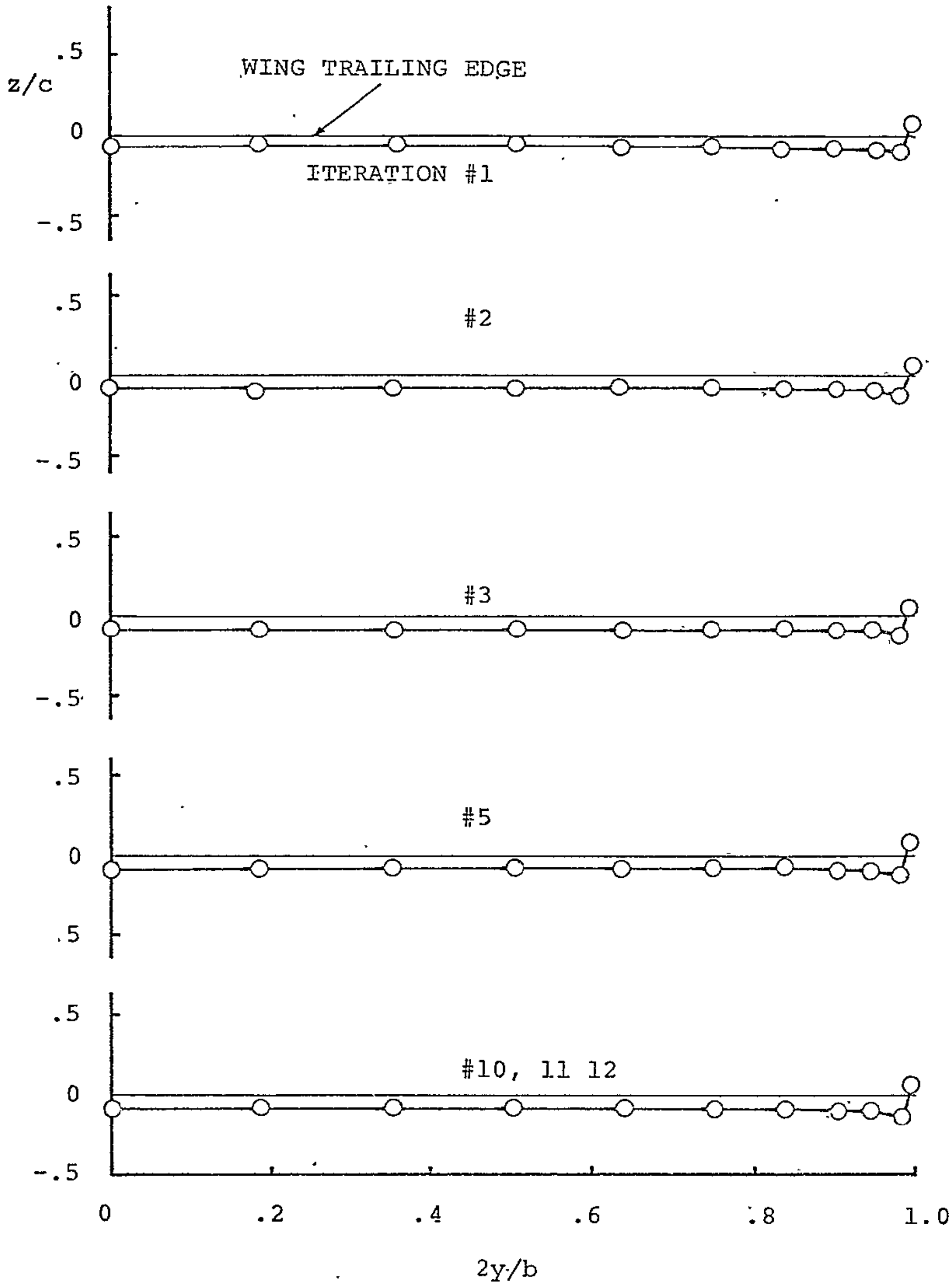

Figure Bla. Evolution of the Rolled-up Wake Pattern Through Successive Iterations, at a Station Situated 1 Chord Lengths Behind the Trailing Edge, for a Rectangular Wing of AR = 8, at $\alpha = 5°$, with NX = 4, NY = 10, $\Delta x_W = .5c$.

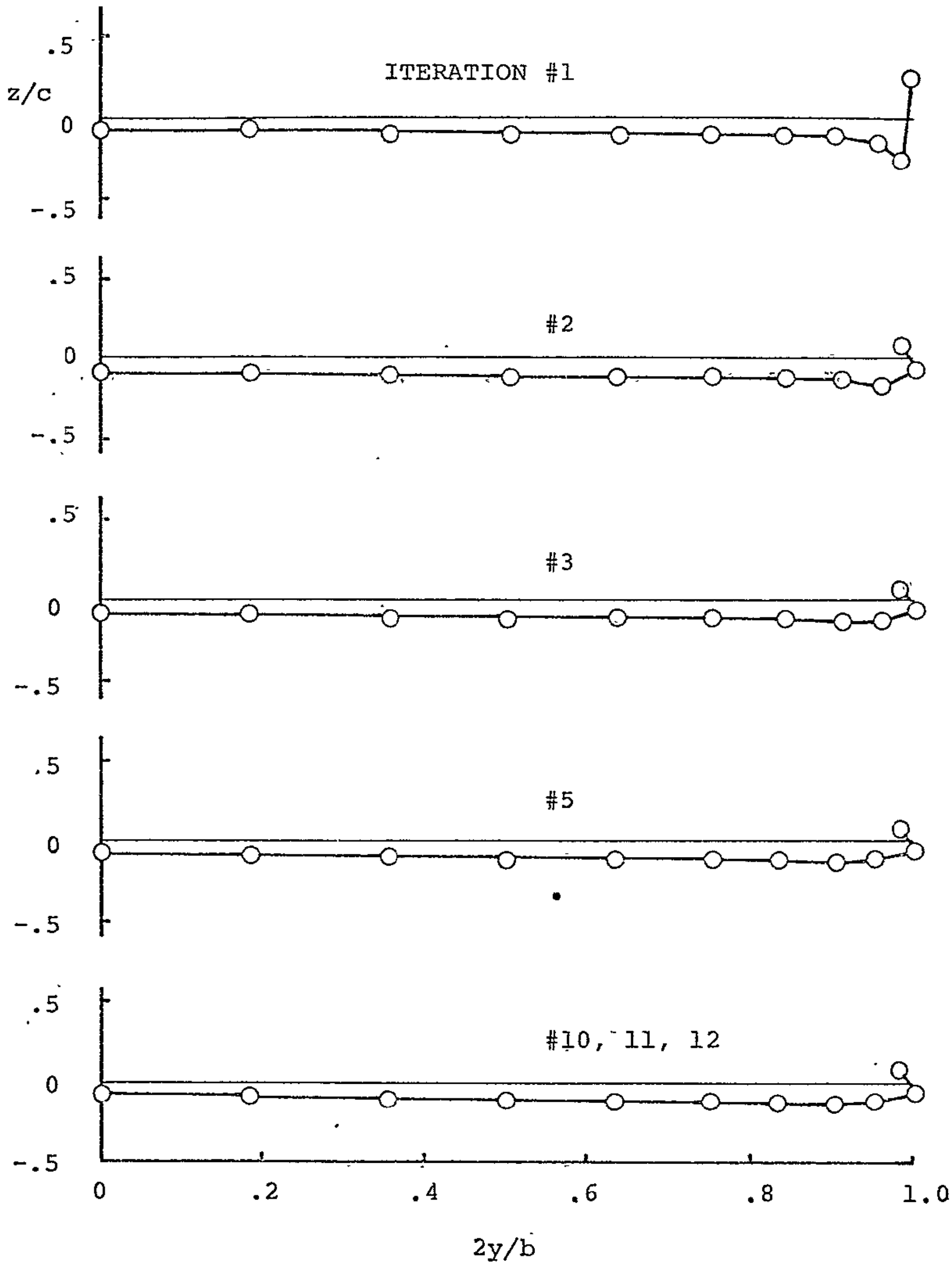

Figure B1b. Evolution of the Rolled-up Wake Pattern Through Successive Iterations, at a Station Situated 2 Chord Lengths Behind the Trailing Edge, for the Wing Planform of Figure B1a

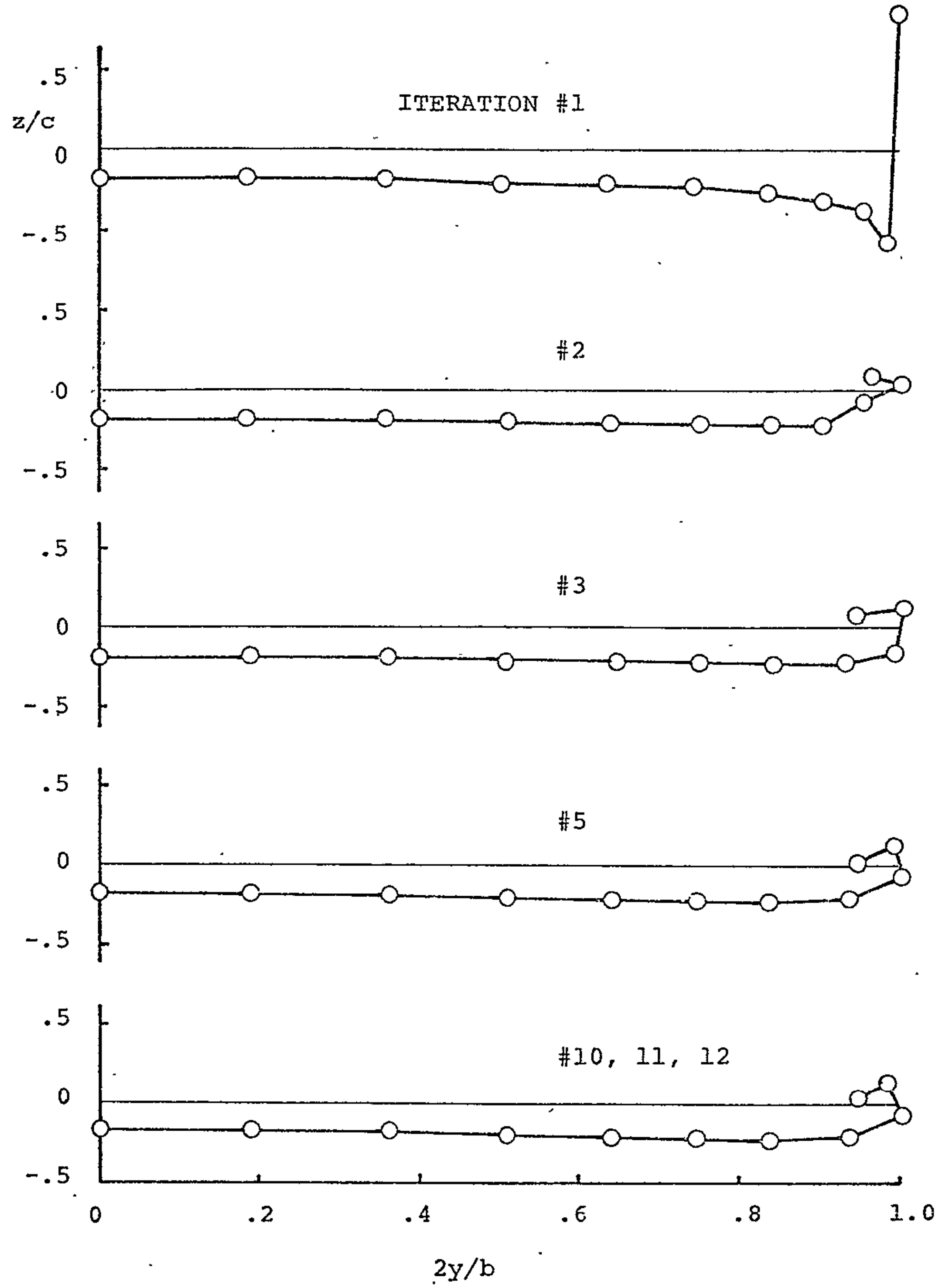

Figure Blc. Evolution of the Rolled-up Wake Pattern Through Successive Iterations, at a Station Situated 5 Chord Lengths Behind the Trailing Edge, for the Wing of Figure Bla

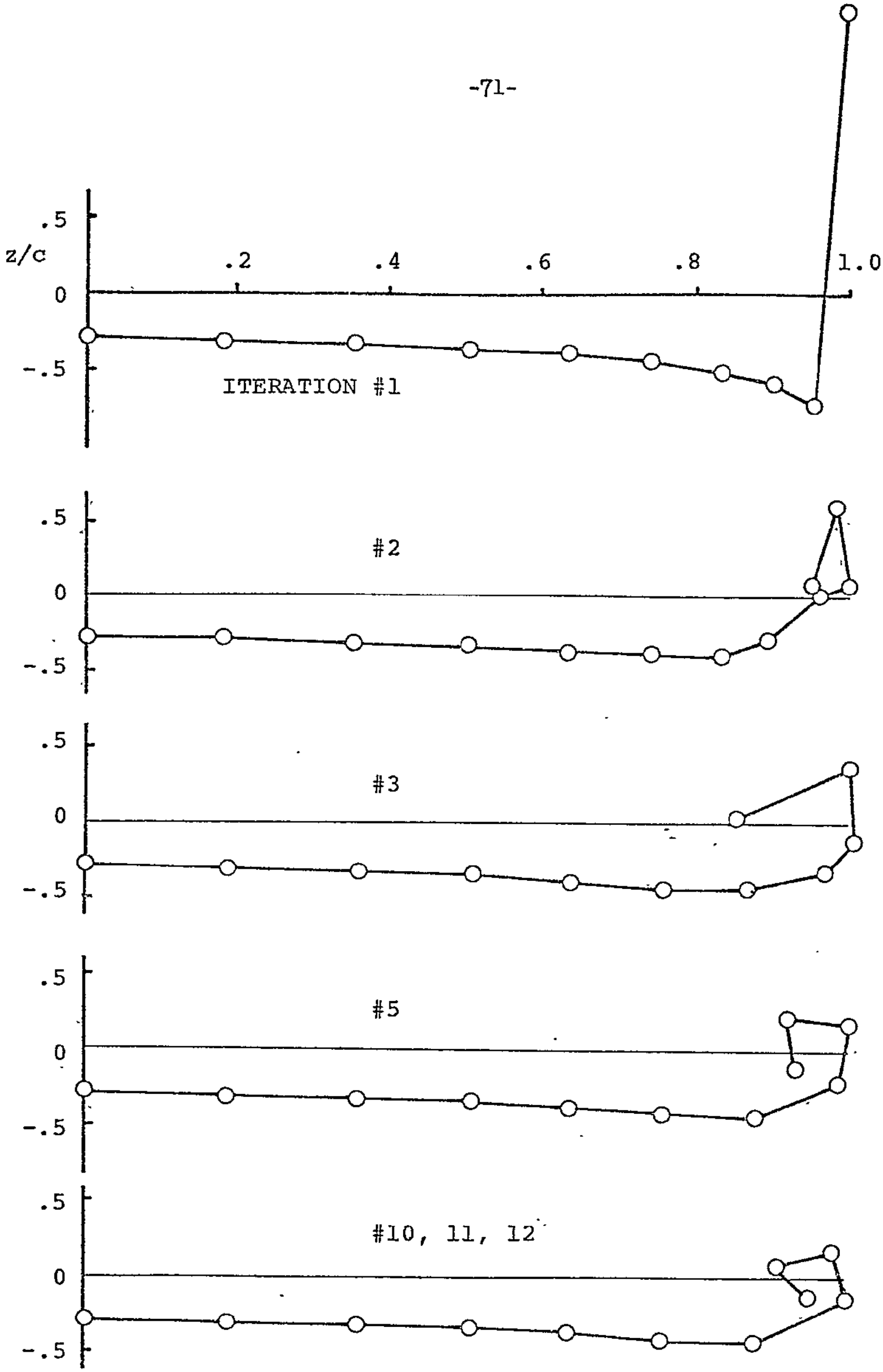

Figure Bld. Evolution of the Rolled-up Wake Pattern Through Successive Iterations, at a Station Situated 10 Chord Lengths Behind the Trailing Edge, for the Wing of Figure Bla.

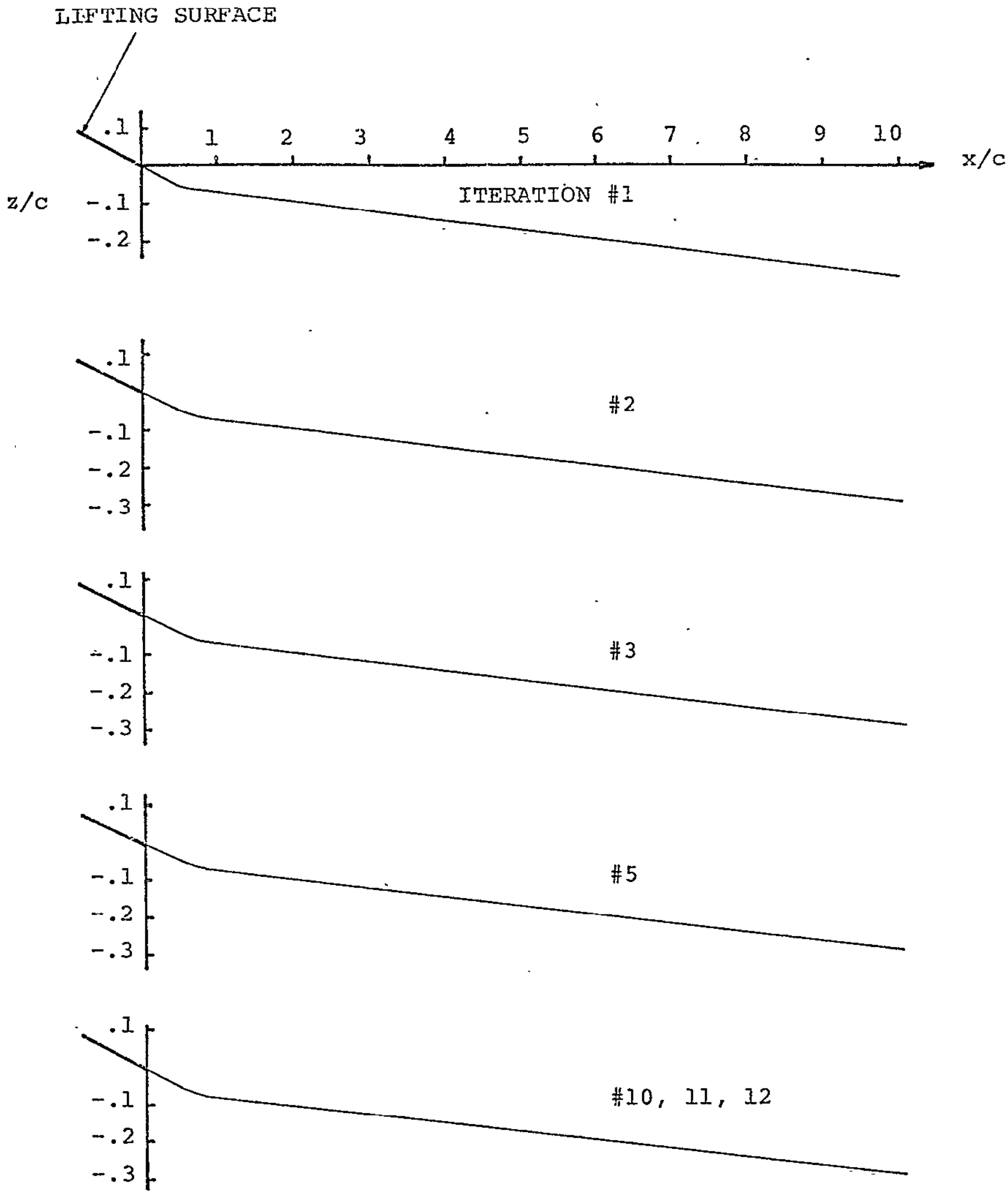

Figure B2a. Evolution of Wake Streamline #1 Through Successive Iterations for the Planform of Figure Bla.

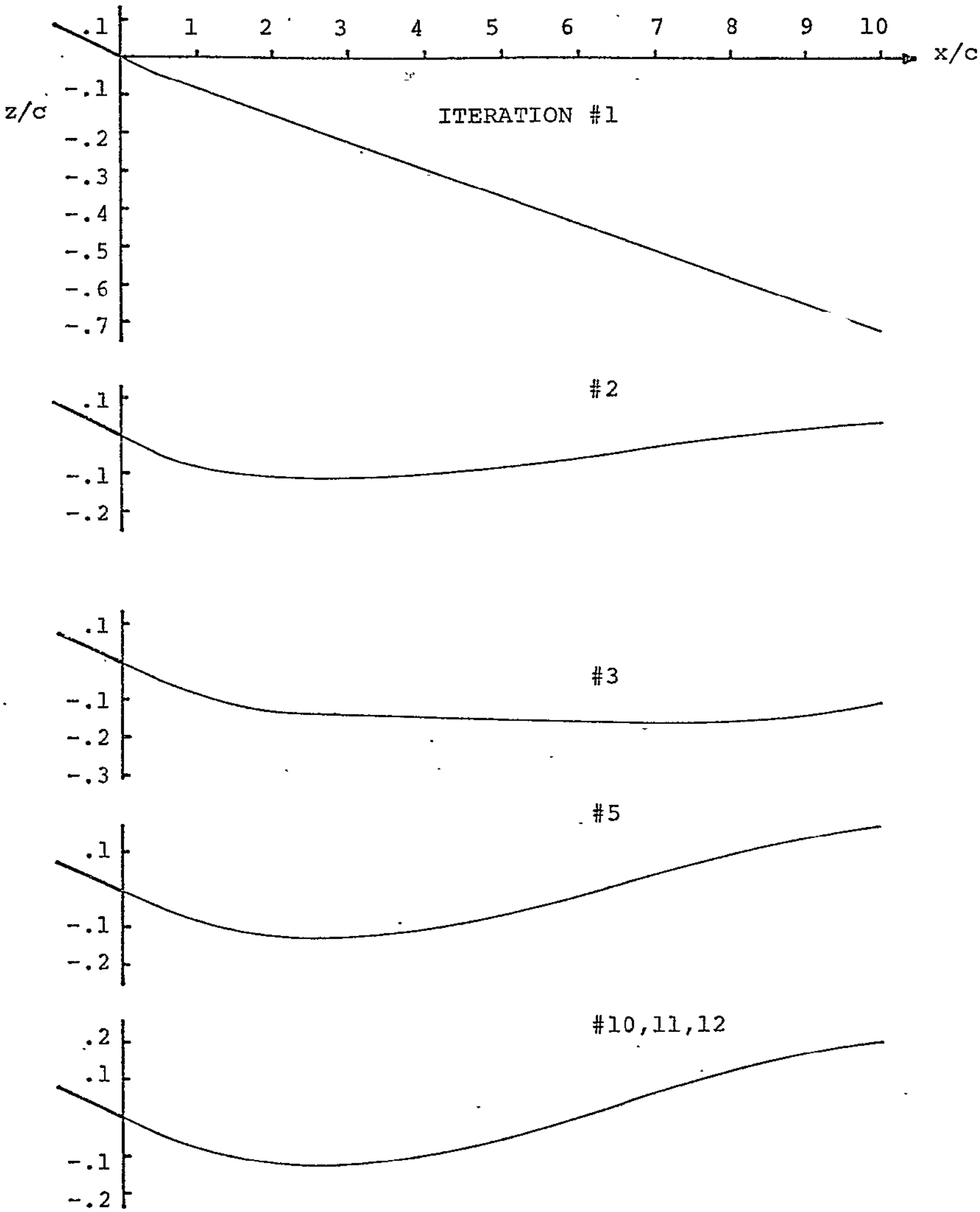

Figure B2b. Evolution of Wake Streamline #9 Through Successive Iterations, for the Planform of Figure B1a.

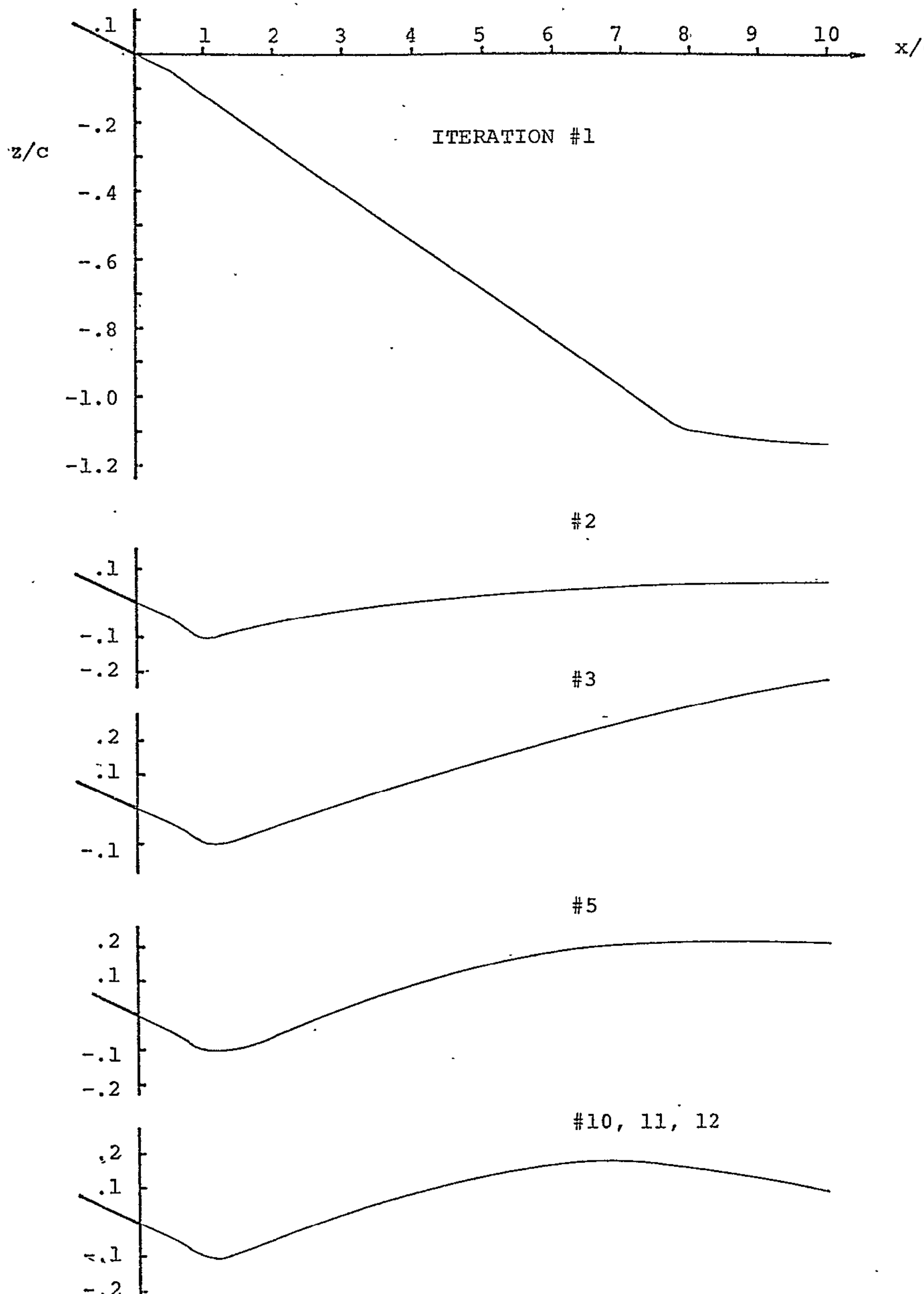

Figure B2c. Evolution of Wake Streamline #10 Through Successive Iterations, for the Planform of Figure B1a.

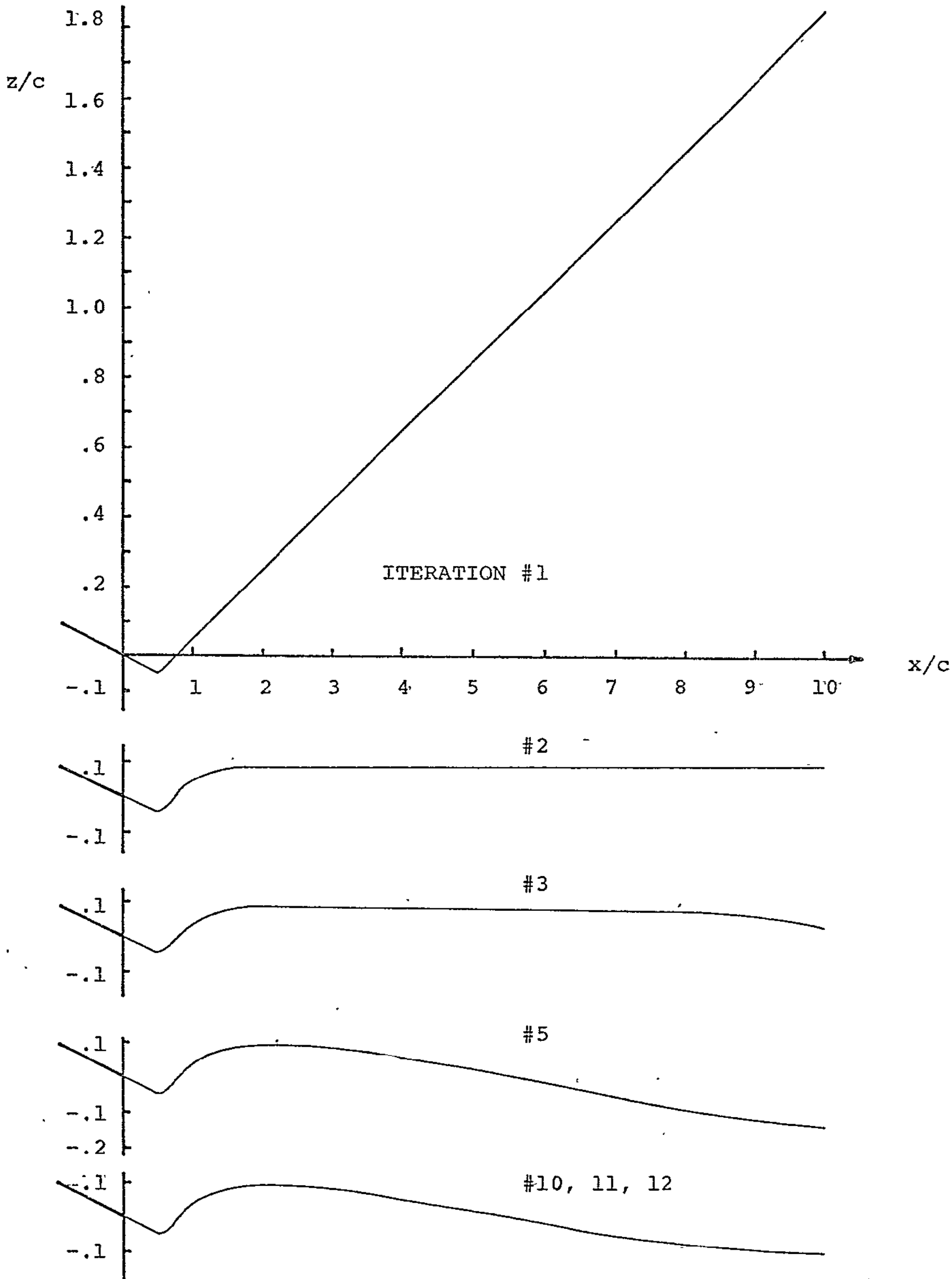

Figure B2d. Evolution of Wake Streamline #11 Through Successive Iterations, for the Planform of Figure B1a.

APPENDIX C

FLOW CHART AND LIST OF THE COMPUTER PROGRAM ILSAWR

C1. Flow Chart of Computer Program ILSAWR

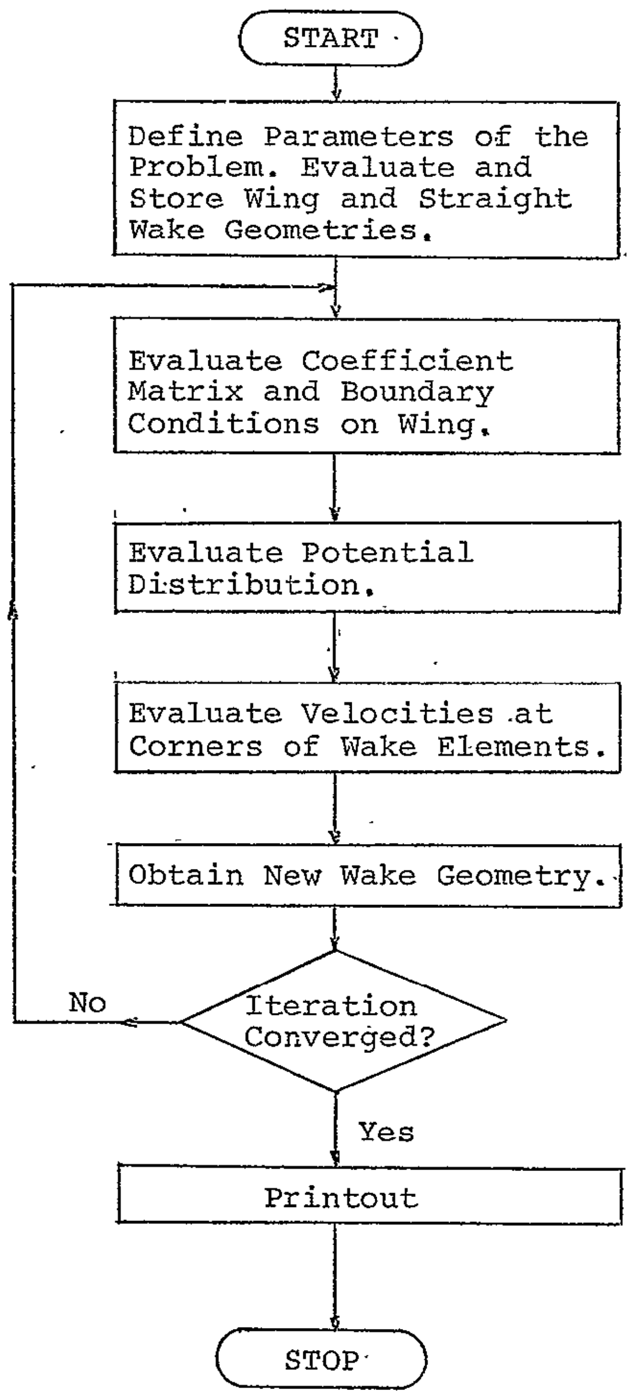

C2. List of Computer Program ILSAWR

```
IV G LEVEL  21                    MAIN                  DATE = 75226             05/22/1
          COMMON/ZZZ1/NX,NY,NZ,NW,REFLEN,SPAN,KSYMMY,KSYMMZ,NSYMMY,NSYMMZ
          COMMON/ZZZ2/TAU,ALFA,TANGLE,TANGTE,CHORD,NTOTAL,UMACH
          COMMON/ZZZ8/AA(2500),SOURCF(250),SINABC,COSABC,ALFABC
          COMMON/ZZZ11/VHKX(2500),VHKY(2500),VHKZ(2500),VKX(250),VKY(250),
         1VKZ(250)
          COMMON/CONTR/NITER
          DIMENSION ITCONT(100)
          DO 10 I=1,15
    10    ITCONT(I)=1
          ITCONT(1)=2
          ITCONT(5)=2
          ITCONT(10)=2
          ITCONT(15)=2
          ITCONT(20)=2
          ITCONT(25)=2
          ITCONT(30)=2
          ITCONT(35)=2
          ITCONT(40)=2
          ITCONT(45)=2
          ITCONT(50)=2
          CALL INITIA(1)
          CALL PRINTA(5)
          CALL GEOMET
          CALL VEC123
    C     CALL PRINTA(3)
          DO 1 NITER=1,12
          IF(NITER.EQ.11)ITCONT(NITER)=2
          IF(NITER.EQ.12)ITCONT(NITER)=2
          IF(ITCONT(NITER).NE.2)GO TO 1000
          CALL COEFF
    C     CALL PRINTB(4)
          TOL=0.001
          CALL GELG(SOURCE,AA,NTOTAL,1,TOL,IER)
          CALL PRINTB(1)
    1000  CONTINUE
          CALL VELMM
    C     CALL VELAUX
          CALL ITER
    1     CONTINUE
          STOP
          END
```

```
      SUBROUTINE INITIA(K)
      COMMON/ZZZ1/NX,NY,NZ,NW,REFLEN,SPAN,KSYMMY,KSYMMZ,NSYMMY,NSYMMZ
      COMMON/ZZZ2/TAU,ALFA,TANGLE,TANGTE,CHORD,NTOTAL,UMACH
      COMMON/ZZZ3/YK(3,11,11,2)
      COMMON/ZZZ6/XPC(250),YPC(250),ZPC(250)
      COMMON/ZZZ7/XP1(250),YP1(250),ZP1(250),XP2(250),YP2(250),
     1ZP2(250),XP3(250),YP3(250),ZP3(250)
      COMMON/ZZZ8/AA(2500),SOURCE(250),SINABC,COSABC,ALFABC
      COMMON/ZZZ9/XPP(250),YPP(250),ZPP(250),XPM(250),YPM(250)
     1,ZPM(250),XMP(250),YMP(250),ZMP(250),XMM(250),YMM(250),
     1ZMM(250),IWAKE(250)
      COMMON/ZZZ10/JNXB(250),NXWAKE,WAKEIN
      GO TO(1,2,3,4),K
1     CONTINUE
      NX=7
      NY=7
      NZ=1
      NXWAKE=11
      WAKEIN=.5
      NW=1
C
C     +1 MEANS THE GEOMETRY OF THE PROBLEM IS SYMMETRIC
C     -1 MEANS THE GEOMETRY OF THE PROBLEM IS ANTISYMMETRIC
C      0 MEANS THE GEOMETRY OF THE PROBLEM IS NEITHER SYMMETRIC NOR ANTI
C
C     IF KSYMMZ .NE. 0 ,THEN NZ=1 (EXCEPT FOR GROUND EFFECT)
C
      KSYMMY=+1
      KSYMMZ=0
      NTOTAL=NX*NY*NZ*NW
      IF(KSYMMY.EQ.0)NTOTAL=NTOTAL*2
      NSYMMY=1
      NSYMMZ=1
      IF(KSYMMY.NE.0)NSYMMY=2
      IF(KSYMMZ.NE.0)NSYMMZ=2
      UMACH=0.0
      REFLEN=1.
      TAU=.00
      SPAN=8.
      ANGLA=0.
      ANGLB=0.
      ALFA=5.
      ALFAR=ALFA*3.14159/180.
      SINALF=SIN(ALFAR)
      COSALF=COS(ALFAR)
C
      ALFABC=0.
      ALFRBC=ALFABC*3.14159/180.
      SINABC=SIN(ALFRBC)
      COSABC=COS(ALFRBC)
C
      BETA=SQRT(1.-UMACH*UMACH)
      XLEZ=-1.
      XTEZ=0.
      CHORD=XTEZ-XLEZ
      XLEZ=XLEZ/(REFLEN*BETA)
      XTEZ=XTEZ/(REFLEN*BETA)
      SPAN=SPAN/REFLEN
```

```
      HFSPAN=.5*SPAN
      XLEP=ANGLA/BETA
      XTEP=ANGLB/BETA
      TAUBAR=TAU*.75*SQRT(3.)*(XTEZ-XLEZ)
      RETURN
2     CONTINUE
      RETURN
3     CONTINUE
      DXX=1./NX
      DYY=1./NY
      NXP=NX+1
      NYP=NY+1
      DO 33 IX=1,NXP
      DO 33 IY=1,NYP
      DO 33 IZ=1,NZ
      XX=(IX-1)*DXX
      YY=(IY-1)*DYY
      CSI=XX*XX
C     THIS IS FOR A UNIFORM Y-MESH
C     ETA=YY
C     THIS IS FOR A NONUNIFORM Y-MESH
      ETA=1.-(1.-YY)**2
      Y=HFSPAN*ETA
C     THIS IS A SEMI-ELLIPTICAL WING PLANFORM
C     XLE=-CHORD*SQRT(1.-(Y*Y)/(HFSPAN*HFSPAN))
C     THIS IS A RECTANGULAR WING PLANFORM
      XTE=XTEZ
      XLE=XLEZ
      XO=XLE+(XTE-XLE)*CSI
      IF(IZ.EQ.1)SIGNZ=+1
      IF(IZ.EQ.2)SIGNZ=-1
      ZO=SIGNZ*TAUBAR*XX*(1.-CSI)*SQRT(1.-ETA**2)
      X=+XO*COSALF+ZO*SINALF
      Z=-XO*SINALF+ZO*COSALF
      YK(1,IX,IY,IZ)=X
      YK(2,IX,IY,IZ)=Y
      YK(3,IX,IY,IZ)=Z
33    CONTINUE
      RETURN
4     CONTINUE
      RETURN
      END
```

```
      SUBROUTINE GECMET
C
C     THIS SUBROUTINE IS FOR QUADRILATERAL ELEMENTS
C
      COMMON/ZZZ1/NX,NY,NZ,NW,REFLEN,SPAN,KSYMMY,KSYMMZ,NSYMMY,NSYMMZ
      COMMON/ZZZ2/TAU,ALFA,TANGLE,TANGTE,CHORD,NTOTAL,UMACH
      COMMON/ZZZ3/YK(3,11,11,2)
      COMMON/ZZZ6/XPC(250),YPC(250),ZPC(250)
      COMMON/ZZZ7/XP1(250),YP1(250),ZP1(250),XP2(250),YP2(250),
     1ZP2(250),XP3(250),YP3(250),ZP3(250)
      COMMON/ZZZ9/XPP(250),YPP(250),ZPP(250),XPM(250),YPM(250)
     1,ZPM(250),XMP(250),YMP(250),ZMP(250),XMM(250),YMM(250),
     1ZMM(250),IWAKE(250)
      COMMON/ZZZ10/JNXB(250),NXWAKF,WAKEIN
C
      INDEX(JW,JX,JY,JZ,MW,MWX,MWXY)=JW+MW*(JX-1)+MWX*(JY-1)+MWXY*(JZ-1)
C
      NWX=NW*NX
      NWXY=NWX*NY
      NWXYZ=NWXY*NZ
C
      CALL INITIA(3)
C
      DO 200 IX=1,NX
      DO 200 IY=1,NY
      DO 200 IZ=1,NZ
C
C     --      -+
C     +-      ++
C
      IW=1
      IND=INDEX(IW,IX,IY,IZ,NW,NWX,NWXY)
      IF(IZ.EQ.2)GO TO 906
      IXMM=IX
      IXPM=IX+1
      IXPP=IX+1
      IXMP=IX
      IYMM=IY
      IYPM=IY
      IYPP=IY+1
      IYMP=IY+1
      IZMM=IZ
      IZPM=IZ
      IZPP=IZ
      IZMP=IZ
C
C     -+      --
C     ++      +-
C
      GO TO 999
906   CONTINUE
      IXMM=IX
      IXMP=IX
      IXPP=IX+1
      IXPM=IX+1
      IYMM=IY+1
      IYMP=IY
      IYPP=IY
```

```
      IYPM=IY+1
      IZMM=IZ
      IZMP=IZ
      IZPP=IZ
      IZPM=IZ
999   CONTINUE
C
      XPP(IND)=YK(1,IXPP,IYPP,IZPP)
      YPP(IND)=YK(2,IXPP,IYPP,IZPP)
      ZPP(IND)=YK(3,IXPP,IYPP,IZPP)
      XPM(IND)=YK(1,IXPM,IYPM,IZPM)
      YPM(IND)=YK(2,IXPM,IYPM,IZPM)
      ZPM(IND)=YK(3,IXPM,IYPM,IZPM)
      XMP(IND)=YK(1,IXMP,IYMP,IZMP)
      YMP(IND)=YK(2,IXMP,IYMP,IZMP)
      ZMP(IND)=YK(3,IXMP,IYMP,IZMP)
      XMM(IND)=YK(1,IXMM,IYMM,IZMM)
      YMM(IND)=YK(2,IXMM,IYMM,IZMM)
      ZMM(IND)=YK(3,IXMM,IYMM,IZMM)
C     WRITE(6,199)IND,XPP(IND),YPP(IND),ZPP(IND),XPM(IND),YPM(IND)
C    1,ZPM(IND),XMP(IND),YMP(IND),ZMP(IND),XMM(IND),YMM(IND),ZMM(IND)
199   FORMAT(/'IND=',I2,/'PP',3X,3F10.4/'PM',3X,3F10.4/'MP',
     13X,3F10.4/'MM',3X,3F10.4)
      IWAKE(IND)=0
      IF(IX.EQ.NX)IWAKE(IND)=1
200   CONTINUE
      IF(KSYMMY.NE.0)GO TO 701
      DO 300 IR=1,NWXYZ
      IL=IR+NWXYZ
      XPP(IL)=+XMP(IR)
      XMP(IL)=+XPP(IR)
      XPM(IL)=+XMM(IR)
      XMM(IL)=+XPM(IR)
      YPP(IL)=-YMP(IR)
      YMP(IL)=-YPP(IR)
      YPM(IL)=-YMM(IR)
      YMM(IL)=-YPM(IR)
      ZPP(IL)=+ZMP(IR)
      ZMP(IL)=+ZPP(IR)
      ZPM(IL)=+ZMM(IR)
      ZMM(IL)=+ZPM(IR)
      IWAKE(IL)=IWAKE(IR)
300   CONTINUE
701   CONTINUE
C
C     POINTS FOR WAKE
C
      NWTOT=NXWAKE*NY
      DO 1 IY=1,NY
      DO 1 IX=1,NXWAKE
      JNXW=IX+(IY-1)*NXWAKE
      JNXB(JNXW)=IY*NX
1     CONTINUE
      DO 10 IY=1,NY
      DO 10 IX=1,NXWAKE
      II=IY*NX
      IND=NTOTAL+IX+(IY-1)*NXWAKE
      FACTOR=1.
```

```
      IF(IX.EQ.NXWAKE)FACTOR=100.
      XMM(IND)=XPM(II)+WAKEIN*(IX-1)
      XMP(IND)=XPP(II)+WAKEIN*(IX-1)
      XPP(IND)=XPP(II)+WAKEIN*IX*FACTOR
      XPM(IND)=XPM(II)+WAKEIN*IX*FACTOR
      YMM(IND)=YPM(II)
      ZMM(IND)=ZPM(II)
      YMP(IND)=YPP(II)
      ZMP(IND)=ZPP(II)
      YPP(IND)=YPP(II)
      ZPP(IND)=ZPP(II)
      YPM(IND)=YPM(II)
      ZPM(IND)=ZPM(II)
10    CONTINUE
      RETURN
      END
```

```
      SUBROUTINE VFC123
      COMMON/ZZZ1/NX,NY,NZ,NW,REFLEN,SPAN,KSYMMY,KSYMMZ,NSYMMY,NSYMMZ
      COMMON/ZZZ2/TAU,ALFA,TANGLE,TANGTE,CHORD,NTOTAL,UMACH
      COMMON/ZZZ3/YK(3,11,11,2)
      COMMON/ZZZ6/XPC(250),YPC(250),ZPC(250)
      COMMON/ZZZ7/XP1(250),YP1(250),ZP1(250),XP2(250),YP2(250),
     1ZP2(250),XP3(250),YP3(250),ZP3(250)
      COMMON/ZZZ9/XPP(250),YPP(250),ZPP(250),XPM(250),YPM(250)
     1,ZPM(250),XMP(250),YMP(250),ZMP(250),XMM(250),YMM(250),
     1ZMM(250),IWAKE(250)
      DO 200 IND=1,NTOTAL
      XPC(IND)=(XPP(IND)+XPM(IND)+XMP(IND)+XMM(IND))/4.
      YPC(IND)=(YPP(IND)+YPM(IND)+YMP(IND)+YMM(IND))/4.
      ZPC(IND)=(ZPP(IND)+ZPM(IND)+ZMP(IND)+ZMM(IND))/4.
      XP1(IND)=(XPP(IND)+XPM(IND)-XMP(IND)-XMM(IND))/4.
      YP1(IND)=(YPP(IND)+YPM(IND)-YMP(IND)-YMM(IND))/4.
      ZP1(IND)=(ZPP(IND)+ZPM(IND)-ZMP(IND)-ZMM(IND))/4.
      XP2(IND)=(XPP(IND)-XPM(IND)+XMP(IND)-XMM(IND))/4.
      YP2(IND)=(YPP(IND)-YPM(IND)+YMP(IND)-YMM(IND))/4.
      ZP2(IND)=(ZPP(IND)-ZPM(IND)+ZMP(IND)-ZMM(IND))/4.
      XP3(IND)=(XPP(IND)-XPM(IND)-XMP(IND)+XMM(IND))/4.
      YP3(IND)=(YPP(IND)-YPM(IND)-YMP(IND)+YMM(IND))/4.
      ZP3(IND)=(ZPP(IND)-ZPM(IND)-ZMP(IND)+ZMM(IND))/4.
  200 CONTINUE
      RETURN
      END
```

```
      SUBROUTINE PRINTA(KPRINT)
      COMMON/ZZZ1/NX,NY,NZ,NW,REFLEN,SPAN,KSYMMY,KSYMMZ,NSYMMY,NSYMMZ
      COMMON/ZZZ2/TAU,ALFA,TANGLE,TANGTE,CHORD,NTOTAL,UMACH
      COMMON/ZZZ3/YK(3,11,11,2)
      COMMON/ZZZ6/XPC(250),YPC(250),ZPC(250)
      COMMON/ZZZ7/XP1(250),YP1(250),ZP1(250),XP2(250),YP2(250),
     1ZP2(250),XP3(250),YP3(250),ZP3(250)
      COMMON/ZZZ8/AA(2500),SOURCE(250),SINABC,COSABC,ALFABC
      COMMON/ZZZ9/XPP(250),YPP(250),ZPP(250),XPM(250),YPM(250)
     1,ZPM(250),XMP(250),YMP(250),ZMP(250),XMM(250),YMM(250),
     1ZMM(250),IWAKE(250)
      COMMON/ZZZ10/JNXB(250),NXWAKE,WAKEIN
      COMMON/CONTR/NITER
      NTP=NTOTAL+1
      NTBW=NTOTAL+NY*NXWAKE
      NY4=4*(NY-1)
      GO TO(1,2,3,4,5,6),KPRINT
1     CONTINUE
      RETURN
2     CONTINUE
      NXP=NX+1
      NYP=NY+1
      DO 35 IZ=1,NZ
      DO 35 IY=1,NYP
      DO 35 IX=1,NXP
      DO 35 J=1,3
      WRITE(6,2500)J,IX,IY,IZ,YK(J,IX,IY,IZ)
2500   FORMAT('YK(',I1,',',I1,',',I1,',',I1,')=',E15.6)
35    CONTINUE
      RETURN
3     CONTINUE
      WRITE(6,400)
400   FORMAT(2X,'IND',4X,'XPC',7X,'YPC',7X,'ZPC',7X,'XP1',7X'YP1',7X,
     1'ZP1',7X,'XP2',7X,'YP2',7X,'ZP2',7X,'XP3',7X,'YP3',7X'ZP3')
      DO 45 I=1,NTOTAL
45    WRITE(6,500)I,XPC(I),YPC(I),ZPC(I),XP1(I),YP1(I),ZP1(I),XP2(I),
     1YP2(I),ZP2(I),XP3(I),YP3(I),ZP3(I)
500   FORMAT(1X,I3,12F10.5)
      RETURN
4     CONTINUE
      RETURN
5     CONTINUE
      WRITE(6,550)
550   FORMAT(//2X,'SPECIFICATIONS OF THE PROBLEM'/)
      WRITE(6,555)NX,NY,NZ,NW,NTOTAL,KSYMMY,KSYMMZ,REFLEN,SPAN,TAU,
     1ALFA,ALFABC,UMACH,NXWAKE,WAKEIN
555   FORMAT(2X,'NX=',I2/2X,'NY=',I2/2X,'NZ=',I2/2X,'NW=',I2/
     12X,'NTOTAL=',I3//2X,'KSYMMY=',I2/2X,'KSYMMZ=',I2//
     12X,'REFERENCE LENGTH=',F6.2/2X,'SPAN/REF LENGTH =',F6.2/
     12X,'THICKNESS=',F9.5//2X,'ALFA=',F7.3/2X,'ALFABC=',F7.3//
     12X,'MACH NUMBER =',F7.3//2X,'NXWAKE=',I3,//
     12X,'WAKEIN=',F7.3)
      WRITE(6,556)TANGLE,TANGTE,CHORD
556   FORMAT(2X,'TANGLE=',F6.2/2X,'TANGTE=',F6.2//2X,'CHORD=',F6.2//)
      RETURN
6     CONTINUE
      RETURN
      END
```

```
      SUBROUTINE PRINTB(KPRINT)
      COMMON/ZZZ1/NX,NY,NZ,NW,REFLEN,SPAN,KSYMMY,KSYMMZ,NSYMMY,NSYMMZ
      COMMON/ZZZ2/TAU,ALFA,TANGLE,TANGTE,CHORD,NTOTAL,UMACH
      COMMON/ZZZ6/XPC(250),YPC(250),ZPC(250)
      COMMON/ZZZ7/XP1(250),YP1(250),ZP1(250),XP2(250),YP2(250),
     1ZP2(250),XP3(250),YP3(250),ZP3(250)
      COMMON/ZZZ8/AA(2500),SOURCE(250),SINABC,COSABC,ALFABC
      NWX=NW*NX
      NWXY=NWX*NY
      NWXYZ=NWXY*NZ
      NY4=4*(NY-1)
      GO TO(1,2,3,4,5,6,7),KPRINT
1     CONTINUE
      WRITE(6,100)
100   FORMAT(///2X,'THE DISTRIBUTION OF THE DOUBLET STRENGTH DH')
      INDFIN=0
      IPRINT=0
      DO 25 ISYMY=1,2
      IF(ISYMY.EQ.2.AND.KSYMMY.NE.0)GO TO 25
      IF(ISYMY.EQ.1)WRITE(6,120)
120   FORMAT(//5X,'RIGHTHAND SIDE')
      IF(ISYMY.EQ.2)WRITE(6,140)
140   FORMAT(//5X,'LEFTHAND SIDE')
      DO 25 IZ=1,NZ
      INDFIN=INDFIN+NWXY
      IPRINT=IPRINT+1
      IND=NWXY*(IPRINT-1)
      DO 25 IX=1,NX
      WRITE(6,300)
      DO 25 IW=1,NW
      IWX=IW*IX
      IND=IND+1
      WRITE(6,200)(SOURCE(KK),KK=IND,INDFIN,NWX)
25    CONTINUE
200   FORMAT(8E15.5)
300   FORMAT(/)
      RETURN
2     CONTINUE
      RETURN
3     CONTINUE
      RETURN
4     CONTINUE
      WRITE(6,770)
770   FORMAT(///'DISTRIBUTION OF AA(I,J)'/)
      DO 77 I=1,NTOTAL
      WRITE(6,771)I
      N1=I
      N2=NTOTAL*NTOTAL
771   FORMAT(2X,'INDEX=',I2)
      IF(NY.LE.4.OR.NY.GE.8)WRITE(6,772)(AA(K),K=N1,N2,NTOTAL)
772   FORMAT(8E15.6/8E15.6/8E15.6/8E15.6/8E15.6)
      IF(NY.EQ.5)WRITE(6,775)(AA(K),K=N1,N2,NTOTAL)
775   FORMAT(5E15.6)
      IF(NY.EQ.6)WRITE(6,776)(AA(K),K=N1,N2,NTOTAL)
776   FORMAT(6E15.6)
      IF(NY.EQ.7)WRITE(6,777)(AA(K),K=N1,N2,NTOTAL)
777   FORMAT(7E15.6)
77    CONTINUE
```

```
      RETURN
5     CONTINUE
      RETURN
6     CONTINUE
      WRITE(6,881)
881   FORMAT(///2X,'THE DISTRIBUTION OF SURFACE NORMAL'/)
      NXW=NX*NW
      NXWY=NXW*NY
      DO 883 IX=1,NXW
      WRITE(6,882)(SOURCE(KK),KK=IX,NXWY,NXW)
882   FORMAT(8E15.6)
883   CONTINUE
      RETURN
7     CONTINUE
      RETURN
      END
```

```
      SUBROUTINE DFBUG(K)
      WRITE(6,1)K
1     FORMAT(2X,'ERROR CODE=',I2)
      RETURN
      END
```

```
      SUBROUTINE VFLMN
      COMMON/ZZZ1/NX,NY,NZ,NW,REFLEN,SPAN,KSYMMY,KSYMMZ,NSYMMY,NSYMMZ
      COMMON/ZZZ2/TAU,ALFA,TANGLE,TANGTE,CHORD,NTOTAL,UMACH
      COMMON/ZZZ6/XPC(250),YPC(250),ZPC(250)
      COMMON/ZZZ7/XP1(250),YP1(250),ZP1(250),XP2(250),YP2(250),
     1ZP2(250),XP3(250),YP3(250),ZP3(250)
      COMMON/ZZZ8/AA(2500),SOURCE(250),SINABC,COSABC,ALFABC
      COMMON/ZZZ9/XPP(250),YPP(250),ZPP(250),XPM(250),YPM(250)
     1,ZPM(250),XMP(250),YMP(250),ZMP(250),XMM(250),YMM(250),
     1ZMM(250),IWAKE(250)
      COMMON/ZZZ10/JNXB(250),NXWAKE,WAKEIN
      COMMON/ZZZ11/VHKX(2500),VHKY(2500),VHKZ(2500),VKX(250),VKY(250),
     1VKZ(250)
      COMMON/ZZZ12/VXWAKE(250),VYWAKE(250),VZWAKE(250)
      COMMON/CONTR/NITER
      DOTPRO(X1,Y1,Z1,X2,Y2,Z2)=X1*X2+Y1*Y2+Z1*Z2
      PROMIX(XX1,YY1,ZZ1,XX2,YY2,ZZ2,XX3,YY3,ZZ3)=(YY2*ZZ3-YY3*ZZ2)*XX1
     1-(XX2*ZZ3-XX3*ZZ2)*YY1+(XX2*YY3-XX3*YY2)*ZZ1
      NT2S=NTOTAL**2
C
      NYP=NY+1
      NWT=NXWAKE*NY
      NWTP=NWT+NXWAKE
      NTBW=NTOTAL+NWT
C
C
      DO 2 I=1,250
      VXWAKE(I)=0.
      VYWAKE(I)=0.
      VZWAKE(I)=0.
2     CONTINUE
      DO 250 JNXBW=1,NTBW
      DO 250 INXW=1,NWT
      DO 250 ISYMMY=1,NSYMMY
      DO 250 ISYMMZ=1,NSYMMZ
      SIGNY=3.-2*ISYMMY
      SIGNZ=3.-2*ISYMMZ
      JNXW=JNXBW-NTOTAL
      IF(JNXBW.LE.NTOTAL)JNX=JNXBW
      IF(JNXBW.GT.NTOTAL)JNX=JNXB(JNXW)
C
      INDEX=NTOTAL+INXW
      Q1X=XPP(JNXBW)-XMM(INDEX)
      Q1Y=YPP(JNXBW)-YMM(INDEX)*SIGNY
      Q1Z=ZPP(JNXBW)-ZMM(INDEX)*SIGNZ
      Q2X=XMP(JNXBW)-XMM(INDEX)
      Q2Y=YMP(JNXBW)-YMM(INDEX)*SIGNY
      Q2Z=ZMP(JNXBW)-ZMM(INDEX)*SIGNZ
      Q3X=XMM(JNXBW)-XMM(INDEX)
      Q3Y=YMM(JNXBW)-YMM(INDEX)*SIGNY
      Q3Z=ZMM(JNXBW)-ZMM(INDEX)*SIGNZ
      Q4X=XPM(JNXBW)-XMM(INDEX)
      Q4Y=YPM(JNXBW)-YMM(INDEX)*SIGNY
      Q4Z=ZPM(JNXBW)-ZMM(INDEX)*SIGNZ
      Q1Q1=DOTPRO(Q1X,Q1Y,Q1Z,Q1X,Q1Y,Q1Z)
      Q2Q2=DOTPRO(Q2X,Q2Y,Q2Z,Q2X,Q2Y,Q2Z)
      Q3Q3=DOTPRO(Q3X,Q3Y,Q3Z,Q3X,Q3Y,Q3Z)
      Q4Q4=DOTPRO(Q4X,Q4Y,Q4Z,Q4X,Q4Y,Q4Z)
```

```
      Q1Q2=DOTPRO(Q1X,Q1Y,Q1Z,Q2X,Q2Y,Q2Z)
      Q1Q4=DOTPRO(Q1X,Q1Y,Q1Z,Q4X,Q4Y,Q4Z)
      Q2Q3=DOTPRO(Q2X,Q2Y,Q2Z,Q3X,Q3Y,Q3Z)
      Q3Q4=DOTPRO(Q3X,Q3Y,Q3Z,Q4X,Q4Y,Q4Z)
      Q1=SQRT(Q1Q1)
      Q2=SQRT(Q2Q2)
      Q3=SQRT(Q3Q3)
      Q4=SQRT(Q4Q4)
      Q41X=Q4Y*Q1Z-Q4Z*Q1Y
      Q41Y=-(Q4X*Q1Z-Q4Z*Q1X)
      Q41Z=Q4X*Q1Y-Q4Y*Q1X
      Q41SQ=DOTPRO(Q41X,Q41Y,Q41Z,Q41X,Q41Y,Q41Z)
      Q12X=Q1Y*Q2Z-Q1Z*Q2Y
      Q12Y=-(Q1X*Q2Z-Q1Z*Q2X)
      Q12Z=Q1X*Q2Y-Q1Y*Q2X
      Q12SQ=DOTPRO(Q12X,Q12Y,Q12Z,Q12X,Q12Y,Q12Z)
      Q23X=Q2Y*Q3Z-Q2Z*Q3Y
      Q23Y=-(Q2X*Q3Z-Q2Z*Q3X)
      Q23Z=Q2X*Q3Y-Q2Y*Q3X
      Q23SQ=DOTPRO(Q23X,Q23Y,Q23Z,Q23X,Q23Y,Q23Z)
      Q34X=Q3Y*Q4Z-Q3Z*Q4Y
      Q34Y=-(Q3X*Q4Z-Q3Z*Q4X)
      Q34Z=Q3X*Q4Y-Q3Y*Q4X
      Q34SQ=DOTPRO(Q34X,Q34Y,Q34Z,Q34X,Q34Y,Q34Z)
C
      PART1=0.
      IF(Q41SQ.NE.0.)PART1=((Q4Q4-Q1Q4)/Q4+(Q1Q1-Q1Q4)/Q1)/Q41SQ
      PART2=0.
      IF(Q12SQ.NE.0.)PART2=((Q1Q1-Q1Q2)/Q1+(Q2Q2-Q1Q2)/Q2)/Q12SQ
      PART3=0.
      IF(Q23SQ.NE.0.)PART3=((Q2Q2-Q2Q3)/Q2+(Q3Q3-Q2Q3)/Q3)/Q23SQ
      PART4=0.
      IF(Q34SQ.NE.0.)PART4=((Q3Q3-Q3Q4)/Q3+(Q4Q4-Q3Q4)/Q4)/Q34SQ
      VX=Q41X*PART1+Q12X*PART2+Q23X*PART3+Q34X*PART4
      VY=(Q41Y*PART1+Q12Y*PART2+Q23Y*PART3+Q34Y*PART4)*SIGNY
      VZ=Q41Z*PART1+Q12Z*PART2+Q23Z*PART3+Q34Z*PART4
      VXWAKE(INXW)=VXWAKE(INXW)+VX*SOURCE(JNX)
      VYWAKE(INXW)=VYWAKE(INXW)+VY*SOURCE(JNX)
      VZWAKE(INXW)=VZWAKE(INXW)+VZ*SOURCE(JNX)
250   CONTINUE
      CALL VELPP
      DO 4 I=1,NTOTAL
      VKX(I)=0.
      VKY(I)=0.
      VKZ(I)=0.
4     CONTINUE
      DO 3 I=1,NTOTAL
      DO 3 J=1,NTOTAL
      NNN=I+(J-1)*NTOTAL
      VKX(I)=VKX(I)+SOURCE(J)*VHKX(NNN)
      VKY(I)=VKY(I)+SOURCE(J)*VHKY(NNN)
      VKZ(I)=VKZ(I)+SOURCE(J)*VHKZ(NNN)
3     CONTINUE
      IF(NITER.EQ.1)GO TO 753
      IF(NITER.LE.10)GO TO 2000
753   WRITE(6,5)
5     FORMAT(/10X,'THIS IS THE X-WING VELOCITY'/)
      CALL PRINTV(VKX,NX,NY)
```

```
      WRITE(6,6)
6     FORMAT(/10X,'THIS IS THE X-WAKE VELOCITY'/)
      CALL PRINTV(VXWAKE,NXWAKE,NYP)
      WRITE(6,7)
7     FORMAT(/10X,'THIS IS THE Y-WING VELOCITY'/)
      CALL PRINTV(VKY,NX,NY)
      WRITE(6,8)
8     FORMAT(/10X,'THIS IS THE Y-WAKE VELOCITY'/)
      CALL PRINTV(VYWAKE,NXWAKE,NYP)
      WRITE(6,9)
9     FORMAT(/10X,'THIS IS THE Z-WING VELOCITY'/)
      CALL PRINTV(VKZ,NX,NY)
      WRITE(6,10)
10    FORMAT(/10X,'THIS IS THE Z-WAKE VELCCITY'/)
      CALL PRINTV(VZWAKE,NXWAKE,NYP)
2000  CONTINUE
      RETURN
      END
```

```
      SUBROUTINE PRINTV(VECTOR,N1,N2)
      DIMENSION VECTOR(1)
      WRITE(6,3)
      DO 1 IX=1,N1
      WRITF(6,2)(VECTCR(IX+N1*(IY-1)),IY=1,N2)
1     CONTINUE
2     FORMAT(8E15.6)
      WRITE(6,3)
3     FORMAT(/)
      RETURN
      END
```

```
      SUBROUTINE COEFF
      COMMON/ZZZ1/NX,NY,NZ,NW,REFLEN,SPAN,KSYMMY,KSYMMZ,NSYMMY,NSYMMZ
      COMMON/ZZZ2/TAU,ALFA,TANGLE,TANGTF,CHORD,NTOTAL,UMACH
      COMMON/ZZZ6/XPC(250),YPC(250),ZPC(250)
      COMMON/ZZZ7/XP1(250),YP1(250),ZP1(250),XP2(250),YP2(250),
     1ZP2(250),XP3(250),YP3(250),ZP3(250)
      COMMON/ZZZ8/AA(2500),SOURCE(250),SINABC,COSABC,ALFABC
      COMMON/ZZZ9/XPP(250),YPP(250),ZPP(250),XPM(250),YPM(250)
     1,ZPM(250),XMP(250),YMP(250),ZMP(250),XMM(250),YMM(250),
     1ZMM(250),IWAKE(250)
      COMMON/ZZZ10/JNXB(250),NXWAKE,WAKEIN
      COMMON/ZZZ11/VHKX(2500),VHKY(2500),VHKZ(2500),VKX(250),VKY(250),
     1VKZ(250)
      DIMENSION XUNORM(250),YUNORM(250),ZUNORM(250)
      DOTPRO(X1,Y1,Z1,X2,Y2,Z2)=X1*X2+Y1*Y2+Z1*Z2
      PROMIX(XX1,YY1,ZZ1,XX2,YY2,ZZ2,XX3,YY3,ZZ3)=(YY2*ZZ3-YY3*ZZ2)*XX1
     1-(XX2*ZZ3-XX3*ZZ2)*YY1+(XX2*YY3-XX3*YY2)*ZZ1
      NT2S=NTOTAL**2
C
C
      DO 9 NNN=1,NT2S
C     VHKX(NNN)=0.
C     VHKY(NNN)=0.
      VHKZ(NNN)=0.
9     AA(NNN)=0.
C      CALCULATION OF THE SURFACE NORMAL
C
      DO 140 JNX=1,NTOTAL
C
      XD1=XPP(JNX)-XMM(JNX)
      YD1=YPP(JNX)-YMM(JNX)
      ZD1=ZPP(JNX)-ZMM(JNX)
      XD2=XMP(JNX)-XPM(JNX)
      YD2=YMP(JNX)-YPM(JNX)
      ZD2=ZMP(JNX)-ZPM(JNX)
      CRX=YD1*ZD2-ZD1*YD2
      CRY=-(XD1*ZD2-ZD1*XD2)
      CRZ=XD1*YD2-YD1*XD2
      ABN=SQRT(DOTPRO(CRX,CRY,CRZ,CRX,CRY,CRZ))
      XUNORM(JNX)=CRX/ABN
      YUNORM(JNX)=CRY/ABN
      ZUNORM(JNX)=CRZ/ABN
140   CONTINUE
      NTBW=NTOTAL+NXWAKE*NY
      DO 250 JNXBW=1,NTBW
C
      DO 250 INX=1,NTOTAL
      DO 250 ISYMMY=1,NSYMMY
      DO 250 ISYMMZ=1,NSYMMZ
      SIGNY=3.-2*ISYMMY
      SIGNZ=3.-2*ISYMMZ
C
      JNXW=JNXBW-NTOTAL
      IF(JNXBW.LE.NTOTAL)JNX=JNXBW
      IF(JNXBW.GT.NTOTAL)JNX=JNXB(JNXW)
      NNN=INX+(JNX-1)*NTOTAL
C
      Q1X=XPP(JNXBW)-XPC(INX)
```

```
      Q1Y=YPP(JNXBW)-YPC(INX)*SIGNY
      Q1Z=ZPP(JNXBW)-ZPC(INX)*SIGNZ
      Q2X=XMP(JNXBW)-XPC(INX)
      Q2Y=YMP(JNXBW)-YPC(INX)*SIGNY
      Q2Z=ZMP(JNXBW)-ZPC(INX)*SIGNZ
      Q3X=XMM(JNXBW)-XPC(INX)
      Q3Y=YMM(JNXBW)-YPC(INX)*SIGNY
      Q3Z=ZMM(JNXBW)-ZPC(INX)*SIGNZ
      Q4X=XPM(JNXBW)-XPC(INX)
      Q4Y=YPM(JNXBW)-YPC(INX)*SIGNY
      Q4Z=ZPM(JNXBW)-ZPC(INX)*SIGNZ
      Q1Q1=DOTPRO(Q1X,Q1Y,Q1Z,Q1X,Q1Y,Q1Z)
      Q2Q2=DOTPRO(Q2X,Q2Y,Q2Z,Q2X,Q2Y,Q2Z)
      Q3Q3=DOTPRO(Q3X,Q3Y,Q3Z,Q3X,Q3Y,Q3Z)
      Q4Q4=DOTPRO(Q4X,Q4Y,Q4Z,Q4X,Q4Y,Q4Z)
      Q1Q2=DOTPRO(Q1X,Q1Y,Q1Z,Q2X,Q2Y,Q2Z)
      Q1Q4=DOTPRO(Q1X,Q1Y,Q1Z,Q4X,Q4Y,Q4Z)
      Q2Q3=DOTPRO(Q2X,Q2Y,Q2Z,Q3X,Q3Y,Q3Z)
      Q3Q4=DOTPRO(Q3X,Q3Y,Q3Z,Q4X,Q4Y,Q4Z)
      Q1=SQRT(Q1Q1)
      Q2=SQRT(Q2Q2)
      Q3=SQRT(Q3Q3)
      Q4=SQRT(Q4Q4)
      Q41X=Q4Y*Q1Z-Q4Z*Q1Y
      Q41Y=-(Q4X*Q1Z-Q4Z*Q1X)
      Q41Z=Q4X*Q1Y-Q4Y*Q1X
      Q41SQ=DOTPRO(Q41X,Q41Y,Q41Z,Q41X,Q41Y,Q41Z)
      Q12X=Q1Y*Q2Z-Q1Z*Q2Y
      Q12Y=-(Q1X*Q2Z-Q1Z*Q2X)
      Q12Z=Q1X*Q2Y-Q1Y*Q2X
      Q12SQ=DOTPRO(Q12X,Q12Y,Q12Z,Q12X,Q12Y,Q12Z)
      Q23X=Q2Y*Q3Z-Q2Z*Q3Y
      Q23Y=-(Q2X*Q3Z-Q2Z*Q3X)
      Q23Z=Q2X*Q3Y-Q2Y*Q3X
      Q23SQ=DOTPRO(Q23X,Q23Y,Q23Z,Q23X,Q23Y,Q23Z)
      Q34X=Q3Y*Q4Z-Q3Z*Q4Y
      Q34Y=-(Q3X*Q4Z-Q3Z*Q4X)
      Q34Z=Q3X*Q4Y-Q3Y*Q4X
      Q34SQ=DOTPRO(Q34X,Q34Y,Q34Z,Q34X,Q34Y,Q34Z)
C
      PART1=0.
      IF(Q41SQ.NE.0.)PART1=((Q4Q4-Q1Q4)/Q4+(Q1Q1-Q1Q4)/Q1)/Q41SQ
      PART2=0.
      IF(Q12SQ.NE.0.)PART2=((Q1Q1-Q1Q2)/Q1+(Q2Q2-Q1Q2)/Q2)/Q12SQ
      PART3=0.
      IF(Q23SQ.NE.0.)PART3=((Q2Q2-Q2Q3)/Q2+(Q3Q3-Q2Q3)/Q3)/Q23SQ
      PART4=0.
      IF(Q34SQ.NE.0.)PART4=((Q3Q3-Q3Q4)/Q3+(Q4Q4-Q3Q4)/Q4)/Q34SQ
      VX=Q41X*PART1+Q12X*PART2+Q23X*PART3+Q34X*PART4
      VY=(Q41Y*PART1+Q12Y*PART2+Q23Y*PART3+Q34Y*PART4)*SIGNY
      VZ=Q41Z*PART1+Q12Z*PART2+Q23Z*PART3+Q34Z*PART4
C     VHKX(NNN)=VHKX(NNN)+VX
C     VHKY(NNN)=VHKY(NNN)+VY
      VHKZ(NNN)=VHKZ(NNN)+VZ
      FACTOR=DOTPRO(VX,VY,VZ,XUNORM(INX),YUNORM(INX),ZUNORM(INX))
      AA(NNN)=AA(NNN)+FACTOR
C
C     THE NEXT FEW LINES ARE A FEW CHECK STATEMENTS
```

```
C       SOURCE(INX)=SOURCE(INX)+FACTOR
250     CONTINUE
C       WRITE(6,152)
152     FORMAT(20X,'THIS IS THE MATRIX AA'//)
C       WRITE(6,151)(AA(I),I=1,NT2S)
C       WRITE(6,153)
153     FORMAT(//20X,'THIS IS THE MATRIX SOURCE'//)
C       WRITE(6,151)(SOURCE(I),I=1,NTOTAL)
151     FORMAT(8F15.6)
        DO 154    I=1,NTOTAL
        SOURCE(I)=-(XUNORM(I)*COSABC+ZUNORM(I)*SINABC)
154     CONTINUE
        RETURN
        END
```

```
      SUBROUTINE VELPP
      COMMON/ZZZ1/NX,NY,NZ,NW,REFLEN,SPAN,KSYMMY,KSYMMZ,NSYMMY,NSYMMZ
      COMMON/ZZZ2/TAU,ALFA,TANGLE,TANGTE,CHORD,NTOTAL,UMACH
      COMMON/ZZZ6/XPC(250),YPC(250),ZPC(250)
      COMMON/ZZZ7/XP1(250),YP1(250),ZP1(250),XP2(250),YP2(250),
     1ZP2(250),XP3(250),YP3(250),ZP3(250)
      COMMON/ZZZ8/AA(2500),SOURCE(250),SINABC,COSABC,ALFABC
      COMMON/ZZZ9/XPP(250),YPP(250),ZPP(250),XPM(250),YPM(250)
     1,ZPM(250),XMP(250),YMP(250),ZMP(250),XMM(250),YMM(250),
     1ZMM(250),IWAKE(250)
      COMMON/ZZZ10/JNXB(250),NXWAKE,WAKEIN
      COMMON/ZZZ11/VHKX(2500),VHKY(2500),VHKZ(2500),VKX(250),VKY(250),
     1VKZ(250)
      COMMON/ZZZ12/VXWAKE(250),VYWAKE(250),VZWAKE(250)
      DOTPRO(X1,Y1,Z1,X2,Y2,Z2)=X1*X2+Y1*Y2+Z1*Z2
      PROMIX(XX1,YY1,ZZ1,XX2,YY2,ZZ2,XX3,YY3,ZZ3)=(YY2*ZZ3-YY3*ZZ2)*XX1
     1-(XX2*ZZ3-XX3*ZZ2)*YY1+(XX2*YY3-XX3*YY2)*ZZ1
      NT2S=NTOTAL**2
C
      NWT=NXWAKE*NY
      NWTP1=NWT+1
      NWTP=NWT+NXWAKE
      NTBW=NTOTAL+NWT
C
C     INITIALIZATION OF THE WAKE VELOCITY AT THE CORNERS
C
      DO 250 JNXBW=1,NTBW
      DO 250 INXW=NWTP1,NWTP
      DO 250 ISYMMY=1,NSYMMY
      DO 250 ISYMMZ=1,NSYMMZ
      SIGNY=3.-2*ISYMMY
      SIGNZ=3.-2*ISYMMZ
      JNXW=JNXBW-NTOTAL
      IF(JNXBW.LE.NTOTAL)JNX=JNXBW
      IF(JNXBW.GT.NTOTAL)JNX=JNXB(JNXW)
C
      INDEX=NTOTAL+INXW-NXWAKE
      Q1X=XPP(JNXBW)-XMP(INDEX)
      Q1Y=YPP(JNXBW)-YMP(INDEX)*SIGNY
      Q1Z=ZPP(JNXBW)-ZMP(INDEX)*SIGNZ
      Q2X=XMP(JNXBW)-XMP(INDEX)
      Q2Y=YMP(JNXBW)-YMP(INDEX)*SIGNY
      Q2Z=ZMP(JNXBW)-ZMP(INDEX)*SIGNZ
      Q3X=XMM(JNXBW)-XMP(INDEX)
      Q3Y=YMM(JNXBW)-YMP(INDEX)*SIGNY
      Q3Z=ZMM(JNXBW)-ZMP(INDEX)*SIGNZ
      Q4X=XPM(JNXBW)-XMP(INDEX)
      Q4Y=YPM(JNXBW)-YMP(INDEX)*SIGNY
      Q4Z=ZPM(JNXBW)-ZMP(INDEX)*SIGNZ
      Q1Q1=DOTPRO(Q1X,Q1Y,Q1Z,Q1X,Q1Y,Q1Z)
      Q2Q2=DOTPRO(Q2X,Q2Y,Q2Z,Q2X,Q2Y,Q2Z)
      Q3Q3=DOTPRO(Q3X,Q3Y,Q3Z,Q3X,Q3Y,Q3Z)
      Q4Q4=DOTPRO(Q4X,Q4Y,Q4Z,Q4X,Q4Y,Q4Z)
      Q1Q2=DOTPRO(Q1X,Q1Y,Q1Z,Q2X,Q2Y,Q2Z)
      Q1Q4=DOTPRO(Q1X,Q1Y,Q1Z,Q4X,Q4Y,Q4Z)
      Q2Q3=DOTPRO(Q2X,Q2Y,Q2Z,Q3X,Q3Y,Q3Z)
      Q3Q4=DOTPRO(Q3X,Q3Y,Q3Z,Q4X,Q4Y,Q4Z)
      Q1=SQRT(Q1Q1)
```

```
      Q2=SQRT(Q2Q2)
      Q3=SQRT(Q3Q3)
      Q4=SQRT(Q4Q4)
      Q41X=Q4Y*Q1Z-Q4Z*Q1Y
      Q41Y=-(Q4X*Q1Z-Q4Z*Q1X)
      Q41Z=Q4X*Q1Y-Q4Y*Q1X
      Q41SQ=DOTPRO(Q41X,Q41Y,Q41Z,Q41X,Q41Y,Q41Z)
      Q12X=Q1Y*Q2Z-Q1Z*Q2Y
      Q12Y=-(Q1X*Q2Z-Q1Z*Q2X)
      Q12Z=Q1X*Q2Y-Q1Y*Q2X
      Q12SQ=DOTPRO(Q12X,Q12Y,Q12Z,Q12X,Q12Y,Q12Z)
      Q23X=Q2Y*Q3Z-Q2Z*Q3Y
      Q23Y=-(Q2X*Q3Z-Q2Z*Q3X)
      Q23Z=Q2X*Q3Y-Q2Y*Q3X
      Q23SQ=DOTPRO(Q23X,Q23Y,Q23Z,Q23X,Q23Y,Q23Z)
      Q34X=Q3Y*Q4Z-Q3Z*Q4Y
      Q34Y=-(Q3X*Q4Z-Q3Z*Q4X)
      Q34Z=Q3X*Q4Y-Q3Y*Q4X
      Q34SQ=DOTPRO(Q34X,Q34Y,Q34Z,Q34X,Q34Y,Q34Z)
C
      PART1=0.
      IF(Q41SQ.NE.0.)PART1=((Q4Q4-Q1Q4)/Q4+(Q1Q1-Q1Q4)/Q1)/Q41SQ
      PART2=0.
      IF(Q12SQ.NE.0.)PART2=((Q1Q1-Q1Q2)/Q1+(Q2Q2-Q1Q2)/Q2)/Q12SQ
      PART3=0.
      IF(Q23SQ.NE.0.)PART3=((Q2Q2-Q2Q3)/Q2+(Q3Q3-Q2Q3)/Q3)/Q23SQ
      PART4=0.
      IF(Q34SQ.NE.0.)PART4=((Q3Q3-Q3Q4)/Q3+(Q4Q4-Q3Q4)/Q4)/Q34SQ
      VX=Q41X*PART1+Q12X*PART2+Q23X*PART3+Q34X*PART4
      VY=(Q41Y*PART1+Q12Y*PART2+Q23Y*PART3+Q34Y*PART4)*SIGNY
      VZ=Q41Z*PART1+Q12Z*PART2+Q23Z*PART3+Q34Z*PART4
      IF(INXW.LE.NWT)GO TO 250
      VXWAKE(INXW)=VXWAKE(INXW)+VX*SOURCE(JNX)
      VYWAKE(INXW)=VYWAKE(INXW)+VY*SOURCE(JNX)
      VZWAKE(INXW)=VZWAKE(INXW)+VZ*SOURCE(JNX)
250   CONTINUE
      RETURN
      END
```

```
      SUBROUTINE ITER
      COMMON/ZZZ1/NX,NY,NZ,NW,REFLEN,SPAN,KSYMMY,KSYMMZ,NSYMMY,NSYMMZ
      COMMON/ZZZ2/TAU,ALFA,TANGLE,TANGTE,CHORD,NTOTAL,UMACH
      COMMON/ZZZ6/XPC(250),YPC(250),ZPC(250)
      COMMON/ZZZ7/XP1(250),YP1(250),ZP1(250),XP2(250),YP2(250),
     1ZP2(250),XP3(250),YP3(250),ZP3(250)
      COMMON/ZZZ8/AA(900),SOURCE(250),SINABC,COSABC,ALFABC
      COMMON/ZZZ9/XPP(250),YPP(250),ZPP(250),XPM(250),YPM(250)
     1,ZPM(250),XMP(250),YMP(250),ZMP(250),XMM(250),YMM(250),
     1ZMM(250),IWAKE(250)
      COMMON/ZZZ10/JNXB(250),NXWAKE,WAKEIN
      COMMON/ZZZ11/VHKX(900),VHKY(900),VHKZ(900),VKX(250),VKY(250),
     1VKZ(250)
      COMMON/ZZZ12/VXWAKE(250),VYWAKE(250),VZWAKE(250)
      COMMON/CONTR/NITER
      DIMENSION XXX(250),YYY(250),ZZZ(250),VXW(250),VYW(250),VZW(250)
      DIMENSION INDICA(100)
      DOTPRO(X1,Y1,Z1,X2,Y2,Z2)=X1*X2+Y1*Y2+Z1*Z2
C
C
      NXWAKP=NXWAKE+1
      ALFAR=ALFA*3.14159/180.
      TANALF=TAN(ALFAR)
      NYP=NY+1
      DO 1 IX=1,NXWAKE
      DO 1 IY=1,NY
      IXP=IX+1
      IYP=IY+1
      IELEM=NTOTAL+IX+(IY-1)*NXWAKE
      INODE1=IXP+(IYP-1)*NXWAKP
      INODE2=IX +(IYP-1)*NXWAKP
      INODE3=IX +(IY -1)*NXWAKP
      INODE4=IXP+(IY -1)*NXWAKP
C
      XXX(INODE1)=XPP(IELEM)
      YYY(INODE1)=YPP(IELEM)
      ZZZ(INODE1)=ZPP(IELEM)
C
      XXX(INODE2)=XMP(IELEM)
      YYY(INODE2)=YMP(IELEM)
      ZZZ(INODE2)=ZMP(IELEM)
C
      XXX(INODE3)=XMM(IELEM)
      YYY(INODE3)=YMM(IELEM)
      ZZZ(INODE3)=ZMM(IELEM)
C
      XXX(INODE4)=XPM(IELEM)
      YYY(INODE4)=YPM(IELEM)
      ZZZ(INODE4)=ZPM(IELEM)
C
1     CONTINUE
      DO 50 IX=1,NXWAKP
      DO 50 IY=1,NYP
      INDICA(IY)=IY*NXWAKP
      INODE=IX+(IY-1)*NXWAKP
      INDEX1=INODE-(IY-1)
      VXW(INODE)=VXWAKE(INDEX1)+1.
      VYW(INODE)=VYWAKE(INDEX1)
```

```
      VZW(INODE)=VZWAKE(INDEX1)
      IF(IX.EQ.NXWAKP)VXW(INODE)=0.
      IF(IX.EQ.NXWAKP)VYW(INODE)=0.
      IF(IX.EQ.NXWAKP)VZW(INODF)=0.
      IF(IX.EQ.1)VZW(INODE)=-TANALF
      IF(IX.EQ.1)VYW(INCDE)=0.
      IF(IX.EQ.1)VXW(INODE)=1.
50    CONTINUE
C
C
C     WRITE(6,51)
51    FORMAT(/3X,'PRINTCUT CF THE WAKE X-VELOCITY'/)
C     CALL PRINTV(VXW,NXWAKP,NYP)
      WRITE(6,52)
52    FORMAT(/3X,'PRINTCUT OF THE WAKE Y-VELOCITY'/)
      CALL PRINTV(VYW,NXWAKP,NYP)
      WRITE(6,53)
53    FORMAT(/3X,'PRINTOUT OF THE WAKE Z-VELOCITY'/)
      CALL PRINTV(VZW,NXWAKP,NYP)
      IF(NITER.GT.1)GC TO 1000
      WRITE(6,100)
100   FORMAT(/3X,'PRINTOUT OF THE WAKE CORNER COORDINATES BFFORE')
      WRITE(6,201)
201   FORMAT(3X,'ITERATION IN THE X-DIRECTION'/)
      CALL PRINTV(XXX,NXWAKP,NYP)
      WRITE(6,202)
202   FORMAT(/3X,'PRINTOUT OF THE WAKE CORNER COORDINATES BEFORE')
      WRITE(6,203)
203   FORMAT(3X,'ITERATION IN THE Y-DIRECTICN'/)
      CALL PRINTV(YYY,NXWAKP,NYP)
      WRITF(6,204)
204   FORMAT(/3X,'PRINTOUT OF THE WAKE CORNER COORDINATES BEFORE')
      WRITE(6,205)
205   FORMAT(3X, 'ITERATICN IN THE Z-DIRECTION '/)
      CALL PRINTV(ZZZ,NXWAKP,NYP)
1000  CONTINUE
C
C
      DO 3 IX=1,NXWAKP
      DO 3 IY=1,NYP
      INODE=IX+(IY-1)*NXWAKP
      IF(IX.EQ.NXWAKP)GO TO 3
      R=WAKEIN
      VELTOT=SQRT(DOTPRC(VXW(INODE),VYW(INODE),VZW(INODE),
     1VXW(INODE),VYW(INODE),VZW(INODE)))
      IF(VELTOT.EQ.0.)CALL DEBUG(50)
      DELX=R*VXW(INODE)/VELTOT
      DELY=R*VYW(INCDE)/VELTOT
      DELZ=R*VZW(INODE)/VELTOT
C
      INODP1=INODE+1
      IF(INODP1.EQ.INDICA(IY))GO TO 2001
C     XXX(INODP1)=XXX(INODP1)+DELX
      YYY(INODP1)=YYY(INODE)+DELY
C     IF(IX.EQ.1.AND.IY.EQ.NYP)GO TO 2000
      ZZZ(INODP1)=ZZZ(INODE)+DELZ
      GO TO 3
2000  CONTINUE
```

```
      IF(NITER.EQ.1)ZZZ(INODP1)=ZZZ(INODE)+DELZ
C
C     BRING THE WHOLE VORTEX IN LINE WITH THE LAST Z
C
      INDEX1=INODP1+1
      INDEX2=NXWAKE+(IY-1)*NXWAKE
C     DO 2 INDEX=INDEX1,INDEX2
C2     ZZZ(INDEX)=ZZZ(INODP1)
C
      GO TO 3
2001  CONTINUE
      YYY(INODP1)=YYY(INODE)
      ZZZ(INODP1)=ZZZ(INODE)
C
3     CONTINUE
C
      DO 4 IX=1,NXWAKE
      DO 4 IY=1,NY
      IELEM=NTOTAL+IX+(IY-1)*NXWAKE
      IXP=IX+1
      IYP=IY+1
      INODE1=IXP+(IYP-1)*NXWAKP
      INODE2=IX +(IYP-1)*NXWAKP
      INODE3=IX +(IY -1)*NXWAKP
      INODE4=IXP+(IY -1)*NXWAKP
C
      XPP(IELEM)=XXX(INODE1)
      YPP(IELEM)=YYY(INODE1)
      ZPP(IELEM)=ZZZ(INODE1)
C
      XPM(IELEM)=XXX(INODE4)
      YPM(IELEM)=YYY(INODE4)
      ZPM(IELEM)=ZZZ(INODE4)
C
      IF(IX.EQ.1)GO TO 4
C
      XMM(IELEM)=XXX(INODE3)
      YMM(IELEM)=YYY(INODE3)
      ZMM(IELEM)=ZZZ(INODE3)
C
      XMP(IELEM)=XXX(INODE2)
      YMP(IELEM)=YYY(INODE2)
      ZMP(IELEM)=ZZZ(INODE2)
C
C
4     CONTINUE
      IF(NITER.LE.10)GO TO 738
C     WRITE(6,400)NITER
400   FORMAT(/3X,'AFTER',I3,2X,'ITERATIONS, THE X-CORNER ')
C     WRITE(6,401)
401   FORMAT(3X,'COORDINATES OF THE WAKE ARE'/)
C     CALL PRINTV(XXX,NXWAKP,NYP)
      WRITE(6,402)NITER
402   FORMAT(/3X,'AFTER',I3,2X,'ITERATIONS, THE Y-CORNER')
      WRITE(6,403)
403   FORMAT(3X,'COORDINATES OF THE WAKE ARE'/)
      DO 601 IX=1,NXWAKP
      DO 601 IY=1,NYP
```

```
      INODE=IX+(IY-1)*NXWAKP
      YYY(INODE)=(1./(SPAN/2.))*YYY(INODE)
601   CONTINUE
      CALL PRINTV(YYY,NXWAKP,NYP)
      WRITE(6,404)NITER
404   FORMAT(/3X,'AFTER',I3,2X,'ITERATIONS, THE Z-CORNER')
      WRITE(6,405)
405   FORMAT(3X,'COORDINATES OF THE WAKE ARE'/)
      CALL PRINTV(ZZZ,NXWAKP,NYP)
738   CONTINUF
      RETURN
      END
```

C3. Printout of Computer Program ILSAWR

```
SPECIFICATIONS OF THE PROBLEM

NX= 7
NY= 7
NZ= 1
NW= 1
NTOTAL= 49

KSYMMY= 1
KSYMMZ= 0

REFERENCE LENGTH=  1.00
SPAN/REF LENGTH =  8.00
THICKNESS=  0.0

ALFA=  5.000
ALFABC=  0.0

MACH NUMBER =  0.0

NXWAKE= 11

WAKEIN=  0.500
TANGLE=  0.0
TANGTE=  0.0

CHORD=  1.00
```

PRINTOUT OF THE WAKE CORNER COORDINATES BEFORE
ITERATION IN THE X-DIRECTION

-0.118756E-06	-0.118756E-06	-0.118756E-06	-0.118756E-06	-0.118756E-06	-0.118756E-06	-0.118756E-06	-0.118756E-06
0.500000E 00	0.500000E 00	0.500000E 00	0.500000E 00	0.500000E 00	0.500000E 00	0.500000E 00	0.500000E 00
0.100000E 01	0.100000E 01	0.100000E 01	0.100000E 01	0.100000E 01	0.100000E 01	0.100000E 01	0.100000E 01
0.150000E 01	0.150000E 01	0.150000E 01	0.150000E 01	0.150000E 01	0.150000E 01	0.150000E 01	0.150000E 01
0.200000E 01	0.200000E 01	0.200000E 01	0.200000E 01	0.200000E 01	0.200000E 01	0.200000E 01	0.200000E 01
0.250000E 01	0.250000E 01	0.250000E 01	0.250000E 01	0.250000E 01	0.250000E 01	0.250000E 01	0.250000E 01
0.300000E 01	0.300000E 01	0.300000E 01	0.300000E 01	0.300000E 01	0.300000E 01	0.300000E 01	0.300000E 01
0.350000E 01	0.350000E 01	0.350000E 01	0.350000E 01	0.350000E 01	0.350000E 01	0.350000E 01	0.350000E 01
0.400000E 01	0.400000E 01	0.400000E 01	0.400000E 01	0.400000E 01	0.400000E 01	0.400000E 01	0.400000E 01
0.450000E 01	0.450000E 01	0.450000E 01	0.450000E 01	0.450000E 01	0.450000E 01	0.450000E 01	0.450000E 01
0.500000E 01	0.500000E 01	0.500000E 01	0.500000E 01	0.500000E 01	0.500000E 01	0.500000E 01	0.500000E 01
0.550000E 03	0.550000E 03	0.550000E 03	0.550000E 03	0.550000E 03	0.550000E 03	0.550000E 03	0.550000E 03

PRINTOUT OF THE WAKE CORNER COORDINATES BEFORE
ITERATION IN THE Z-DIRECTION

0.103898E-07	0.103898E-07	0.103898E-07	0.103898E-07	0.103898E-07	0.103898E-07	0.103898E-07	0.103898E-07
0.103898E-07	0.103898E-07	0.103898E-07	0.103898E-07	0.103898E-07	0.103898E-07	0.103898E-07	0.103898E-07
0.103898E-07	0.103898E-07	0.103898E-07	0.103898E-07	0.103898E-07	0.103898E-07	0.103898E-07	0.103898E-07
0.103898E-07	0.103898E-07	0.103898E-07	0.103898E-07	0.103898E-07	0.103898E-07	0.103898E-07	0.103898E-07
0.103898E-07	0.103898E-07	0.103898E-07	0.103898E-07	0.103898E-07	0.103898E-07	0.103898E-07	0.103898E-07
0.103898E-07	0.103898E-07	0.103898E-07	0.103898E-07	0.103898E-07	0.103898E-07	0.103898E-07	0.103898E-07
0.103898E-07	0.103898E-07	0.103898E-07	0.103898E-07	0.103898E-07	0.103898E-07	0.103898E-07	0.103898E-07
0.103898E-07	0.103898E-07	0.103898E-07	0.103898E-07	0.103898E-07	0.103898E-07	0.103898E-07	0.103898E-07
0.103898E-07	0.103898E-07	0.103898E-07	0.103898E-07	0.103898E-07	0.103898E-07	0.103898E-07	0.103898E-07
0.103898E-07	0.103898E-07	0.103898E-07	0.103898E-07	0.103898E-07	0.103898E-07	0.103898E-07	0.103898E-07
0.103898E-07	0.103898E-07	0.103898E-07	0.103898E-07	0.103898E-07	0.103898E-07	0.103898E-07	0.103898E-07
0.103898E-07	0.103898E-07	0.103898E-07	0.103898E-07	0.103898E-07	0.103898E-07	0.103898E-07	0.103898E-07

PRINTOUT OF THE WAKE CORNER COORDINATES BEFORE
ITERATION IN THE Y-DIRECTION

0.0	0.106122E 01	0.195918E 01	0.269388E 01	0.326531E 01	0.367347E 01	0.391837E 01	0.400000E 01
0.0	0.106122E 01	0.195918E 01	0.269388E 01	0.326531E 01	0.367347E 01	0.391837E 01	0.400000E 01
0.0	0.106122E 01	0.195918E 01	0.269388E 01	0.326531E 01	0.367347E 01	0.391837E 01	0.400000E 01
0.0	0.106122E 01	0.195918E 01	0.269388E 01	0.326531E 01	0.367347E 01	0.391837E 01	0.400000E 01
0.0	0.106122E 01	0.195918E 01	0.269388E 01	0.326531E 01	0.367347E 01	0.391837E 01	0.400000E 01
0.0	0.106122E 01	0.195918E 01	0.269388E 01	0.326531E 01	0.367347E 01	0.391837E 01	0.400000E 01
0.0	0.106122E 01	0.195918E 01	0.269388E 01	0.326531E 01	0.367347E 01	0.391837E 01	0.400000E 01
0.0	0.106122E 01	0.195918E 01	0.269388E 01	0.326531E 01	0.367347E 01	0.391837E 01	0.400000E 01
0.0	0.106122E 01	0.195918E 01	0.269388E 01	0.326531E 01	0.367347E 01	0.391837E 01	0.400000E 01
0.0	0.106122E 01	0.195918E 01	0.269388E 01	0.326531E 01	0.367347E 01	0.391837E 01	0.400000E 01
0.0	0.106122E 01	0.195918E 01	0.269388E 01	0.326531E 01	0.367347E 01	0.391837E 01	0.400000E 01
0.0	0.106122E 01	0.195918E 01	0.269388E 01	0.326531E 01	0.367347E 01	0.391837E 01	0.400000E 01

THE DISTRIBUTION OF THE DOUBLET STRENGTH DH

RIGHTHAND SIDE

-0.39589E-02	-0.38849E-02	-0.37125E-02	-0.34288E-02	-0.30008E-02	-0.23927E-02	-0.15925E-02
-0.68218E-02	-0.66766E-02	-0.63782E-02	-0.58863E-02	-0.51416E-02	-0.40764E-02	-0.26464E-02
-0.97730E-02	-0.95619E-02	-0.91271E-02	-0.84065E-02	-0.73069E-02	-0.57133E-02	-0.35749E-02
-0.12560E-01	-0.12283E-01	-0.11710E-01	-0.10753E-01	-0.92783E-02	-0.71273E-02	-0.43533E-02
-0.15061E-01	-0.14720E-01	-0.14011E-01	-0.12818E-01	-0.10967E-01	-0.82876E-02	-0.49955E-02
-0.17136E-01	-0.16737E-01	-0.15904E-01	-0.14494E-01	-0.12303E-01	-0.91863E-02	-0.54982E-02
-0.18558E-01	-0.18116E-01	-0.17189E-01	-0.15618E-01	-0.13183E-01	-0.97781E-02	-0.58347E-02

THIS IS THE X-WAKE VELOCITY

-0.480406E-02	-0.477409E-02	-0.468118E-02	-0.454247E-02	-0.441279E-02	-0.449149E-02	-0.641041E-02	0.380451E-02
-0.160820E-02	-0.160449E-02	-0.158455E-02	-0.152060E-02	-0.132858E-02	-0.903000E-03	-0.440632E-03	-0.276148E-03
-0.853070E-03	-0.847636E-03	-0.821968E-03	-0.748443E-03	-0.597090E-03	-0.403298E-03	-0.263797E-03	-0.218201E-03
-0.532014E-03	-0.524415E-03	-0.495605E-03	-0.432221E-03	-0.336061E-03	-0.240564E-03	-0.178985E-03	-0.158966E-03
-0.361373E-03	-0.353009E-03	-0.325844E-03	-0.277185E-03	-0.216465E-03	-0.163272E-03	-0.130310E-03	-0.119560E-03
-0.258570E-03	-0.250580E-03	-0.227359E-03	-0.191435E-03	-0.151761E-03	-0.119269E-03	-0.994833E-04	-0.930089E-04
-0.191673E-03	-0.184665E-03	-0.165822E-03	-0.139445E-03	-0.112607E-03	-0.913251E-04	-0.785680E-04	-0.743386E-04
-0.145832E-03	-0.139999E-03	-0.125161E-03	-0.105748E-03	-0.868635E-04	-0.723506E-04	-0.635738E-04	-0.606698E-04
-0.113191E-03	-0.108481E-03	-0.969310E-04	-0.824915E-04	-0.688900E-04	-0.585701E-04	-0.524171E-04	-0.503959E-04
-0.894483E-04	-0.857113E-04	-0.767820E-04	-0.659464E-04	-0.559298E-04	-0.483691E-04	-0.438477E-04	-0.423570E-04
-0.717442E-04	-0.688077E-04	-0.619067E-04	-0.536891E-04	-0.461758E-04	-0.405120E-04	-0.371014E-04	-0.359719E-04

PRINTOUT OF THE WAKE Y-VELOCITY

0.0	0.0	0.0	0.0	0.0	0.0	0.0	0.0
0.0	-0.716022E-04	-0.175023E-03	-0.355480E-03	-0.643119E-03	-0.932307E-03	-0.994839E-03	-0.961138E-03
0.0	-0.624721E-04	-0.146541E-03	-0.264779E-03	-0.389637E-03	-0.451965E-03	-0.450023E-03	-0.440730E-03
0.0	-0.549076E-04	-0.119214E-03	-0.190576E-03	-0.245147E-03	-0.264493E-03	-0.261429E-03	-0.257859E-03
0.0	-0.463545E-04	-0.939147E-04	-0.137361E-03	-0.164443E-03	-0.172431E-03	-0.170783E-03	-0.169176E-03
0.0	-0.379370E-04	-0.728592E-04	-0.100491E-03	-0.115661E-03	-0.119803E-03	-0.118961E-03	-0.118196E-03
0.0	-0.305000E-04	-0.563585E-04	-0.748018E-04	-0.846302E-04	-0.870027E-04	-0.866350E-04	-0.865576E-04
0.0	-0.242877E-04	-0.437568E-04	-0.567539E-04	-0.630960E-04	-0.652968E-04	-0.656978E-04	-0.654446E-04
0.0	-0.191143E-04	-0.337828E-04	-0.430350E-04	-0.471937E-04	-0.479207E-04	-0.475501E-04	-0.475683E-04
0.0	-0.151972E-04	-0.266060E-04	-0.337119E-04	-0.370468E-04	-0.378746E-04	-0.379300E-04	-0.380060E-04
0.0	-0.121347E-04	-0.211475E-04	-0.267766E-04	-0.295841E-04	-0.305684E-04	-0.308213E-04	-0.309056E-04
0.0	0.0	0.0	0.0	0.0	0.0	0.0	0.0

PRINTOUT OF THE WAKE Z-VELOCITY

-0.874885E-01	-0.874885E-01	-0.874885E-01	-0.874885E-01	-0.874885E-01	-0.874885E-01	-0.874885E-01	-0.874885E-01
-0.432382E-01	-0.440590E-01	-0.462579E-01	-0.502368E-01	-0.568230E-01	-0.605203E-01	-0.119565E 00	0.112517E 00
-0.353017E-01	-0.363320E-01	-0.391258E-01	-0.440521E-01	-0.517856E-01	-0.645059E-01	-0.116190E 00	0.115683E 00
-0.312628E-01	-0.324179E-01	-0.355478E-01	-0.409581E-01	-0.492123E-01	-0.623588E-01	-0.114302E 00	0.117486E 00
-0.288760E-01	-0.301112E-01	-0.334463E-01	-0.391316E-01	-0.476605E-01	-0.610232E-01	-0.113099E 00	0.118648E 00
-0.273377E-01	-0.286259E-01	-0.320919E-01	-0.379440E-01	-0.466324E-01	-0.601180E-01	-0.112267E 00	0.119454E 00
-0.262872E-01	-0.276112E-01	-0.311631E-01	-0.371205E-01	-0.459086E-01	-0.594692E-01	-0.111665E 00	0.120042E 00
-0.255382E-01	-0.268866E-01	-0.304969E-01	-0.365245E-01	-0.453760E-01	-0.589868E-01	-0.111211E 00	0.120485E 00
-0.249849E-01	-0.263503E-01	-0.300006E-01	-0.360755E-01	-0.449708E-01	-0.586147E-01	-0.110861E 00	0.120829E 00
-0.245665E-01	-0.259441E-01	-0.296227E-01	-0.357309E-01	-0.446567E-01	-0.583240E-01	-0.110584E 00	0.121102E 00
-0.242425E-01	-0.256287E-01	-0.293274E-01	-0.354595E-01	-0.444069E-01	-0.580906E-01	-0.110361E 00	0.121322E 00
0.0	0.0	0.0	0.0	0.0	0.0	0.0	0.0

AFTER 12 ITERATIONS, THE Y-CORNER
COORDINATES OF THE WAKE ARE

0.0	0.265306E 00	0.489796E 00	0.673469E 00	0.816326E 00	0.918367E 00	0.979592E 00	0.100000E 01
0.0	0.265306E 00	0.489796E 00	0.673469E 00	0.816326E 00	0.918367E 00	0.979592E 00	0.100000E 01
0.0	0.265304E 00	0.489791E 00	0.673462E 00	0.816316E 00	0.918354E 00	0.979583E 00	0.999995E 00
0.0	0.265299E 00	0.489782E 00	0.673458E 00	0.816390E 00	0.919041E 00	0.988532E 00	0.993113E 00
0.0	0.265296E 00	0.489781E 00	0.673488E 00	0.816621E 00	0.920893E 00	0.998054E 00	0.985269E 00
0.0	0.265295E 00	0.489791E 00	0.673563E 00	0.817064E 00	0.923885E 00	0.100617E 01	0.977684E 00
0.0	0.265297E 00	0.489812E 00	0.673681E 00	0.817712E 00	0.927946E 00	0.101180E 01	0.971098E 00
0.0	0.265303E 00	0.489845E 00	0.673843E 00	0.818561E 00	0.933012E 00	0.101475E 01	0.965665E 00
0.0	0.265312E 00	0.489888E 00	0.674047E 00	0.819605E 00	0.939014E 00	0.101530E 01	0.961232E 00
0.0	0.265323E 00	0.489942E 00	0.674289E 00	0.820839E 00	0.945859E 00	0.101386E 01	0.957566E 00
0.0	0.265338E 00	0.490004E 00	0.674565E 00	0.822255E 00	0.953407E 00	0.101085E 01	0.954468E 00
0.0	0.265338E 00	0.490004E 00	0.674565E 00	0.822255E 00	0.953407E 00	0.101085E 01	0.954468E 00

AFTER 12 ITERATIONS, THE Z-CORNER
COORDINATES OF THE WAKE ARE

0.103898E-07	0.103898E-07	0.103898E-07	0.103898E-07	0.103898E-07	0.103898E-07	0.103898E-07	0.103898E-07
-0.435778E-01	-0.435778E-01	-0.435778E-01	-0.435778E-01	-0.435778E-01	-0.435778E-01	-0.435778E-01	-0.435778E-01
-0.651601E-01	-0.655704E-01	-0.666694E-01	-0.686542E-01	-0.719262E-01	-0.776857E-01	-0.102429E 00	0.114439E-01
-0.827836E-01	-0.837079E-01	-0.861989E-01	-0.906252E-01	-0.976425E-01	-0.108422E 00	-0.114252E 00	0.373512E-01
-0.983939E-01	-0.998934E-01	-0.103939E 00	-0.111024E 00	-0.121868E 00	-0.135728E 00	-0.106455E 00	0.496775E-01
-0.112814E 00	-0.114927E 00	-0.120624E 00	-0.130476E 00	-0.145068E 00	-0.160042E 00	-0.838876E-01	0.514905E-01
-0.126466E 00	-0.129219E 00	-0.136625E 00	-0.149292E 00	-0.167490E 00	-0.181624E 00	-0.520228E-01	0.462482E-01
-0.139593E 00	-0.143091E 00	-0.152152E 00	-0.167647E 00	-0.189275E 00	-0.200448E 00	-0.159777E-01	0.371573E-01
-0.152344E 00	-0.156419E 00	-0.167333E 00	-0.185653E 00	-0.210503E 00	-0.216208E 00	0.206399E-01	0.262983E-01
-0.164817E 00	-0.169565E 00	-0.182254E 00	-0.203371E 00	-0.231220E 00	-0.228352E 00	0.556518E-01	0.146913E-01
-0.177079E 00	-0.182505E 00	-0.196972E 00	-0.220852E 00	-0.251465E 00	-0.236203E 00	0.878766E-01	0.265461E-02
-0.177079E 00	-0.182505E 00	-0.196972E 00	-0.220852E 00	-0.251465E 00	-0.236203E 00	0.878766E-01	0.265461E-02